EXPERIMENTAL INVESTIGATION OF FILM COOLING EFFECTIVENESS ON GAS TURBINE BLADES

A Dissertation

by

SHIOU-JIUAN LI

Submitted to the Office of Graduate Studies of
Texas A&M University
in partial fulfillment of the requirements for the degree of

DOCTOR OF PHILOSOPHY

Approved by:

Chair of Committee,	Je-Chin Han
Committee Members,	Sai Lau
	Gerald Morrison
	Hamn-Ching Chen
Head of Department,	Jerald A. Caton

December 2012

Major Subject: Mechanical Engineering

ABSTRACT

High turbine inlet temperature becomes necessary for increasing thermal efficiency of modern gas turbines. To prevent failure of turbine components, advance cooling technologies have been applied to different portions of turbine blades.

The detailed film cooling effectiveness distributions along a rotor blade has been studied under combined effects of upstream trailing edge unsteady wake with coolant ejection by the pressure sensitive paint (PSP). The experiment is conducted in a low speed wind tunnel with a five blade linear cascade and exit Reynolds number is 370,000. The density ratios for both blade and trailing edge coolant ejection range from 1.5 to 2.0. Blade blowing ratios are 0.5 and 1.0 on suction surface and 1.0 and 2.0 on pressure surface. Trailing edge jet blowing ratio and Strouhal number are 1.0 and 0.12, respectively. Results show the unsteady wake reduces overall effectiveness. However, the unsteady wake with trailing edge coolant ejection enhances overall effectiveness. Results also show that the overall effectiveness increases by using heavier coolant for ejection and blade film cooling.

Leading edge film cooling has been investigated using PSP. There are two test models: seven and three-row of film holes for simulating vane and blade, respectively. Four film holes' configurations are used for both models: radial angle cylindrical holes, compound angle cylindrical holes, radial angle shaped holes, and compound angle shaped holes. Density ratios are 1.0 to 2.0 while blowing ratios are 0.5 to 1.5. Experiments were conducted in a low speed wind tunnel with Reynolds number

100,900. The turbulence intensity near test model is about 7%. The results show the shaped holes have overall higher effectiveness than cylindrical holes for both designs. As increasing density ratio, density effect on shaped holes becomes evident. Radial angle holes perform better than compound angle holes as increasing blowing and density ratios. Increasing density ratio generally increases overall effectiveness for all configurations and blowing ratios. One exception occurs for compound angle and radial angle shaped hole of three-row design at lower blowing ratio. Effectiveness along stagnation row reduces as increasing density ratio due to coolant jet with insufficient momentum caused by heavier density coolant, shaped hole, and stagnation row.

DEDICATION

Bi-Shia Lin, Jr-Yuan Lin, Jr-Chang Lin, Hsiu-Han Li, and Yan-De Li, thanks for every support and encouragement from my family members.

ACKNOWLEDGEMENTS

I would like to express deep gratitude to my advisor Professor J.C. Han for instructing me to conduct research in the Turbine Heat Transfer Laboratory, consistent encouragement, and financial support. I would like to thank the Professor. S. Lau, Professor G. Morrison, and Professor H.C. Chen for giving their precious time on the advisory committee. Acknowledgments are also to my colleagues Dr. Rallabandy, Dr. Lei for experiment instructions and to Mr. Yang, Mr. Wu, and Mr. Chu for friendship. Finally, I thank to all my family members and friends for their support, understanding and patience.

NOMENCLATURE

C	Oxygen concentration
C_D	Discharge coefficient
C_X	Axial chord of blade = 17cm
D	Diameter of the leading edge model (semi-cylinder)
DR	Blade surface coolant to mainstream density ratio
DR_t	Trailing edge coolant to mainstream density ratio
d	Film cooling hole diameter
d_r	Wake rod diameter
d_t	Ejection hole diameter
I	Coolant to mainstream momentum flux ratio
L	Length of film coolant hole
M	Film cooling mass flux (blowing) ratio $=\rho_c V_c/\rho_M V_M$
M_t	Trailing edge coolant ejection mass flux (blowing) ratio $=\rho_t V_t/\rho_M V_M$
N	Rotating speed of spoke wheel, rpm
n	Number of spoke wheel rods, 16
P	Spacing between consecutive holes on same film cooling row
PL	Length of blade on pressure side along curved surface = 25.4cm
P_{O2}	Partial pressure of oxygen
P_T	Total pressure
P_s	Static pressure

P_t Spacing between consecutive ejection holes

S Strouhal Number = $2\pi Nnd_r/60V_1$

SL Length of blade on suction side along curved surface = 33cm

s Distance from the stagnation line

Tu Turbulence intensity

T_c Coolant temperature

T_f Film temperature

T_m Mainstream temperature

V_M Local mainstream velocity, m/s

V_c Coolant velocity, m/s

V_m Mainstream temperature

V_1 Cascade inlet velocity, m/s

V_2 Cascade exit velocity, m/s

W_{air} Molecular weight of air

W_{fg} Molecular weight of foreign gas

z Distance along the blade span measured from the bottom of the measure area

α film cooling hole incline angle to the surface

β film cooling hole incline angle to the stream-wise direction

γ film cooling hole forward expansion angle

δ film cooling hole lateral expansion angle

θ angle to stagnation line

η Film cooling effectiveness

$\bar{\eta}$ Span-wise averaged film cooling effectiveness

ρ_c Coolant density, kg/m^3

ρ_M Mainstream density, kg/m^3

$\dot{m}_c$ Coolant mass flow rate

TABLE OF CONTENTS

LIST OF FIGURES

LIST OF TABLES

1. INTRODUCTION

Raising emphasis on efficiency in the gas turbine industry has led to a demand for turbine blades to withstand higher temperatures. Reliable cooling of the turbine blade is therefore imperative to increase the efficiency of the gas-turbine.

There are vast amount of literature discussing various methods of cooling the blade internally and externally over the past few decades [1, 2]. The aim of internal cooling is to increase heat transfer between blade internal passages and cooling air as shown in Fig. 1.1. A certain amount of cooling air is from compressor and goes through the channel inside the blade for internal cooling. There are several heat transfer techniques used to augment heat transfer between blade inner wall and coolant for different portions the gas turbine blade. Jet impingement is commonly used at blade leading edge inner channel. In the middle portion of the blade, angled ribs has been used to break the boundary layer and create secondary flow for heat transfer enhancement. Pin fins and dimples are usually put at trailing edge for enhancement.

The well known method for external cooling is the film cooling as shown in Fig. 1.2. Film cooling has been widely used as an active method to protect high temperature and high pressure blades. Relatively cooler air from compressor is injected through discrete holes on blade to from a protective thin film between the hot mainstream and the blade called film cooling. Turbine blade film cooling has been studied extensively in literature over the past few decades in the following categories.

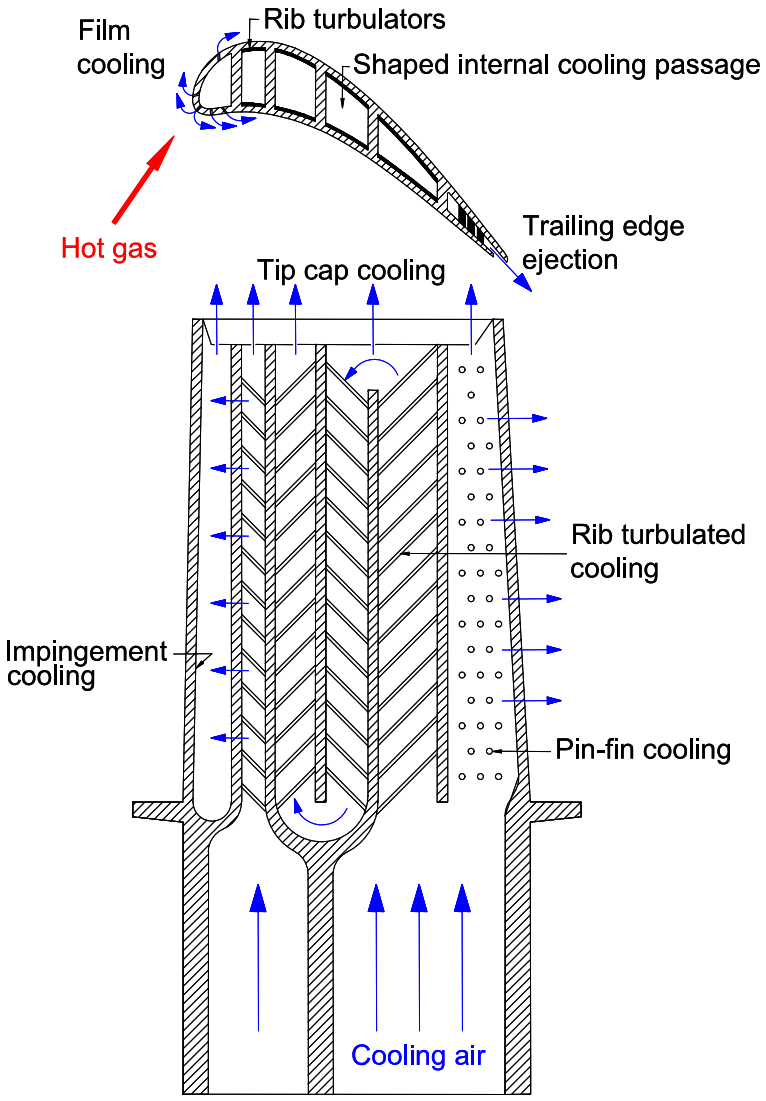

Fig. 1.1 Gas turbine blade internal cooling techniques

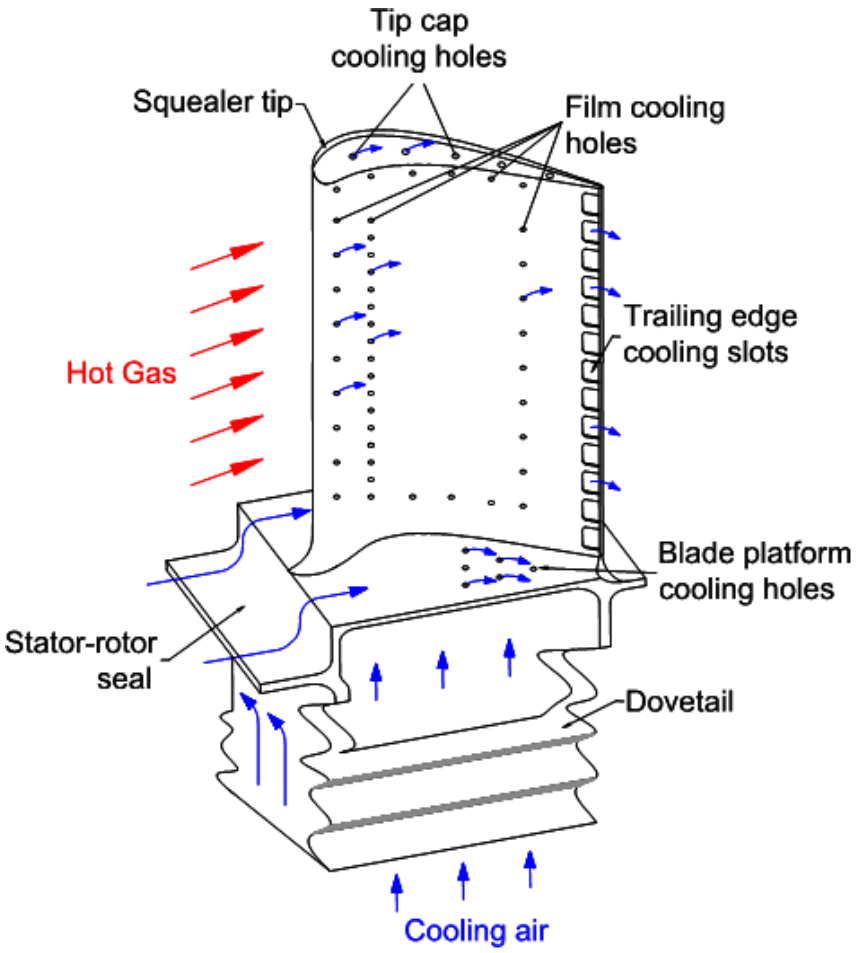

Fig. 1.2 Gas turbine blade film cooling techniques

1.1 Literature Review on Hole Shape

Film holes' configurations changed flow filed and influenced film cooling effectiveness. Goldstein et al. [3] concluded that shaped holes appreciably increased film cooling effectiveness laterally because of increasing the spreading of the secondary flow. Another reason is that the mean velocity of the secondary flow is decreased with the larger exit area of shaped hole. Goldstein et al. also [4] obtained results for film holes with compound angle which was contributed to reduce lift-off effect at higher blowing ratios. Rallabandi et al. [5] investigated flat plate film cooling with a step positioned upstream of a row of film cooling holes. They concluded step had a positive effect on film cooling for simple angled and compound angled cylindrical holes near the holes but had a negative effect for either simple angled or compound angled fan-shaped holes. Gritsch et al. [6] studied three holes' configurations on film cooling. It showed that laid-back fan-shaped holes had best film cooling compared with cylindrical, fan-shaped holes, particularly at higher blowing ratios. However, this study is limited to lower density ratios. Guo et al. [7] performed four film-hole shapes on showerhead film cooling on leading edge model for density ratio equal to unity. It showed shaped hole performed better that cylindrical holes at higher blowing ratios. Waye et al. [8] investigated film cooling effectiveness of axial holes embedded in various trench configurations. They concluded narrow trench provided best film cooling due to coolant with better lateral spreading.

1.2 Literature Review on Blowing Ratio and Density Ratio Effects

Blowing ratio (M) is defined as the coolant to mainstream mass flux ratio. Density ratio (DR) has been defined as the coolant to mainstream density ratio. Sinha et al. [9] studied both blowing ratio effect and density ratio effect on film cooling effectiveness using a plate with simple angled holes. At lower blowing ratios, the film coolant was found to adhere to the surface of the plate. On increasing the blowing ratios, the film coolant tended to lift-off from the blade surface, owing to the larger inertia due to the higher momentum of the coolant. Other studies [4, 10, 11] also had reached the similar conclusions using different methods. Furthermore, blowing ratio had been extensively studied to determine optimum film cooling effectiveness. The optimum blowing ratio is different for different film-hole shapes. Goldstein et al. [12] and Jubran et al. [13] reached the same conclusion that the optimum blowing ratio is around 0.5 for cylindrical holes. Typical coolant to mainstream density ratios in gas turbine engines are around 2.0. However, simulating this density ratio in the laboratory is difficult, because it requires cooling the secondary air to temperatures much lower than the ambient [9, 14] and heating mainstream air. Instead, foreign gases have been used to simulate the effect of density ratio [3, 15]. Sinha et al. [9] observed a significant improvement in film cooling effectiveness at higher density ratios due to the suppression of lift-off at higher blowing ratios. Wright et al. [16] experimentally studied density ratio effect of the flat plate film cooling. They concluded that increasing density ratio decreased centerline film cooling effectiveness but increased laterally averaged film cooling effectiveness due to enhance the spreading of the jets.

1.3 Literature Review on Free Stream Turbulence Effect

The flow condition on film cooling and heat transfer frequently studied is turbulence intensity. Choi et al. [17] reported that heat transfer on blade surface increased by increasing Reynolds number and free-stream turbulence due to suppress separation and promote boundary layer transition for low Re flow. Ekkad et al. [18] studied free-stream turbulence on leading edge film cooling and reported that turbulence reduced film cooling significantly at lower blowing ratio for density ratio 1 and 1.5. Bons et al. [19] presented high free-stream turbulence results on film cooling with turbulent intensity (Tu) up to 17% and density ratio close to unity. They found that effectiveness dramatically reduced right behind the holes at low to moderate blowing ratios. However, high turbulence helped reduce extent of coolant lift-off and result in higher effectiveness for higher blowing ratios. Also, high Tu created a more uniform film between adjacent holes and had higher effectiveness. Saumweber et al. [20] concluded effectiveness reduced at lower blowing ratios but slightly increased at higher blowing ratios as increasing turbulence intensity for cylindrical holes. For shaped holes, increasing turbulence level had a detrimental effect on effectiveness even for higher blowing ratio. Ethridge et al. [21] investigated film cooling performance under strong curvature on suction side of first-stage turbine vane. They found effectiveness for these holes was much higher than holes with a similar injection angle on a flat plate.

1.4 Literature Review on Leading Edge Film Cooling

There are several film cooling investigations focusing on leading edge region. El-Gabry et al. [22] provided that film cooling effectiveness with a pulsing film is lower

than that with a continue film at the same blowing ratio for a cylindrical leading edge model. Maikell et al. [23] simulated leading edge model constructed of a high conductive material to represent actually engine conditions with and without thermal barrier coating (TBC). They found that film cooling effectiveness had increased in the interface between the model and the TBC. However, effectiveness decreased on the external surface of TBC compared with the models without TBC. Rozati et al. [24] simulated Syngas ash particles in film cooled leading edge region. They concluded the percentage of particles deposited decreased with increasing blowing ratios and erosive wear was highest with 5μm and 7 μm particles in the film holes. Gue et al. [25] presents a three-dimensional conjugate heat transfer prediction on a cylindrical leading edge model with film cooling. This conjugate analysis considered both the internal convective heat transfer and external film cooling including heat conduction in the solid. The results clearly showed the leading edge overall cooling performance significantly affected by heat conduction through the cylinder solid wall.

1.5 Literature Review on Unsteady Wake

Rotor blades in a gas turbine engine experience intermittent wakes typically around S=0.1~0.4 and shocks due to the stator vanes located immediately upstream of the blades. These unsteady phenomena will trigger the laminar-turbulent transition along the blade surface [26]. An intermittency based model has been developed by Mayle et al. [27] to predict transitional heat transfer along the blade surface and this model has been shown to be fairly accurate in by Han et al. [28] and Zhang et al. [29]. Moreover, flow

transition to turbulence is further hastened due to film cooling holes on blades surface [30].

Spoke wheel type wake generators have been widely used in literature to simulate transition on rotor blades [29-33]. LDV and traversing hot-wires have been used to measure the phase averaged structure of the wake with better spatial resolution. Data of Stieger et al. [34] and Bijak-Bartosik et al. [35] show wake inside the passage between two rotor blades. Because of the wake, an increase in turbulent kinetic energy along the suction surface is measured. This also further confirms the picture of laminar-turbulent transition built in the literature.

Several studies on a linear cascade with rotating a spoke-wheel wake generator installed upstream of a typical high pressure film cooled model turbine blade have been conducted in the Turbine Heat Transfer Lab at Texas A&M University to study heat transfer coefficient and film cooling effectiveness. A reduction in film cooling effectiveness due to the unsteady wake is observed across the blade shown by Mehendale et al. [36] and Du et al [37]. Rallabandi et al. [38] provides a comprehensive parametric study such as blowing ratio, density ratio under different wake strength conditions. Teng et al. [39] used cold-wire anemometry to measure the mean and fluctuating temperature profiles within the film cooling jet. Increased turbulence in the boundary layer can be clearly observed in the unsteady wake case which reveals shorter coolant traces. A significant Strouhal number effect in a cascade characterizing the unsteady wake effect on leading edge film cooling was identified by the researchers [35, 40].

1.6 Literature Review on Unsteady Wake with Trailing Edge Coolant Ejection

Film cooling effectiveness and heat transfer along blade under unsteady wake with trailing edge coolant ejection had been investigated by Du et al. [41, 42] and Li et al. [43]. Du et al. acquired heat transfer coefficient distributions and film cooling effectiveness using thermochromic liquid crystals. However, the ejection blowing ratio was only 0.5 which did not match with engine conditions. Li et al. extended ejection blowing ratio to 1.0 which was close to engine conditions. They concluded adding coolant ejection increased turbulence intensity, and the ejection coolant was carried by unsteady wake toward blade surface to protect it. Therefore, the overall effectiveness slightly increased.

1.7 Literature Review on Measurement Techniques

Several experimental techniques have been used to determine film cooling effectiveness. For almost identical conditions, the thermal methods (IR [44, 45] and liquid crystal [46]) show a higher film cooling effectiveness than mass-transfer analogy method discussed in detail by [4, 11, 47]. When comparing film cooling effectiveness measured by the naphthalene sublimation [4, 48] mass transfer analogy and the transient liquid crystal methodology [10] on a flat plate, Goldstein et al. [4] found that a consistent 10-20% lower values measured by mass transfer method compared values with by heat transfer method. The reason is that data from heat transfer method already includes lateral conduction effect. A similar conclusion was arrived by Wright et al. [11] using the Pressure Sensitive Paint (PSP) mass transfer analogy. The validity of the heat-mass transfer analogy for film cooling effectiveness measurement requires the reasonable

approximation that the turbulent Lewis number be equal to unity, based on works by Nicoll et al. [49] and Jones [15]. More recently, the PSP analogy has made it possible to present high resolution conduction error free contours of film cooling effectiveness [50, 51, 52]. Therefore, we choose this method to obtain film cooling effectiveness and get high resolution results.

2. PRESSURE SENSITIVE PAINT MEASURMENT THEORY AND DATA ANALYSIS *

Foreign gas film-cooling effectiveness measurements are based on the reasonable approximation that the turbulent Lewis number (ratio of eddy thermal diffusivity to eddy mass diffusivity) is equal to 1, according to an analysis by Jones [15].

This work uses the Pressure Sensitive Paint (PSP) mass transfer analogy. The PSP (UniFIB UF405 from ISSI Inc.) is applied to the area of interest on the blade (shown in Fig. 2.1). When excited with light of wavelength of around 430nm (in the blue range of the visible spectrum), the paint emits a light at a higher wavelength (around 600nm). The intensity of the light emitted by the paint is proportional to the absolute partial pressure of oxygen. The principle is explained in Fig. 2.1). For the current case, the lighting source is a narrow range continuous blue LED light. The emitted light is recorded using a Cooke Sensicam CCD camera equipped with a low-pass filter (transmitting wavelengths above 550nm only). This filter is provided to ensure that the camera does not capture any of the incident blue light.

A calibration is performed Fig. 2.1(b) correlating the intensity of the light emitted to the partial pressure of oxygen. To compensate for non-uniformities in the lighting, the ordinate in the plot is normalized with reference (wind-off) intensity. Further, in the calibration, it is noted that the intensity of the light emitted by the PSP is

*Reprinted with permission from "Influence of Unsteady Wake with Trailing Edge Coolant Ejection on Turbine Blade Film Cooling" by Li, S.J., Rallabandi, A.P., and Han, J.C., 2012. Journal of Turbomachinery, Vol. 134(6), 061026-1~061026-9, Copyright [2012] by Journal of Turbomachinery.

also a function of temperature. Since our tests are conducted in a low speed wind tunnel with incompressible flow (located inside a room maintained at 22C by a central air conditioning system), this issue is not expected to play a role for the case under consideration.

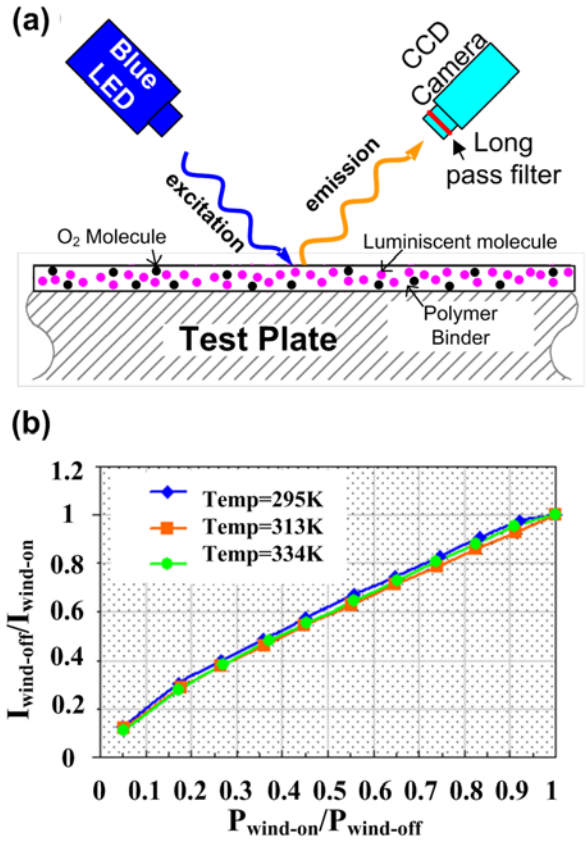

Fig. 2.1 (a) Principle of measurement using PSP (b) Calibration curve for PSP at three different temperatures

In this study, two kinds of foreign gas are used to simulate required density ratio. CO_2 is used as coolant to obtain density ratio of 1.5; a mixture of 15% SF_6 and 85% Ar (by volume), from Praxair Inc. is used to obtain an effective density ratio of 2.0. The coolant flow rates are controlled by rotameters.

To determine film cooling effectiveness for a given configuration, four tests are required. 200 images are averaged for each test to reduce random noise contamination. Test 1(black image) involves switching off the LED light and capturing an image in a dark room to determine the background noise intensity. The corresponding intensity field is called I_b. Test 2 (reference image) involves switching on the LED light, focusing the camera on the region of interest and acquiring a set of images without turning on the mainstream (I_r). Test 3 (air image) involves establishing mainstream and coolant flow rates at the appropriate blowing ratio using air as a coolant and acquiring a set of images (I_{air}). Finally, test 4 (coolant image) is conducted, establishing the desired blowing ratio using a coolant (either CO_2 or the 15% SF_6 and 85% Ar mixture), recorded as (I_{fg}).

These recorded intensities can be converted into pressures using the calibration in Fig. 2.1(b). In determining $P_{wind\text{-}on}= (P_{O2})_{air}$ the corresponding measured intensity is $I_{wind\text{-}on}=I_{air}–I_b$. Corresponding with the $P_{wind\text{-}on}= (P_{O2})_{fg}$ case, $I_{wind\text{-}on}=I_{fg}–I_b$. For both cases, $I_{wind\text{-}off}=I_r–I_b$ and $P_{wind\text{-}off}$ =1 bar. Knowing $(P_{O2})_{air}$ and $(P_{O2})_{fg}$, the film cooling effectiveness can be estimated by using Eq.(1).

$$\eta = 1 - \frac{1}{\left(\frac{(P_{O_2})_{air}}{(P_{O_2})_{fg}} - 1\right)\frac{W_{fg}}{W_{air}} + 1} \tag{1}$$

The term W_{fg}/ W_{air} is the molecular ratio (or density ratio) of the foreign gas to air - and arises because the partial pressure of oxygen (measured by the PSP) is proportional to the molar concentration of oxygen. The turbulent Lewis number (assumed to be equal to unity) is the ratio of the turbulent thermal diffusivity to the turbulent mass diffusivity. The molecular weight ratio term arises because mass fraction of oxygen does not equal its mole fraction when a high density foreign gas is injected.

All effectiveness values reported in this work are time averaged values (200 images), and not phase-averaged values. As the flow field surround the blade is unsteady, the effectiveness distribution along the blade would also be expected to vary with the phase of the upstream wake rod. However, the response time of the currently used PSP is not quick enough to resolve this time-variation.

3. EXPERIMENTAL SETUP *

3.1 Blade, Rotating Rods, and Wind Tunnel Geometry

Firstly, introducing unsteady wake test wind tunnel. Tests are conducted in a five passage low speed wind tunnel setup (shown in Fig. 3.1(a)) with five blades. The inlet velocity, measured by a Pitot-static probe is maintained at 12m/s, resulting in an exit velocity of around 32.7 m/s, corresponding to an exit Reynolds number, $V_2C_x/\nu=3.7\times10^5$. The upstream vane-generated unsteady wake and coolant ejection impinging on the downstream rotor are simulated by a rotating spoke-wheel type wake generator containing hollow rods equipped with coolant ejection holes. A total of 16 rods are used. The inside and outside diameter of each hollow rod are 3.2mm and 6.3mm, correspondingly. Each hollow rod contains 32 holes, the diameter of each hole is 1.6 mm, distributing uniformly with 3d spacing in the middle portion of the rod. The location of the wake generator plane is 8cm upstream of the blade row. The wake generator and hole direction is arranged such that the wake rod and coolant ejection are aligned along the flow streamline upstream of the leading edge of the instrumented blade. The tested rotating speed of the wake generator is fixed at 140rpm, corresponding with values of Strouhal number of 0.12 for all tests. In this study, the Strouhal number is defined as:

$$S = \frac{2\pi N n d_r}{60 V_1} \tag{2}$$

*Reprinted with permission from "Influence of Unsteady Wake with Trailing Edge Coolant Ejection on Turbine Blade Film Cooling" by Li, S.J., Rallabandi, A.P., and Han, J.C., 2012. Journal of Turbomachinery, Vol. 134(6), 061026-1~061026-9, Copyright [2012] by Journal of Turbomachinery.

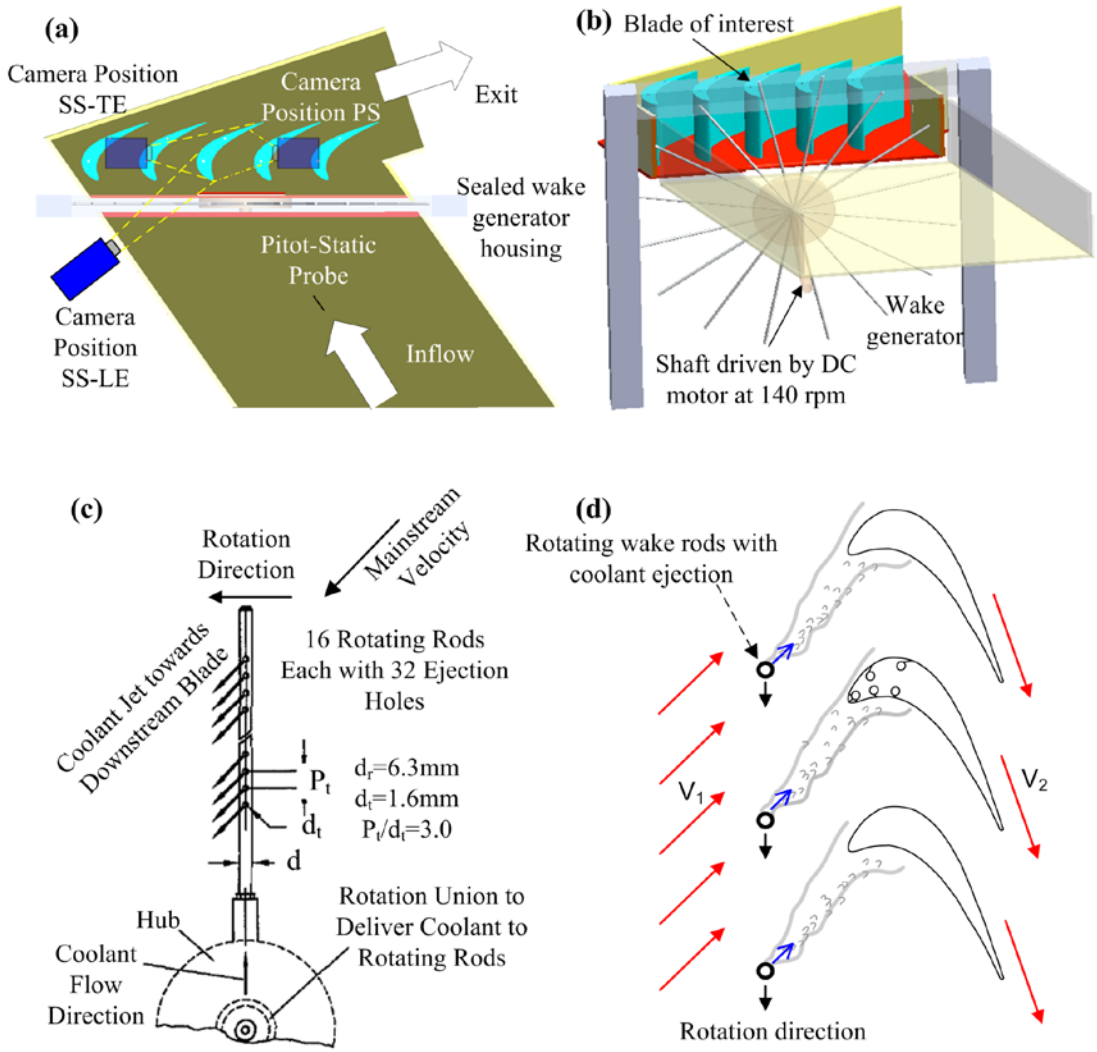

Fig. 3.1 (a), (b): 3D view of suction type wind tunnel with spoke wheel wake generator; (c), (d): Trailing edge coolant ejection configuration

Blades studied are five-times scaled versions of a typical high pressure blade, with a turn angle of 107.49 degrees. The axial chord of the blade is 17cm and the radial span is 25.2cm. The blade pitch is 17cm. The blade (Fig. 3.2) has 7 rows of film cooling holes – three at the leading edge, and two each on both the pressure and suction surfaces. Detailed specifications of the film cooling holes are available in Table 1. In Table 1, the axial angle is the angle made by the center-line of the film cooling hole with the axis of rotation of the blade. The radial angle is the angle that the hole makes with the span (radius) of the blade. The simple angled holes on the suction side (SS1 and SS2) therefore have a radial angle of 90 deg. The tangential angle is the angle the axis of the hole makes with the mainstream. Flow can be controlled separately to each row on the suction and the pressure sides, but flow to the three rows on the leading edge is supplied by the same supply line, as detailed in Fig. 3.2.

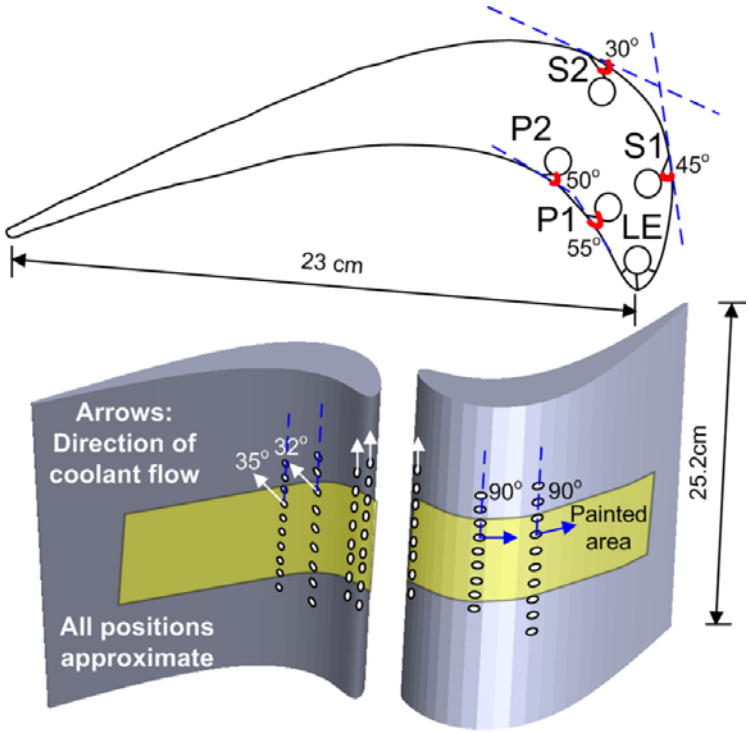

Fig. 3.2 View of blade showing arrangement of cooling holes, coolant supply channels and area painted with PSP

Table 1 Film cooling hole specification

	d(mm)	P/d	L/d	Axial Angle	Radial angle	Tang. Angle
LE	1.65	7.31	2.7	90°	27°	-
SS1	1.9	4.13	7.6	-	90°	45°
SS2	1.78	5.71	12.8	-	90°	30°
PS1	1.78	6.79	4.2	-	32°	55°
PS2	1.78	5.00	6.7	-	35°	50°

3.2 Wind Tunnel Characterization

The velocity distribution of the blade has been measured using a specifically fabricated blade with a total 24 pressure taps along the blade in Fig. 3.3(a). On the suction side, the flow experiences acceleration until 80% of the chord length, after which the velocity stays approximately constant until the exit. On the pressure side, the velocity stays constant at around 16% of the exit velocity until 50% of the blade chord, after which the flow accelerates quickly to reach V_2. The effect of using radial spoke wheels on a linear cascade is not anticipated to be significant in the region of interest, as per a discussion in Han et al. [28] and Ou et al. [30]. Under the test condition of Strouhal number of 0.1, Renolds number of 5.3×10^5, phase averaged measurements of turbulence within the wake based on 100 samples (Fig. 3.3 (b-d)) and show highest intensities reaching 20% as shown in Fig. 3.3 (d). For our test consideration, mainstream without the wake and coolant ejection experiences a time averaged turbulence intensity of 0.7%. With the wake (S=0.12) and no coolant ejection (M_t=0) experiences a turbulence intensity around 13%. With both wake (S=0.12) and coolant ejection (M_t=1) turbulence intensity works out to around 12.7% which a little lower compared no coolant ejection case because addition of ejection to unsteady wake profile increases mainstream velocity and produces more uniformly distributed turbulence intensity profile, which slightly reduces turbulence intensity. The detailed test conditions can be found in Table 2.

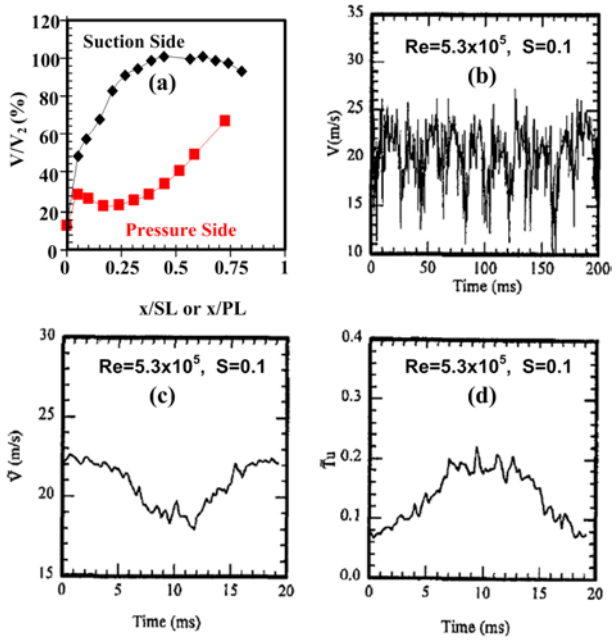

Fig. 3.3 (a) Velocity distribution around model blade (b) Instantaneous hot-wire velocity signal (c) Ensemble averaged velocity (d) Ensemble averaged turbulence intensity

Table 2 Test conditions for unsteady flow

Case	S	DR_t	DR	M_t	M
1	0	0	1.5	0	SS:0.5,1.0; PS:1.0,2.0
2	0.12	0	1.5	0	SS:0.5,1.0; PS:1.0,2.0
3	0.12	1.5	1.5	1	SS:0.5,1.0; PS:1.0,2.0
4	0.12	2.0	2.0	1	SS:0.5,1.0; PS:1.0,2.0

3.3 Experimental Uncertainty for Unsteady Flow Film Cooling

The mainstream velocity is measured using a micro-manometer connected to a pitot-static tube located in the cascade upstream of the wake rods. An error analysis based on the Kline-McClintock [53] scheme shows a maximum 2% error in the mainstream velocity. The coolant flows through each coolant passage (shown in the figure on p.18) and rods for coolant ejection are both controlled by individual rotameters. A maximum 6% error (for lowest blowing ratios) and much lower values for higher blowing ratios is anticipated in the coolant flow rate. Uncertainty in measured film cooling effectiveness is also dependent on the intensity of illumination in the regions covered by the PSP. Due to the relative insensitivity of PSP at close-to-atmospheric oxygen pressures, the film cooling effectiveness has a larger uncertainty around 9% at lower effectiveness values, and lower uncertainty at higher effectiveness value.

3.4 Experimental Facilities of Leading Edge Film Cooling

Experimental setup for leading edge film cooling is as shown in Fig. 3.4. The facility is a suction type low speed wind tunnel. The mainstream flow is fixed to maintain a Reynolds number of 100,900 based on the cylinder's diameter. Inlet velocity measured by Pitot-static probe is around 20.4 m/s. Mainstream flow travels through a nozzle before it enters the test tunnel. Leading edge model is a blunt body with semi-cylinder called test section and an after-body. The test section is placed in the wind tunnel, and the center of the cylinder is at 73.7 cm downstream of the nozzle exit. Coolant plenum is right inside the hollow semi-cylinder. Coolant flow from compressor (air) or coolant bottle travels through rotameters and enters semi-cylinder from the

bottom. The coolant inside plenum is discharged to mainstream through the seven-rows or three-rows film cooling holes. To simulate realistic engine condition, a turbulent grid is put at the exit of the nozzle to increase the free stream turbulence of the mainstream flow. Turbulence intensity increases to around 7% with the grid, and turbulence integral length scale is about 1.5cm measured near the cylinder. For PSP measurement, the position of excitation light (LED light) is located at the top of test section and CCD camera position is also shown in Fig. 3.4.

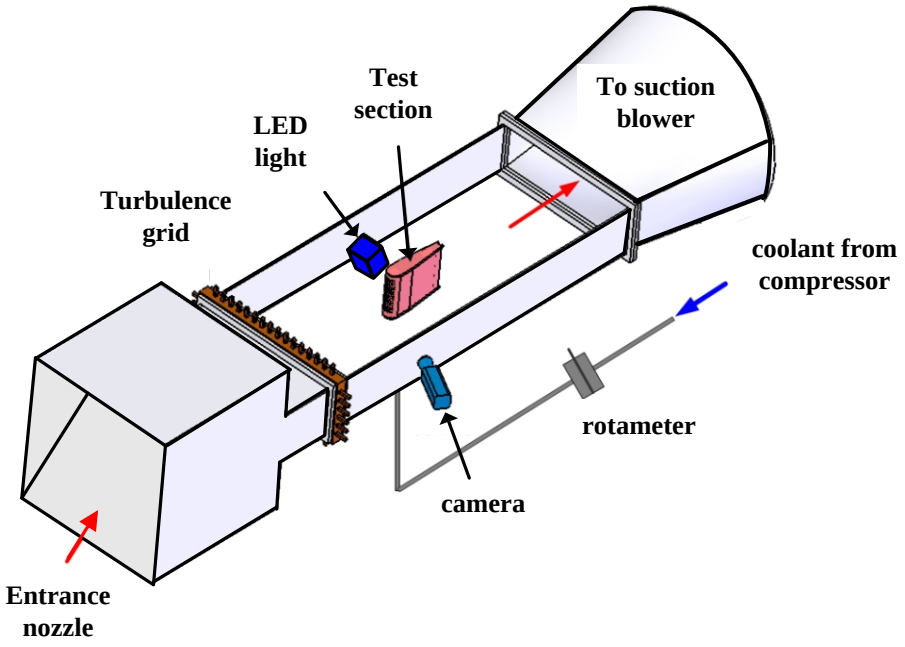

Fig. 3.4 Leading edge film cooling test facility

3.5 Semi-Cylinder Test Section

Leading edge model as show in Fig. 3.5 contains a fix after-body and detachable semi-cylinder which is made of Stereolithography (SLA). The semi-cylinder test sections include two designs: seven-row film cooled model (Fig. 3.6) for simulating rotor and three row film cooled model (Fig. 3.7) for simulating vane. There are four kinds of holes configurations such as radial angle cylindrical holes, compound angle cylindrical holes, radial angle shaped holes, and compound angle shaped holes for each set. Also, all holes' arrangement are in-line pattern. There are eight leading edge film cooled models in total are studied. The dimensions of semi-cylinder are 7.62 cm in diameter, 25.4 cm in height, and 0.64 cm in thickness. For seven-row film holes design, holes' location are at θ=0° (stagnation line), ±15°, ±30° and ±45° as shown in Fig. 3.6.

Either radial angle cylindrical holes (a) or radial angle shaped holes (c), the holes are oriented in the radial (span-wise) direction which is orthogonal to the local mainstream direction. As for compound angle cylindrical holes (b) or shaped holes (d), each row oriented at different angles with respect to the local mainstream because of the constraint of space. The holes' from stagnation row to downstream are orientated at β= 90°, 75°, 67.5°, and 60° to the local mainstream direction as shown in Fig. 3.6 (b) or (d). The three-row film-hole design can be shown in Fig. 3.7. The holes' location are at θ=0° (stagnation line), ±30° on both side of cylinder. The orientation of holes at ±30° is 67.5° (β) to the local mainstream direction for compound angle cylindrical holes (b) or shaped holes (d) in Fig. 3.7. The stagnation row for four holes' configuration is always in radial (span-wise) direction. There are fifteen holes per row with a p/d of 4 for either seven-

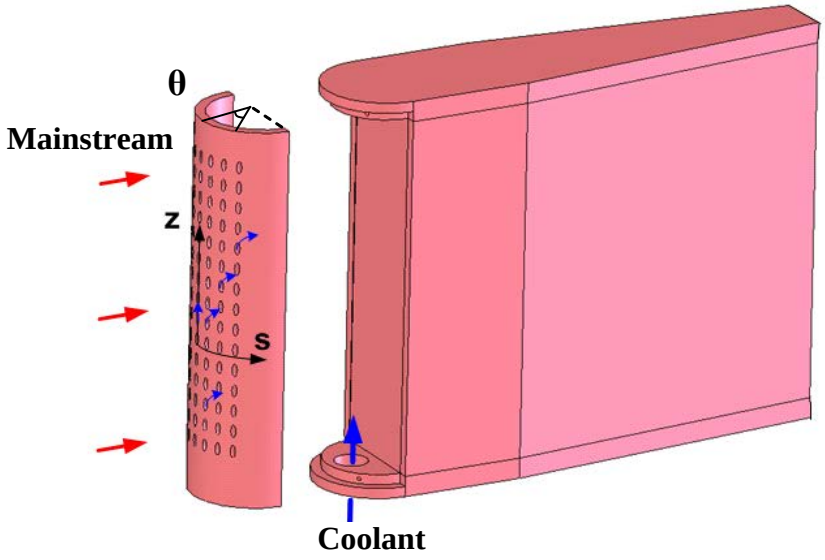

Fig. 3.5 Leading edge film cooling model with semi-cylinder test section and an after-body

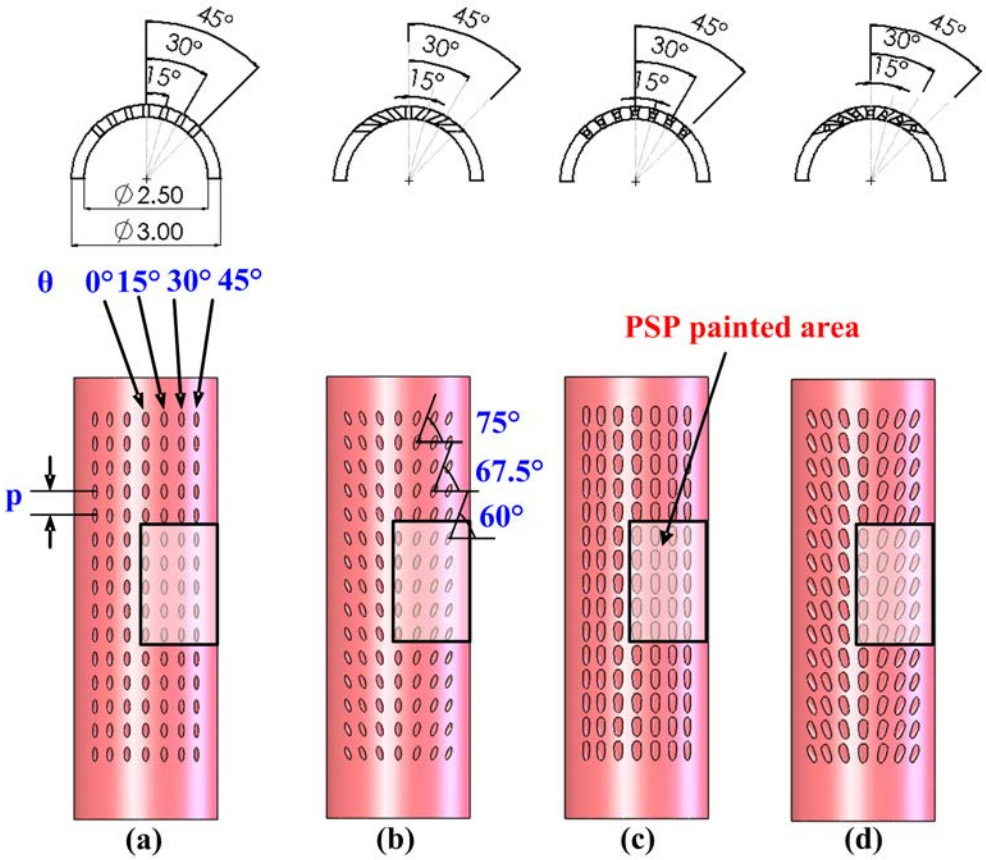

Fig. 3.6 Seven-row film cooled leading edge models (a) Radial angle cylindrical holes (b) Compound angle cylindrical holes (c) Radial angle shaped holes (d) Compound angle shaped holes

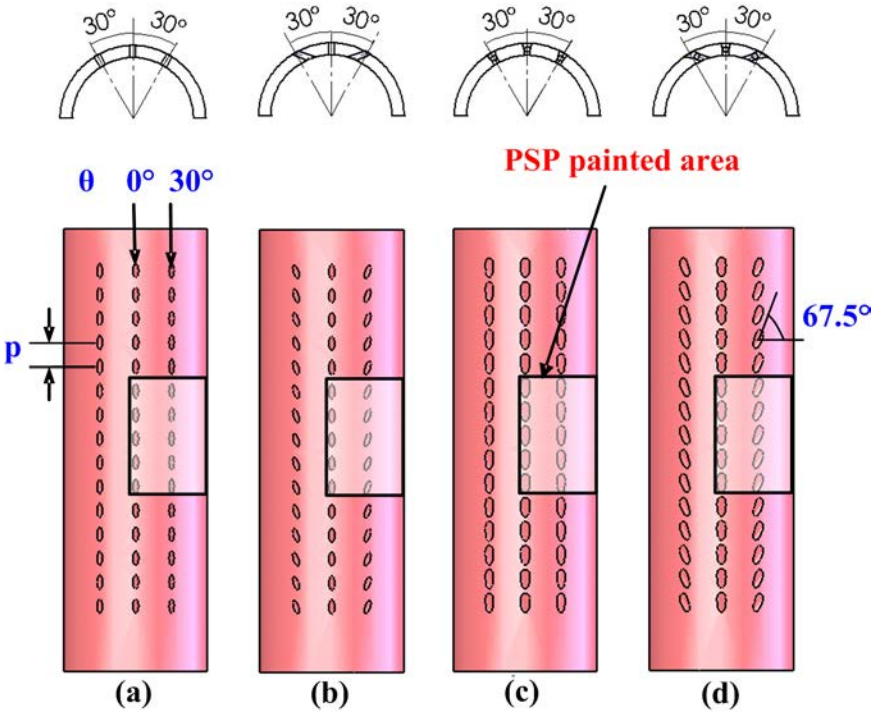

Fig. 3.7 Three-row film cooled leading edge models (a) Radial angle cylindrical holes (b) Compound angle cylindrical holes (c) Radial angle shaped holes (d) Compound angle shaped holes

row or three-row for semi-cylinder test section. For economic purpose, both the top and bottom four rows has been blocked for each row, which means no coolant coming out from these holes. In other words, only middle seven holes are open per row as running experiment. Due to geometric symmetry of semi-cylinder, the flow behavior is similar for both right and left hand side of stagnation line so that data taken are only on right hand side. Because of the edge effect, the reported data only focus on middle five holes per row ever if middle seven holes open as indicated in Fig. 3.6 or 3.7.

The detailed holes orientations of both cylinder holes and shaped hole are shown in Fig. 3.8. For cylindrical holes, the holes' inclined angle (α) is 25° to the model surface and compound angle β is mentioned above. As for shaped holes, laidback fan-shaped holes are used. This means holes with lateral expansion (γ) of 5° from the holes' centerline, and additional 5° (δ) forward expansion to the surface starting in the middle of hole (1/2L). For all four configurations, the metering part (hole inlet) has the same diameter (d=0.3715 cm). However, due to lateral expansion (γ) for shaped holes configuration, an area ratio is about 2 between the expanded cross section at the hole' exit and the metering part. Detailed specifications and dimensions of the film cooling holes are available in Table 3 and 4. The test conditions for both seven-row and three-row designs are as Table 5 and 6.

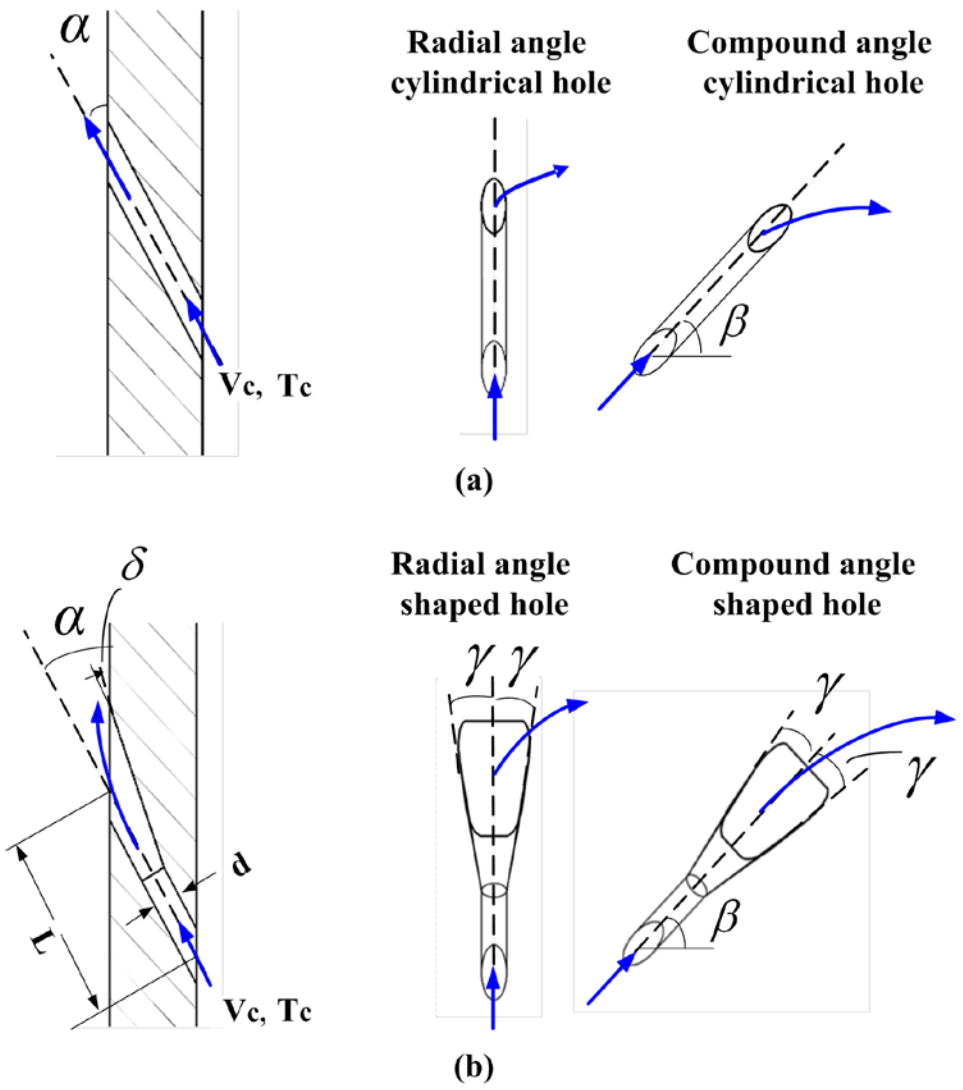

Fig. 3.8 Definition of orientations and hole shape (a) Cylindrical hole (b) Shaped hole

Table 3 Film cooling hole specification for seven-row design

	Design 1 (Seven-row)			
Hole configurations	cylindrical holes		shaped holes	
	radial angle	compound angle	radial angle	compound angle
Hole diameter (d, cm)	0.3715	0.3715	0.3715	0.3715
Diameter ratio (D/d)	24	24	24	24
Hole to hole spacing (p/d)	4d	4d	4d	4d
Ratio of hole length to diameter (L/d)	4.73	4.73~ 5.46	4.73	4.73~ 5.46
Lateral expansion angle (γ)(deg)	0	0	5	5
Forward expansion angle (δ) (deg)	0	0	5	5
Angle to surface (α) (deg)	25	25	25	25
Stream-wise angles (β) (deg)	90	90/75/ 67.5/60	90	90/75/ 67.5/60
Ratio of hole breakout area to metering cross-section area	1.0	1.0	1.9	1.9/1.94/ 1.98/2.1

Table 4 Film cooling hole specification for three-row design

	Design 2 (Three-row)			
Hole configurations	cylindrical holes		shaped holes	
	radial angle	compound angle	radial angle	compound angle
Hole diameter (d, cm)	0.3715	0.3715	0.3715	0.3715
Diameter ratio (D/d)	24	24	24	24
Hole to hole spacing (p/d)	4d	4d	4d	4d
Ratio of hole length to diameter (L/d)	4.73	4.73~ 5.46	4.73	4.73~ 5.46
Lateral expansion angle (γ)(deg)	0	0	5	5
Forward expansion angle (δ) (deg)	0	0	5	5
Angle to surface (α) (deg)	25	25	25	25
Stream-wise angles (β) (deg)	90	90/ 67.5	90	90/67.5
Ratio of hole breakout area to metering cross-section area	1.0	1.0	1.9	1.9/1.98

Table 5 Leading edge seven-row design test conditions

Case	Configuration	DR	M
1	Radial angle cylindrical hole	1, 1.5	0.5, 1.0, 1.5
2	Compound angle cylindrical hole		
3	Radial angle shaped hole		
4	Compound angle shaped hole		

Table 6 Leading edge three-row design test conditions

Case	Configuration	DR	M
1	Radial angle cylindrical hole	1, 1.5, 2	0.5, 1.0, 1.5
2	Compound angle cylindrical hole		
3	Radial angle shaped hole		
4	Compound angle shaped hole		

3.6 Experimental Uncertainty for Leading Edge Film Cooling

The mainstream velocity is measured by a micro-manometer connected to a pitot-static tube upstream the test section. From an error analysis of the Kline-McClintock [53] scheme shows a maximum 2% error in the mainstream velocity. The coolant flows (air, foreign gas) is controlled by rotameters. A maximum 7% error is for lowest blowing ratio but lower values are for higher blowing ratios. Uncertainty of measured film cooling effectiveness also comes from the intensity of illumination regions covered by the PSP. The film cooling effectiveness has a larger uncertainty about 9% at lower effectiveness values but a lower uncertainty at higher effectiveness value.

3.7 Objectives of the Present Studies

There are two main topics in this study and each with several effects to investigate. The general aim of these two topics is to obtain film cooling effectiveness. For heat transfer measurement, there is conduction error near film cooling hole. Heat transfer can be analogy to mass transfer, using Pressure Sensitive Paint (PSP) which is no conduction error to determine film cooling effectiveness.

The objectives of unsteady flow on film cooling are: (1) use PSP measurement technique to obtain the detailed film cooling effectiveness distribution data, (2) document film cooling effectiveness data under unsteady wake condition with and without trailing edge coolant ejection, and (3) compare film cooling effectiveness data with unsteady wake and trailing edge coolant ejection for two coolant-to-mainstream density ratios (DR=1.5, 2.0).

The objectives of leading edge film cooling are: (1) Use PSP measurement technique to obtain the detailed film cooling effectiveness distribution (2) Study leading edge film cooling modeled with a semi-cylinder and two designs of film cooling holes with seven-row and three-row to simulate blade and vane, separately (3) Four film holes configurations are tested for both designs with density ratio from DR = 1.0, 1.5, to 2.0 and blowing ratio from 0.5, 1.0, to 1.5.

4. UNSTEADY FLOW ON FILM COOLING *

In this chapter, the cases (Table 2, shown in p.22) are presented through contour plots, span-wise averaged plots, momentum flux ratio plots for detailed discussion. Two camera angles are used for suction side and one camera angle is used for pressure side to compose these plots. The x-axes on contour plots correspond with the distance along the axial chord (C_x), whereas the x-axes on span-wise averaged line plots correspond with the distance along the curved surface of the blade. Also, the span-wise averaged effectiveness includes the value within the hole row which shows a much higher effectiveness value. Flow conditions can be divided into three types for detailed discussion such as no wake condition (case1), wake condition (case2), and combined wake and coolant ejection condition using CO_2 as coolant (case3) Furthermore, realistic engine condition - high density ratio case (DR=2) with combined wake and coolant ejection condition (case 4) is included to compare with CO_2 case (DR=1.5).

4.1 Critical Parameters Determination

Table 2 presents the test cases for mass transfer measurements using PSP technique in this study. Prior experimental results [41], suggest that the film cooling effectiveness measurements are insensitive of the Mainstream Reynolds number for the range tested (Re = 5.3×10^5 to 7.6×10^5). Based on the economic concerns, it is feasible for

*Reprinted with permission from "Influence of Unsteady Wake with Trailing Edge Coolant Ejection on Turbine Blade Film Cooling" by Li, S.J., Rallabandi, A.P., and Han, J.C., 2012. Journal of Turbomachinery, Vol. 134(6), 061026-1~061026-9, Copyright [2012] by Journal of Turbomachinery.
*Reprinted with permission from "Unsteady Wake and Coolant Density Effects on Turbine Blade Film Cooling Using PSP Technique" by Rallabandi, A.P., Li, S.J., and Han, J.C., 2012. Journal of Heat Transfer, Vol. 134, 081701-1~081701-10, Copyright [2012] by Journal of Heat Transfer.

us to pick up exit Reynolds number of 3.7×10^5 for conducting all tests. The no wake condition data (case1) will be used as reference. The unsteady wake strength is defined by wake Strouhal number which is usually above 0.1 for the real engine conditions. It can be achieved in the test set up by a combination of wake rotation speed (N), the number of rod (n), outer diameter of the hollow rod (d_r), and cascade inlet velocity (V_1). First, we choose CO_2 (DR=1.5) as coolant to discuss effects of wake (case2) and trailing edge coolant ejection (case3). Density ratio for modern engine condition is around 2.0 simulated using mixture coolant of 15% SF_6 and 85 % Ar in this paper (case4). Mass flux for mainstream ($\rho_M V_M$) and trailing edge coolant ejection ($\rho_t V_t$) should be similar in real engine situation. Therefore, we choose coolant ejection blowing ratio M_t = 1, corresponding to 0.53% of mainstream flow. From previous study by Rallabandi, et al. [38], we choose two typical blowing ratios for suction side, M=0.5 and 1.0, with leading edge simultaneously at same corresponding blowing ratios of 0.5 and 1.0. However, due to concave surface effect, we choose two different blowing ratios for pressure side, M=1.0 and 2.0, with leading edge simultaneously at same corresponding blowing ratios of 1.0 and 2.0.

4.2 Wake Strength Determination

The unsteady wake increases the turbulence in the flow-field. It is also well established in literature that turbulence has a detrimental effect on film cooling effectiveness, by inducing mixing between the mainstream and coolant jet. It is important to select reasonable Strouhal number to simulate realistic unsteady wake under the modern engine conditions.

There are three Strouhal number such as S=0, 0.18, and 0.36 selected to see unsteady wake effect on film cooling effectiveness. There is no wake generator installed (the clean wind tunnel) for S=0 case. By increasing the rotation speed of the wake rods, Strouhal number can increase from 0 to 0.18 and from 0.18 to 0.36. Contour plots for showing Strouhal number effect are shown in Fig. 4.1 and 4.2. Carbon dioxide has been used to simulated higher density ratio (DR=1.5). The difference between these two figures is blowing ratio. Results of lower blowing ratio cases on both suction and pressure sides are presented in Fig. 4.1 and higher blowing ratio cases on both sides are shown in Fig. 4.2. On both the suction and pressure sides, the clean wind tunnel case shows a much thicker and longer film cooling effectiveness trace than the S=0.18 case. This implied no wake (S=0) situation providing higher film cooling effectiveness. Under unsteady wake condition, a very significant reduction in film cooling effectiveness due to the increased intermittency and turbulence in the free-stream is noticed, especially at lower blowing ratios. The effect of the unsteady wake on the pressure side is less pronounced. The relatively minor difference between the S=0.18 and S=0.36 on both the suction and pressure side cases indicates that, at high enough Strouhal numbers, film cooling effectiveness becomes relatively independent of Strouhal number. This possible reason is that because the turbulence level corresponding to the S=0.36 case is 15% and the S=0.18 case is 10%. This difference in turbulence level does not result in a large increase in the turbulent diffusivity, therefore, not weakening the film coolng jet.

The span-wise averaged film cooling effectiveness line plots (Fig. 4.3 and 4.4) more clearly and directly show that wake causes reduction in effectiveness. No wake

case (S=0) has much higher effectiveness (black line) than wake cases (S=0.18 and 0.36). Also, the results for S=0.18 and S=0.36 are close to each other due to similar turbulent diffusivity. The unsteady wake effect can be seen as Strouhal numbers is larger than 0.1. Therefore, it is reasonable to pick up S=0.12 to simulate effects of unsteady wake, and trailing edge coolant ejection in the following sections.

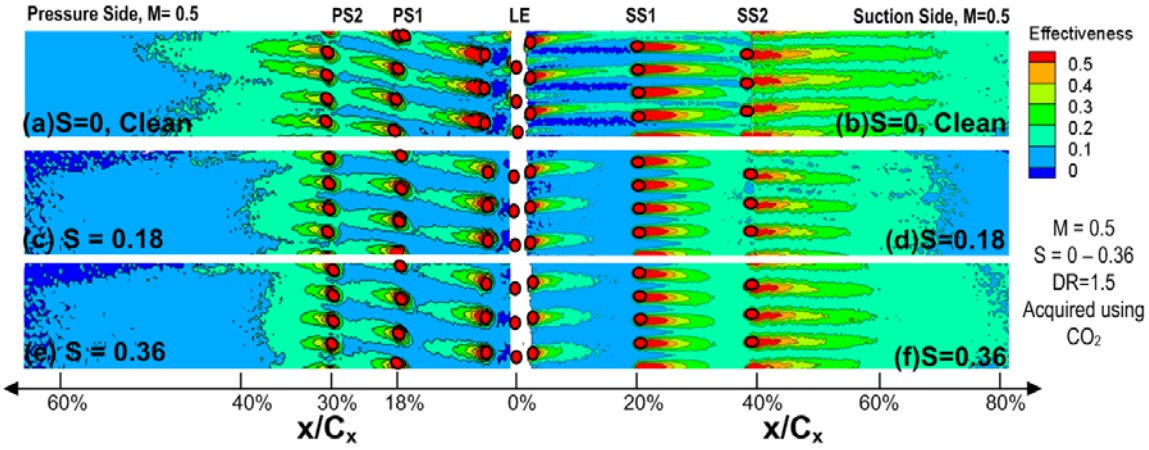

Fig. 4.1 Effect of Strouhal number on film cooling effectiveness, and M=0.5 on both suction side and pressure side for all cases

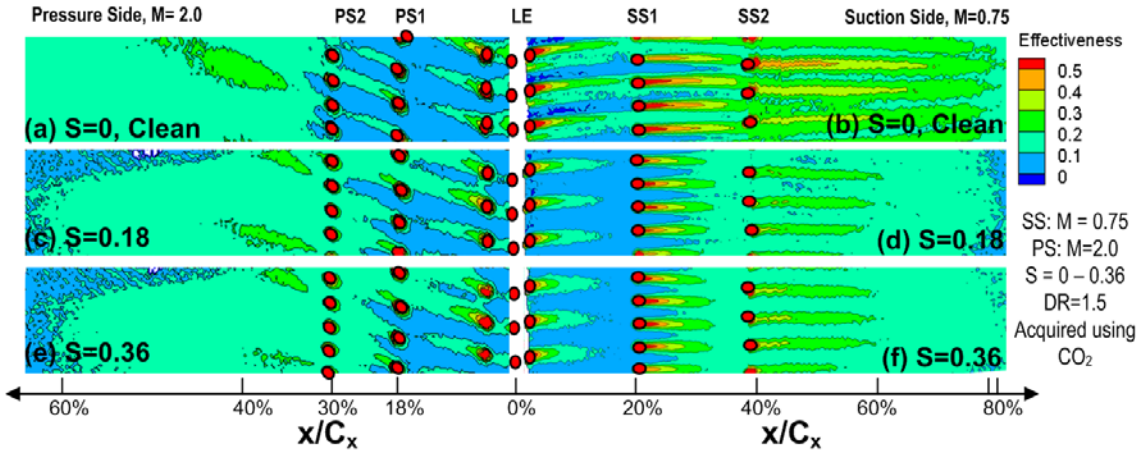

Fig. 4.2 Effect of Strouhal number on film cooling effectiveness, and M=0.75 on suction side and M=2.0 on pressure side for all cases

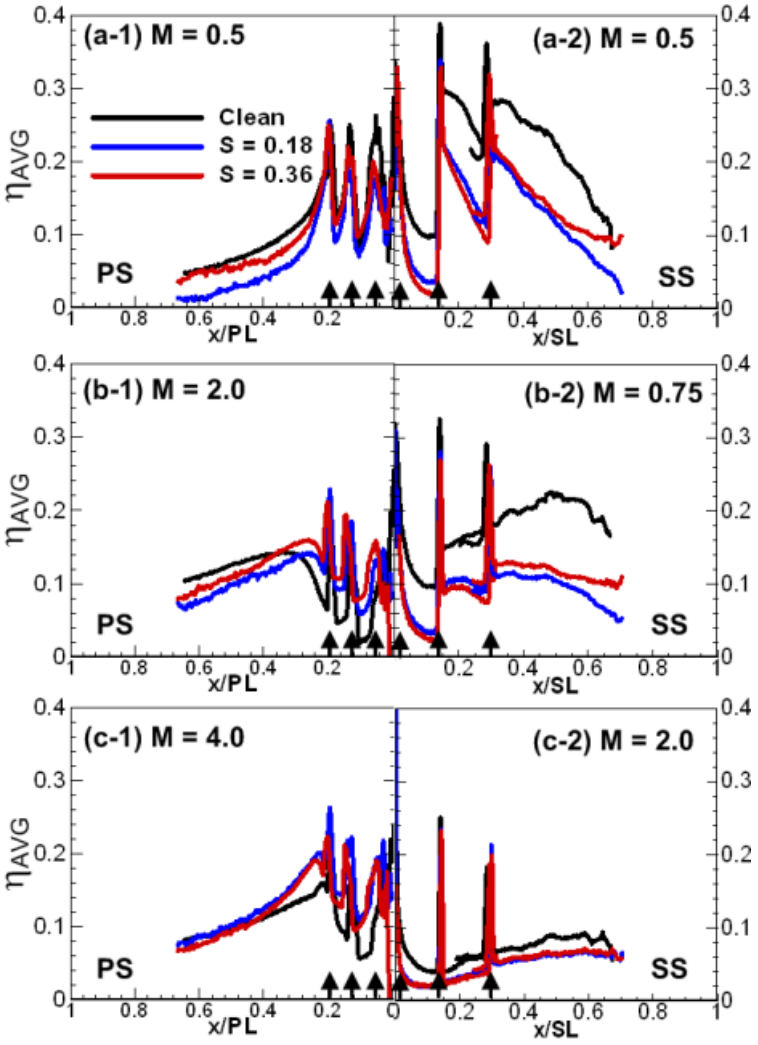

Fig. 4.3 Effect of Strouhal number on film cooling effectiveness for three separate blowing ratios at DR=1.0

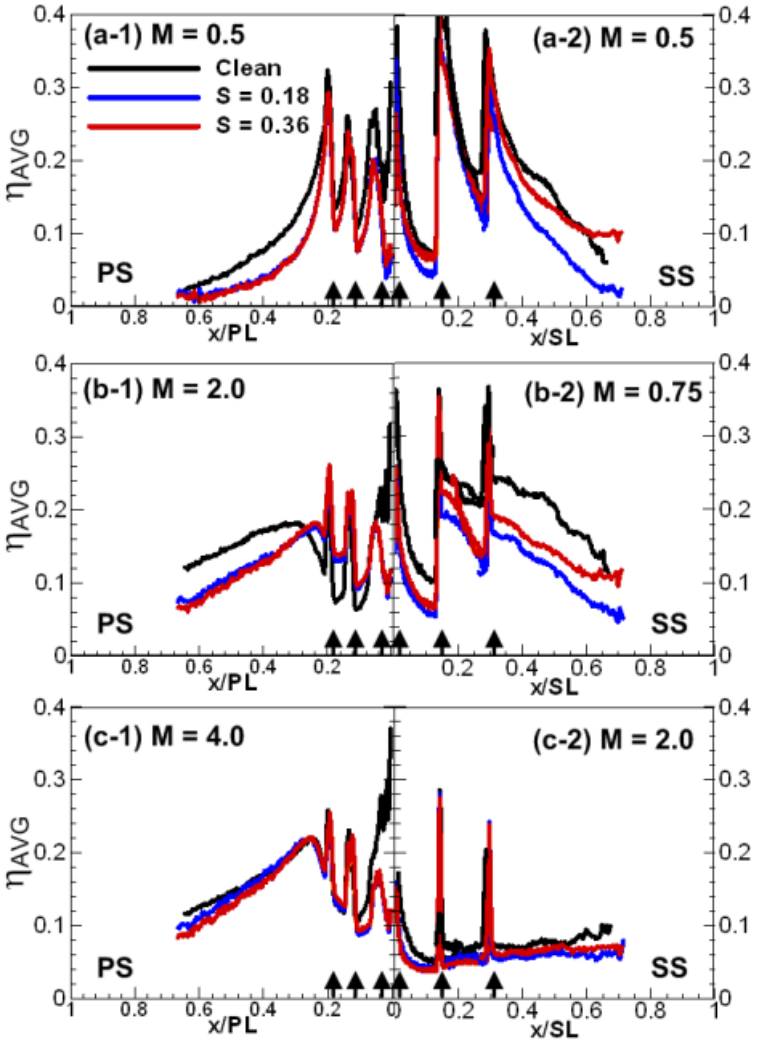

Fig. 4.4 Effect of Strouhal number on film cooling effectiveness for three separate blowing ratios at DR=1.5

4.3 Film Cooling Effectiveness Distribution

Film cooling effectiveness contour plots are shown in Fig. 4.5 and 4.6; span-wise averaged effectiveness line plots are shown in Fig 4.7, 4.8, and 4.9. There are three rows of shower-head radial- angled holes in the leading edge portion of blade, one row each on suction and pressure side, and center-row, or stagnation line of row, (Fig. 4.5, $x/C_x=0$) discharges coolant on to both pressure and suction side. Two rows of simple angle holes on suction side result in a coolant trace aligned with mainstream flow; two rows of compound angle holes on pressure side are result in an inclined coolant effectiveness trace.

4.4 Blowing Ratio Effect

General Trend: At lower blowing ratio (mass flux ratio), low percentage of coolant mixes with mainstream flow. Therefore, coolant remains near blade surface to protect it. As blowing ratio increases, coolant mixes more with mainstream flow, resulting in lower effectiveness. This result can be shown by comparing case 1 at lower blowing ratio (Fig. 4.5) and at higher blowing ratio (Fig. 4.6). The lower blowing ratio is more effective than the higher blowing ratio. The contour plots (Fig. 4.5 and 4.6) also show a coolant accumulation effect, especially at higher blowing ratios. Downstream film cooling rows (SS1, SS2, PS1, PS2) experience finite film cooling effectiveness in the spacing between two holes in the same row due to traces originating from upstream rows. Span-wise averaged effectiveness (Fig. 4.7) also shows the trend mentioned above. Higher blowing ratio (blue dashed line) shows lower effectiveness due to more mixing compared with lower blowing ratio (red dashed line) for both suction and pressure side.

However, higher blowing ratio (blue dashed line) has more coolant accumulation downstream (X/SL>0.3 and X/PL>0.2) than lower blowing ratio (red dashed line), resulting in higher effectiveness.

Suction side: Effectiveness at suction side is high due to convex surface. Best effectiveness is at blowing ratio 0.5. On increasing blowing ratio to 1.0, effectiveness reduces due to more mixing (film cooling lift-off).

Pressure side: Effectiveness levels on pressure side are low due to concave surface on which coolant is easier to mix with mainstream. The coolant jet reattaches with the blade surface at higher blowing ratios downstream of the second row (X/PL>0.2).

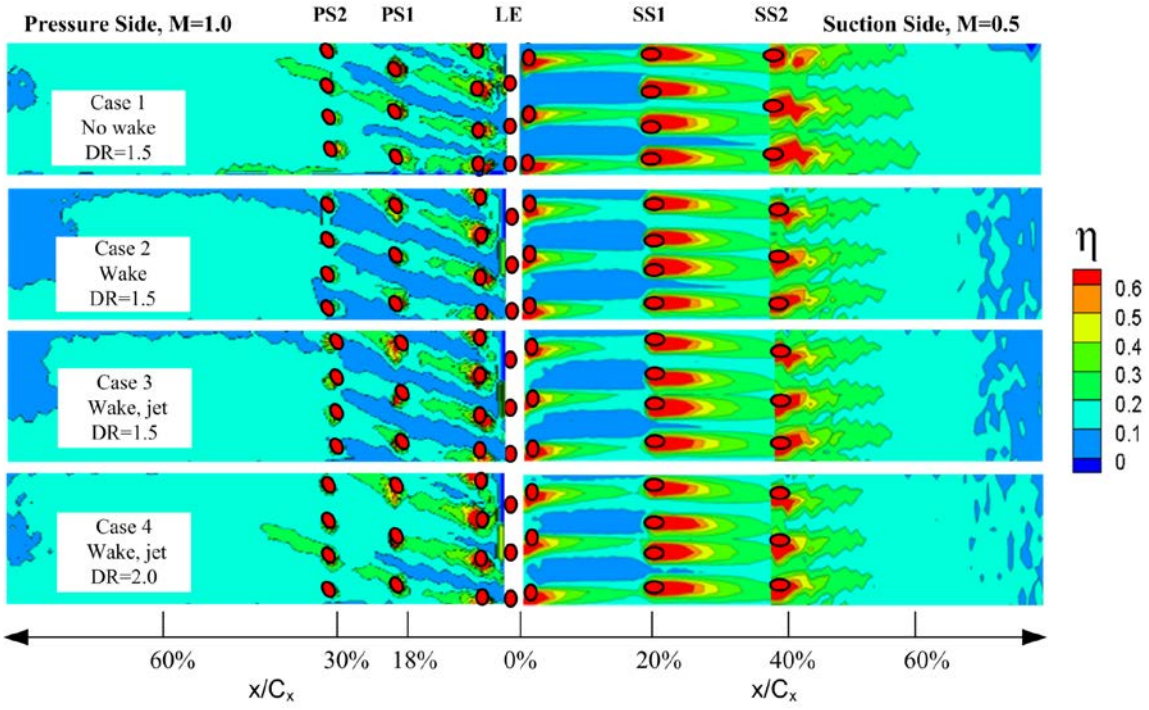

Fig. 4.5 Film cooling effectiveness contour plot for lower blowing ratio cases

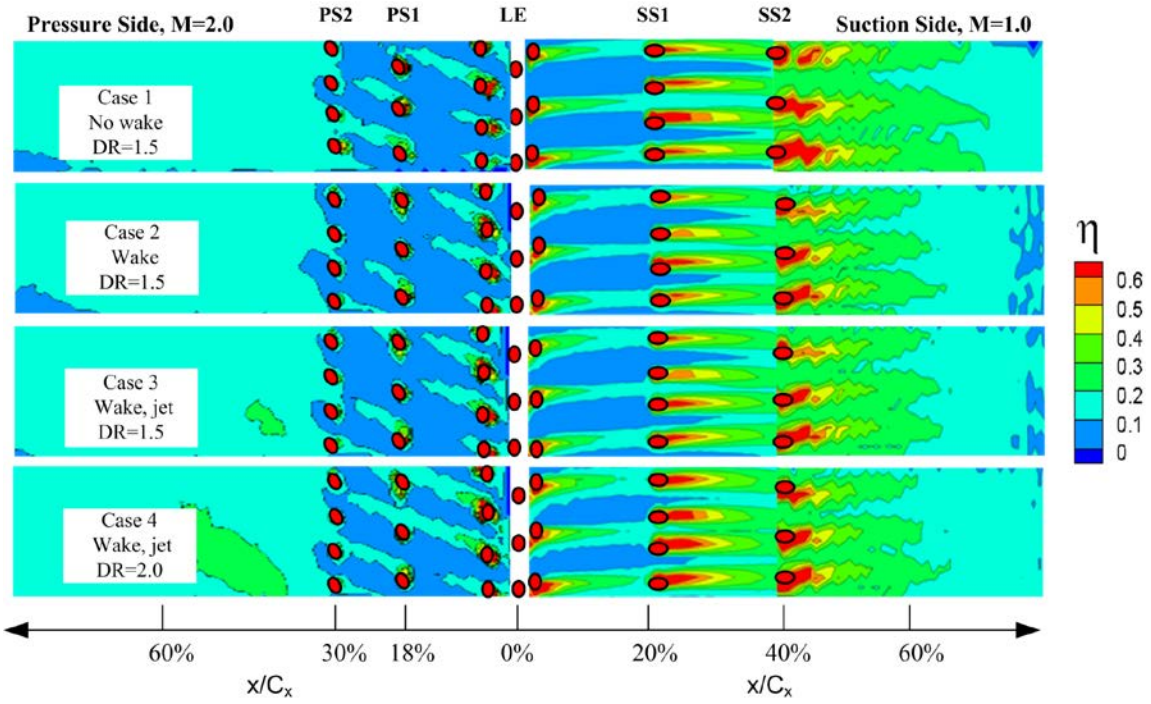

Fig. 4.6 Film cooling effectiveness contour plot for higher blowing ratio cases

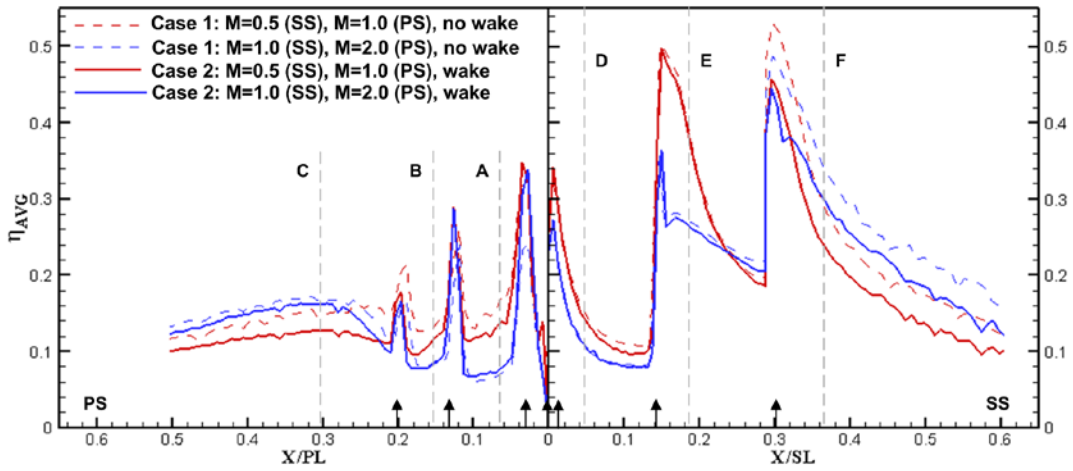

Fig. 4.7 Effect of unsteady wake on span-wise averaged effectiveness, DR=1.5

4.5 Unsteady Wake Effect

Intermittently passing wakes disturb the oncoming mainstream. This unsteady wake (S=0.12) increases the turbulence intensity up to 20% in the flow field, inducing mixing between mainstream and coolant jet. The wake condition (Fig. 4.5 and 4.6, case 2) shows overall lower level effectiveness for all blowing ratios in comparison with the no wake condition (Fig. 4.5 and 4.6, case 1). This implies wake has a detrimental effect on film cooling effectiveness due to extra mixing. The same physics is also demonstrated by the span-wise plots (Fig. 4.7). The wake condition (solid line) shows an overall lower effectiveness value compared with the no wake (dash line).

4.6 Trailing Edge Coolant Ejection Effect

Ejected coolant from upstream rotating rods is carried by unsteady wake and approached on blade surface. Unsteady wake brings more coolant from trailing edge ejection towards blade surface and has an overall small amount increase of effectiveness compared with only wake condition. Comparing conditions of wake (case 2) and wake with jet (case 3) in Fig. 4.5 or 4.6, wake with coolant ejection shows a slightly higher effectiveness level. This result is also presented in Fig 4.8: wake with trailing edge coolant ejection (solid line) shows a slightly higher span-wise averaged effectiveness than the only wake condition (dash line).

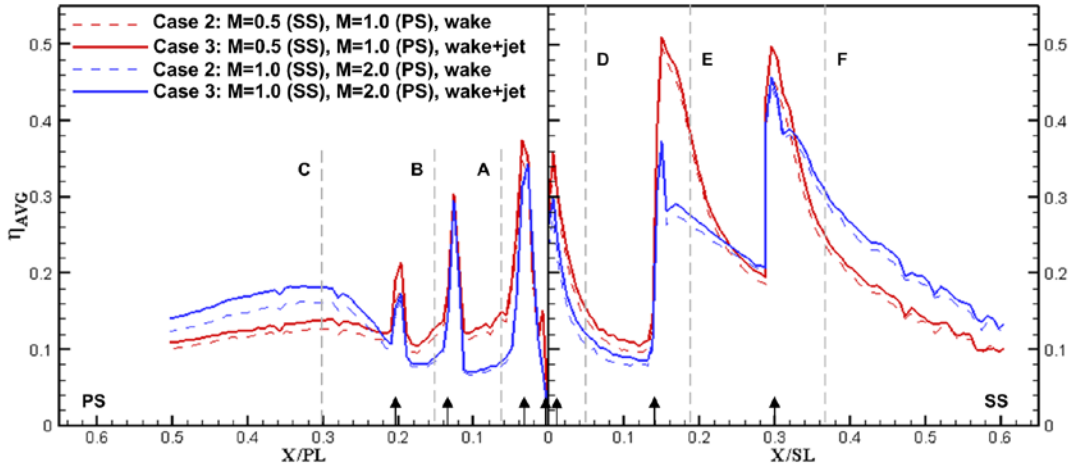

Fig.4.8 Effect of trailing edge coolant ejection on span-wise averaged effectiveness, DR=1.5

4.7 High Density Coolant Effect

Increase the coolant density reduces the velocity of coolant jet, momentum, and jet tendency to lift-off at a given blowing ratio. Density ratio 1.5 and 2.0 are typically encountered for advanced gas turbine engine rotor blade. These ratios are chosen for simulating combined wake and coolant ejection effect. By comparison of Fig. 4.5 case 3 (DR=1.5) and case 4 (DR=2.0), coolant ejection from rods and film coolant from blade at higher density shows higher effectiveness level, especially from leading edge to first row of holes on both side. As indicated in Fig. 4.9, all high blowing ratio cases (blue lines) display lower effectiveness level due to more coolant mixing with mainstream, but show more coolant accumulation downstream (X/SL>0.3 and X/PL>0.2). For all blowing ratios, increasing density ratio from 1.5 (case 3) to 2.0 (case 4) shows overall higher span-wise averaged effectiveness. This is due to two reasons: heavier density coolant to better protect blade surface, and heavier density coolant carried over to the blade surface by upstream wake flow. However, the location after second row on suction side (X/SL>0.3) shows a reverse trend, in which effectiveness of case 3 is larger than case 4. The possible reason is that heavier coolant at blowing ratio 1.0 does not have high enough momentum to carry coolant downstream. This trend also can be shown from case 4 in Fig. 4.5, and 4.6: the effectiveness traces after SS2 for case 4 are shorter than that for case 3.

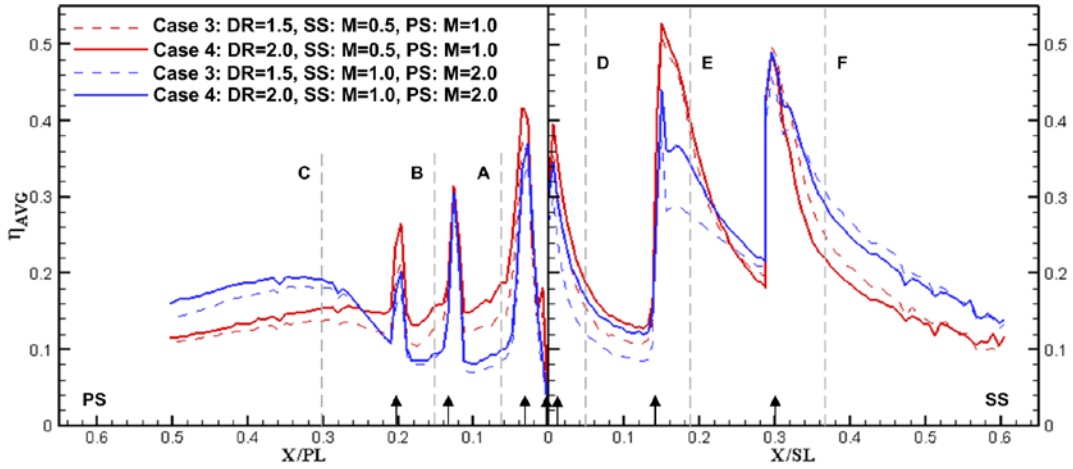

Fig. 4.9 Effect of density ratio on span-wise averaged effectiveness with trailing edge coolant ejection

4.8 Momentum Flux Ratio Effect

Ratio of coolant momentum flux to mainstream momentum flux is defined as momentum flux ratio (I). Momentum flux ratio is a combination of blowing ratio and density ratio. High blowing ratio with heavier density ratio gives similar momentum flux ratio as lower blowing ratio with lower density ratio. This implied film cooling effectiveness can be determined by momentum flux ratio instead of blowing ratio and density ratio. The purpose of presenting results by momentum flux ratio in the paper is to maximum the scale of span-wise averaged effectiveness with momentum flux ratio in selected locations. The momentum flux ratio (I) is defined as follow.

$$I = \frac{\rho_c V_c^{\,2}}{\rho_M V_M^{\,2}} = \frac{(\rho_c V_c / \rho_M V_M)^2}{(\rho_c / \rho_M)} = \frac{M^2}{DR} \tag{3}$$

We pick up six locations to discuss the momentum flux ratio effect as indicated in Figure 4.7, 4.8, or 4.9. Locations A, B, D, and E are right after showerhead or first row on the pressure or suction side. Locations C, and F are at downstream of the second row on pressure or suction side. The results can be seen from Fig. 4.10: effectiveness decreased with increasing momentum flux ratio due to mixing as shown in A, B, D, and E locations. Also, effectiveness further increases with trailing edge jet (case 3) and high coolant density with jet (case 4). However, downstream portion (location C and F) presents a reverse trend. Effectiveness increases with increasing momentum flux ratio due to more coolant accumulation.

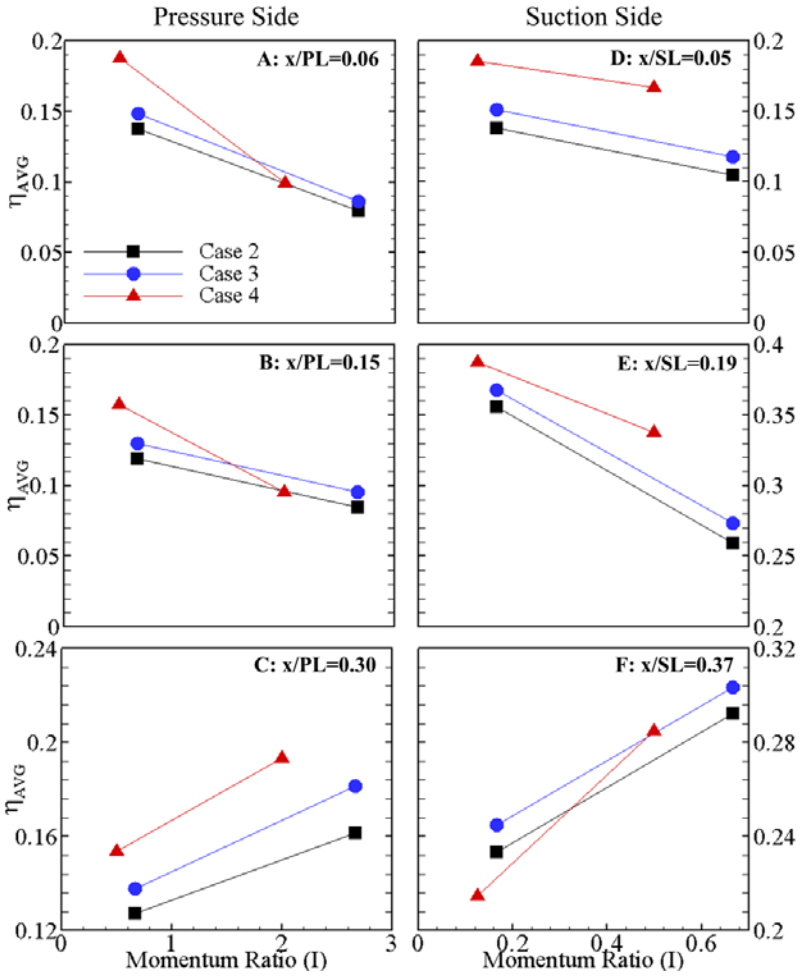

Fig. 4.10 Effect of momentum ratio on film cooling effectiveness at six selected location (A,B,C) for pressure side, (D,E,F) for suction side

5. LEADING EDGE FILM COOLING

5.1 Local Blowing Ratio Distribution

Film cooling effectiveness investigated at three blowing ratios is M= 0.5, 1.0, and 1.5 for all film cooling holes configurations, all density ratios. The blowing ratio is defined as $M=\rho_c V_c/\rho_m V_m$ indicating the coolant mass flux to the mainstream mass flux ratio. According to the above definition, the coolant mass flow rate for a given blowing ratio can be determined from equation as follows and supply to the coolant plenum of semi-cylinder (leading edge test model).

$$\dot{m}_c = nM\rho_m V_m(\pi d^2/4) \tag{4}$$

The pressure differential between the total pressure inside the leading edge semi-cylinder coolant plenum and external static pressure on the semi-cylinder surface is the actual driving force to let coolant eject out through the film cooling holes. As the pressure difference is higher, there is more coolant coming out through the holes. The real coolant velocity from the film cooling holes (V_c) is subject to both the span-wise variation in internal total pressure and circumferential variation in outer static pressure. To determine the real coolant mass flow rate through each hole, the discharge coefficient (C_D) is calculated at the first step based on given total coolant mass flow rate ($\dot{m}_c$), and related pressure (P_T, total pressure inside plenum; P, outer pressure on semi-cylinder surface) as the following equation.

$$\dot{m}_c = \sum_{i=1}^{n} C_D \cdot \rho_c \cdot (\pi d^2/4) \cdot \sqrt{2(P_T - P)/\rho_c} \tag{5}$$

There are three pressure taps placed along the middle five-hole along span-wise direction to measure the total pressure inside the coolant plenum. The result shows that uniform pressure inside plenum so that the effect of span-wise variation in internal pressure on coolant ejection flow can be eliminated in the area of interest. Pressure sensitive paint has been used to measure the outer pressure on the semi-cylinder surface. A constant discharge coefficient C_D is assumed for all the holes at a given blowing ratio. This assumption is based on that the deviation in the discharge coefficients from hole to hole is not significant, and using an average value without introducing significant error. The discharge coefficient C_D can be determined by solving equation (4) and (5) for a given blowing ratio. The coolant velocity from the holes in a row can be calculated by the following equation once obtaining discharge coefficient (C_D).

$$V_{c,local} = C_D \cdot \sqrt{2(P_T - P)/\rho_c} \tag{6}$$

Because the higher outer pressure prohibits the coolant ejecting through film holes from the stagnation row, coolant mass flow rate at stagnation row of holes is lower compared with film holes at downstream rows. The outer static pressure is relatively lower for rows of holes at downstream, and more coolant comes out from these film holes. To better understand the effect of blowing ratio, the local blowing ratio at 15 deg, 30 deg, and 45 deg along leading edge curve surface has been examined. The local blowing ratio is defined as $M_{local} = \rho_c V_{c,local} / \rho_m V_{m,local}$. Local mainstream velocity $(V_{m,local})$ is determined from the local static pressure on the leading edge surface by pressure sensitive paint. Because the local mainstream velocity is zero along stagnation row, the free stream velocity is used to normalize the coolant velocity for the stagnation

row. Although a different denominator is used for the stagnation row, the same notation M_{local} is used to present the local blowing ratios. Because the local blowing ratio distribution for cylindrical hole is similar to that of shaped hole, only results of cylindrical hole is presented in Fig. 5.1 to show local blowing ratio. The higher local mainstream velocity $(V_{m,local})$ results in a lower local blowing ratio (M_{local}) in the downstream rows according to the definition in local blowing ratio formula. For the seven-row design, local blowing ratios for the stagnation row (normalized with $V_{m,local}$) is lowest and 15 deg row is significantly higher than the other two rows (30 deg, and 45 deg). For the three-row design, stagnation row shows local blowing ratio lower than that of 30 deg row.

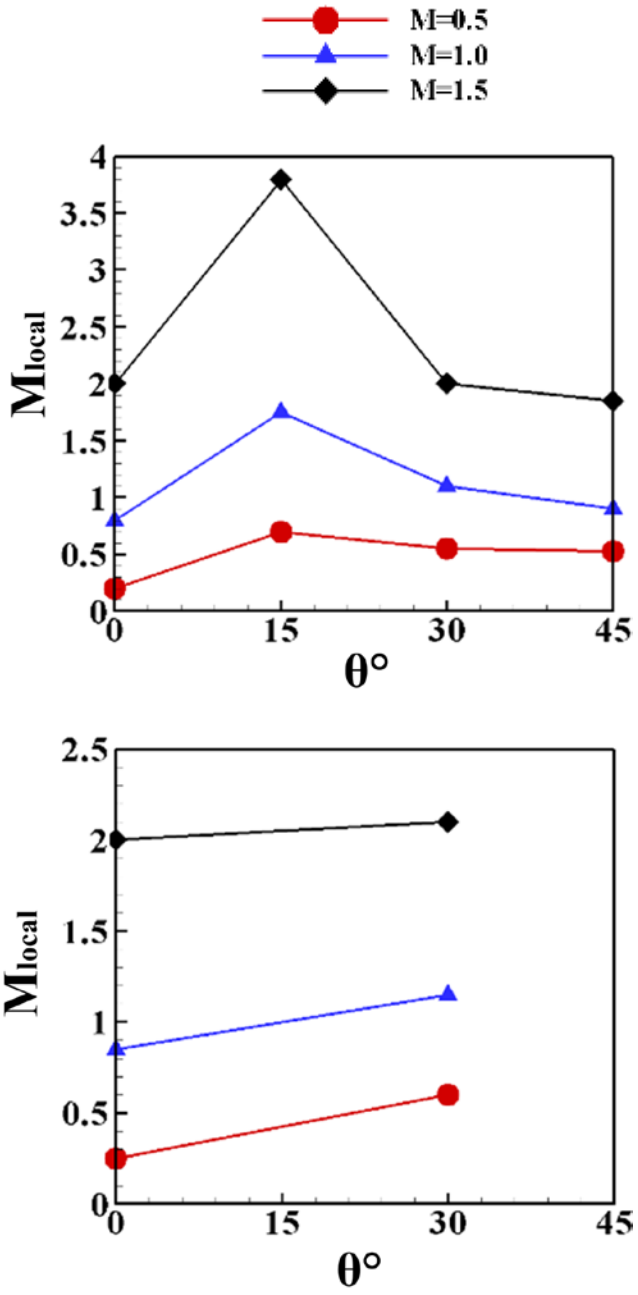

Fig. 5.1 Schematic of local coolant mass flow rate distribution and local blowing ratio: seven-row design (upper) and three-row design (lower)

5.2 Film Cooling Effectiveness Distribution for Seven-Row Design

Coolant of air or foreign gas is from rotor meters and enters the plenum of leading edge semi-cylinder test section. Pressure differential between the internal coolant plenum total pressure and external static pressure is the driving force to make air or foreign gas ejecting through the film cooling holes. As the pressure differential is higher, there is more coolant ejects from the film cooling holes. Along the curved surface of leading edge model, the highest static pressure is at the stagnation line (row). The surface static pressure gradually decreases from stagnation row to downstream. This indicates driving force gradually increases from stagnation row to downstream and the least amount of coolant ejection is right at the stagnation row. This non-uniform coolant ejection will affect the film cooling effectiveness distributions on the leading edge surface compared with flat plate film cooling without any curvature effect. The local coolant mass flow rate distributions can be seen from Fig. 5.2.

For seven-row design, the film-cooling effectiveness distribution (contour plots) along the leading edge models is shown in Fig. 5.3 for four hole configurations such as radial angle cylindrical holes, compound angle cylindrical holes, radial angle shaped holes, and compound angle shaped holes. There are forty night film cooling holes in total to eject coolant to protect leading edge surface for this seven-row design used to simulate vane. In this set of figures, blowing ratio ranges from M=0.5, 1.0, and 1.5. About density ratio, there are only DR=1.0 and 1.5 considered. The x axis is s/d along mainstream direction and the y axis is z/d along the span-wise or radial direction.

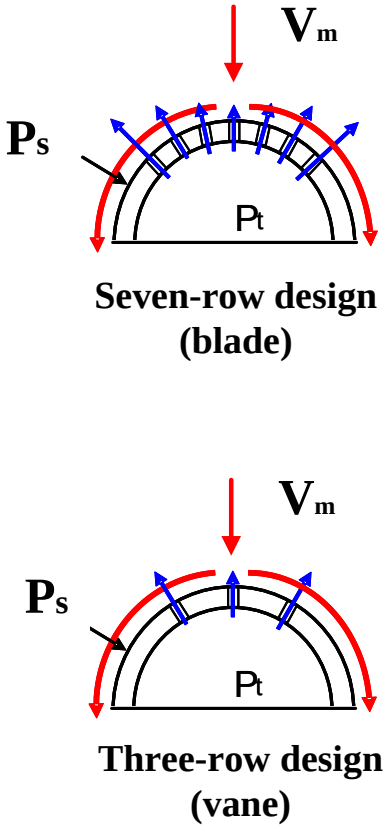

Fig. 5.2 Schematic of local coolant mass flow rate distribution along semi-cylinder

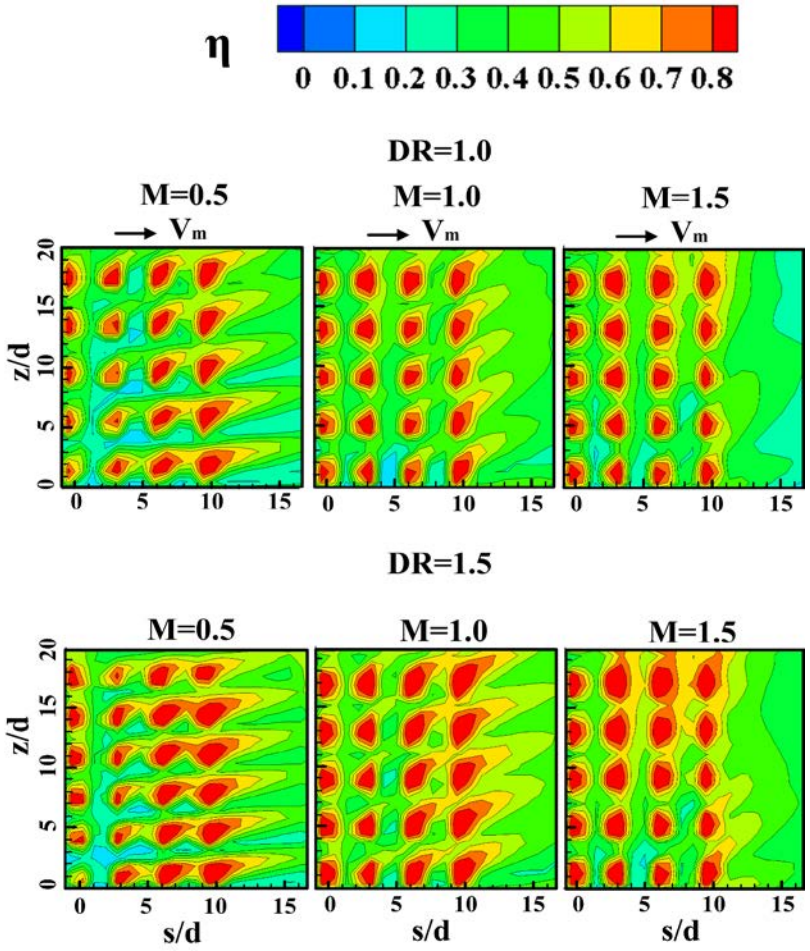

(a) Radial angle cylindrical holes

Fig. 5.3 Film cooling effectiveness distribution for seven-row design

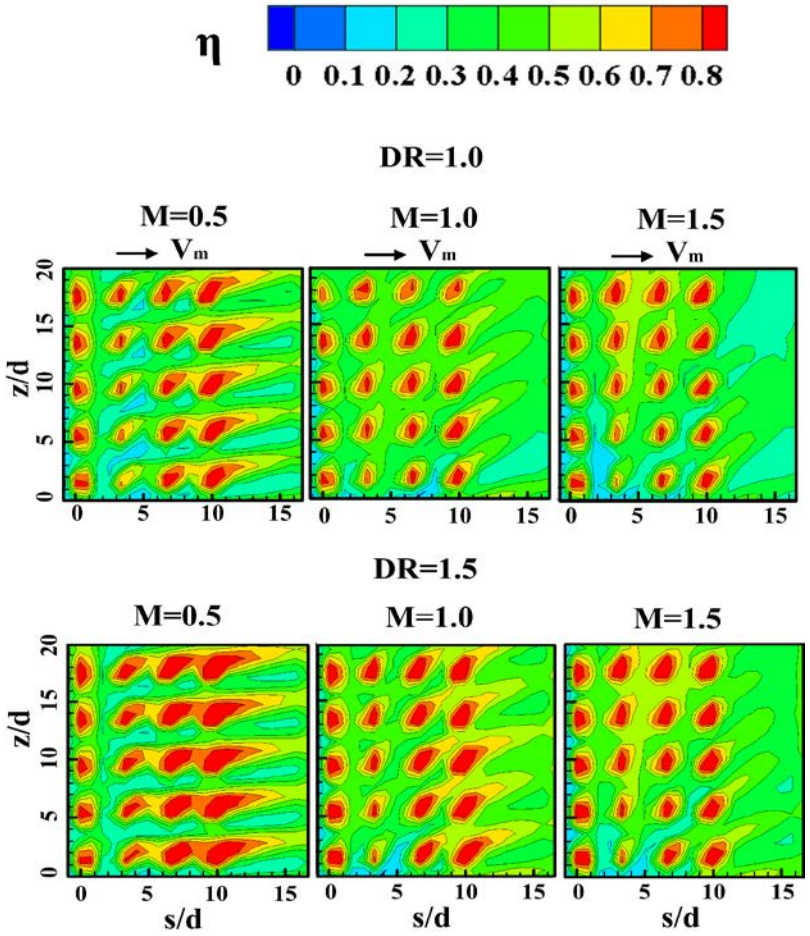

(b) Compound angle cylindrical holes

Fig. 5.3 Continued

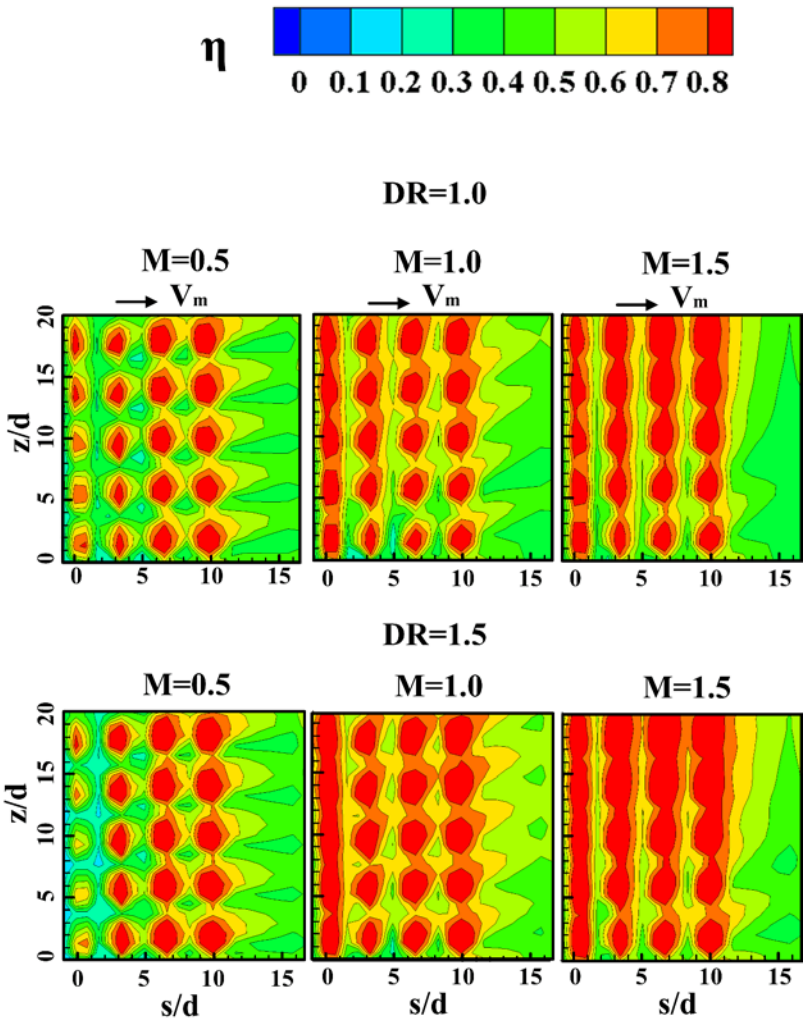

(c) Radial angle shaped holes

Fig. 5.3 Continued

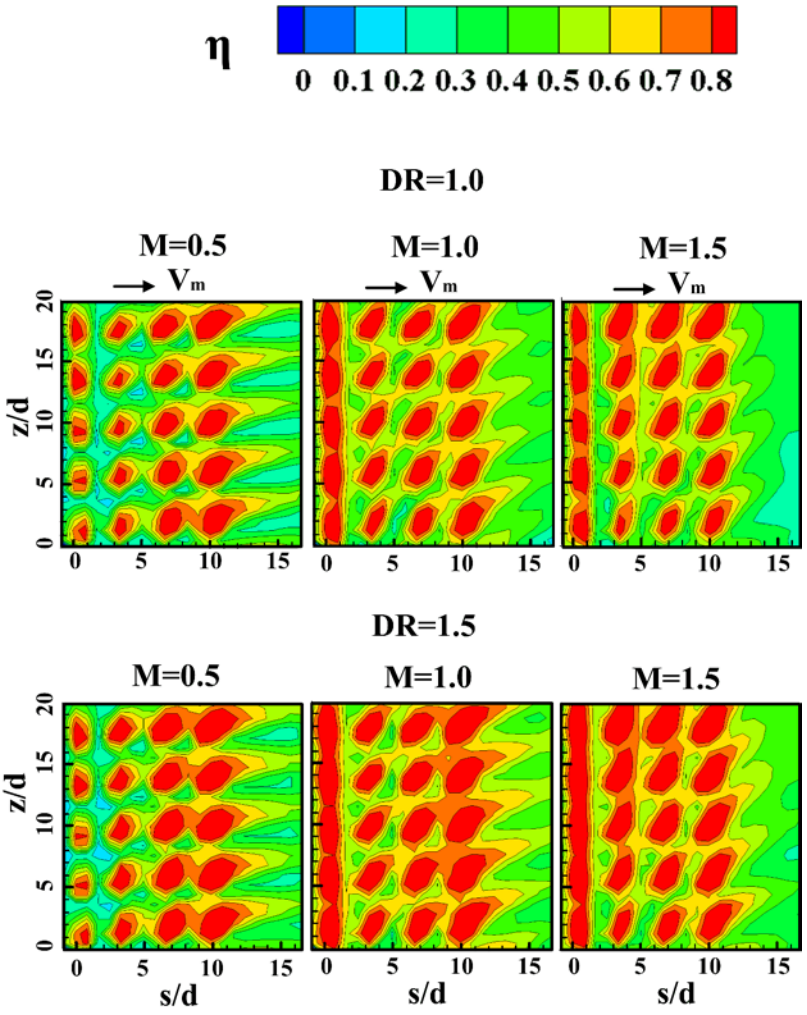

(d) Compound angle shaped holes

Fig. 5.3 Continued

Stagnation line (row) locates at s/d = 0 and follows by first row at s/d ≈ 3, second row at s/d ≈ 6, and third row at s/d ≈ 9. Data presented are only up to s/d =16.5.

Even the film cooling hole configurations are different, there are some common features can be observed along stagnation row (s/d=0) for seven-row design. The overall

trend near the stagnation region is that the mainstream momentum is small for stagnation region and jet interaction with mainstream is weak for all hole configurations. Because the mainstream momentum is small near the stagnation row, this low momentum results in coolant jets from stagnation row easier flowing in the radial direction without being deflected. For example, at lowest average blowing ratio M=0.5, the pressure inside the semi-cylinder test section is low. In the stagnation region, the high outer pressure prohibits coolant ejecting from these stagnation holes. More coolant is directed to the downstream holes. For radial angle cylindrical holes, smaller amount of coolant can eject from film holes for lower blowing ratio M=0.5 case at stagnation row, especially for heavier density coolant (DR=1.5) with lower momentum barely coming out. As increasing blowing ratio to M=1.0 and 1.5 for both density ratio cases (DR=1.0, 1.5), coolant comes out smoothly through the holes of stagnation row. These higher blowing ratio cases have more coolant accumulation in the radial direction at the stagnation row. As for next hole configuration: compound angle cylindrical holes are with an incline angle to the mainstream direction. At stagnation row, lower coolant coverage for this configuration by comparing with radial angle cylindrical holes, particularly for lower density ratio cases (DR=1.0, M=0.5 to 1.5). As density ratio increases to DR=1.5, this situation has been improved by comparison with DR=1.0 cases. In sum, first film hole configuration provides better film cooling effectiveness at stagnation row than the second configuration. The third and forth hole configurations are shaped hole but with different incline angle (radial and compound angle). Shaped hole is with expanded area at the exit of the hole, and this area expansion helps reduce momentum of the coolant jet.

Therefore, lower blowing ratio shaped hole cases (M=0.5, DR=1.0 and 1.5) show lower film cooling effectiveness at stagnation row, As increasing blowing ratio to the higher values (M=1.0 and 1.5) for density ratios of 1.0 and 1.5, coolant jets are with sufficient momentum to eject from film holes and even accumulate along radial direction at stagnation row as shown in contour plots (Fig. 5.3 (c), and (d)).

The film cooling effectiveness distributions of downstream three rows located at s/d ≈ 3, 6, and 9 (seven-row design) are as follows. The general trend is that further downstream rows with more coolant coverage no matter near the holes or between two adjacent film rows due to two reasons. First reason is that coolant accumulation from stagnation row to downstream row. Another reason is that further downstream row with lower pressure difference between inner plenum and external static pressure, and this makes coolant easier ejecting from downstream rows. Take first hole configuration for example to explain the variations of film cooling effectiveness as increasing blowing ratio from M=0.5 to 1.5. As shown in Fig. 5.3 (a) radial angle cylindrical holes, lower blowing ratio and lower density ratio (M=0.5, DR=1.0) case, coolant traces are deflected from radial direction (z) of film holes into mainstream direction (s). This indicated coolant jets of lowing blowing ratio are too weak and easily affects by mainstream flow. As blowing ratio increases to 1.0, coolant traces are in the direction between radial and mainstream direction and show better lateral coolant spread and coverage, especially good at downstream portion. As increasing blowing ratio to M=1.5 (i.e. jet momentum increases), the deflection decreases. This means the jets are less deflected by mainstream at higher blowing ratio. As shown in the contour plot, coolant jets of M=1.5 mostly flow

toward radial direction directly at hole location, and less coolant spread out in lateral direction. Therefore, the overall film cooling effectiveness at higher blowing ratio (M=1.5) is not as good as medium blowing ratio (M=1.0) case, particularly at downstream portion. The higher density ratio cases of first film hole configuration are presented in Fig. 5.3 (a) DR=1.5, M=0.5 to 1.5. As density ratio increases from DR=1 to DR=1.5, the trend of film cooling trance is very similar to that of density ratio one. The only difference is that film cooling effectiveness traces become wider and longer for heavier density coolant (DR=1.5, M=0.5 to 1.5) cases. This indicates higher density coolant has lower momentum, larger tendency to adhere to leading edge surface for protection, resulting in higher film cooling effectiveness. The same hole shape: cylindrical hole but change hole's orientation from radial angle to compound angel (hole configuration 2) to see whether compound angle holes help coolant spread laterally. For lower density ratio cases (Fig. 5.3 (b), DR=1.0), lower blowing ratio (M=0.5) coolant trace still be deflected to mainstream direction even already with compound angle. As increasing blowing ratio to M=1.0 and 1.5, film cooling effectiveness decreases for both right at film cooling holes and between two adjacent rows of holes. This film cooling effectiveness reduction can be explained as coolant mixed more with mainstream for compound angle holes at higher blowing ratios. Increasing density ratio from DR=1.0 to DR=1.5, the film cooling effectiveness level increases, heavier density coolant with better protection. By comparisons of results of radial angle cylindrical holes (Fig. 5.3 (a)) with compound angle cylindrical holes (Fig. 5.3 (b)), contour plots of lower blowing ratio M=0.5 case shows that the compound angle holes has higher effectiveness

than the radial angle holes at downstream portion. However, the results become different for the cases of higher blowing ratios M=1.0 and 1.5, the compound angles cylindrical holes shows lower effectiveness than radial angle cylindrical holes. This is possibility due to less coolant jet can spread-out along curve surface for compound angle hole at higher blowing ratios. For the compound angle cylindrical holes, the compound angles of film cooling holes to from stagnation row to downstream rows reduce so that the coolant jets become relatively less deflected from stagnation to downstream rows. Comparing first and second hole configurations, the overall coolant traces become narrower but longer instead of spread-out for compound angle cylindrical holes due to coolant less spread out.

The shaped holes film cooling effectiveness distributions of downstream three rows located at s/d ≈ 3, 6, and 9 (seven-row design) are in the following discussions. Laidback fan-shaped holes are used there as radial angle shaped holes (Fig. 5.3 (c)), and compound angle shaped holes (Fig. 5.3 (d)). The meter parts (holes' inlet) for cylindrical and shaped holes are the same (with diameter 0.3715 cm). Because of the lateral expansion for shaped holes configuration at holes' exit, the area ratio is equal to two between the cross section at the holes' exit and holes' inlet (metering part, cylindrical holes). The momentum at the shaped holes exit is lower than at cylindrical holes exit due to larger exit hole area. This represents that shaped holes provide lower momentum coolant with larger tendency to adhere to the leading edge surface and result in higher film cooling effectiveness. This can be seen by comparing all contour plots of cylindrical holes (Fig. 5.3 (a) and (b)) with that of shaped holes (Fig. 5.3 (c) and (d)). The shaped

holes cases are with wider effectiveness traces and overall higher film cooling effectiveness. For radial angle shaped hole at lower blowing ratio M=0.5 (Fig. 5.3 (c) DR=1.0), film cooling traces are easier deflected by mainstream into mainstream direction due to lower coolant jet momentum. As blowing ratio is up to M=1.0, coolant jet becomes partially defected by mainstream. At higher blowing ratio M=1.5, coolant jet is strong enough (does not affect by mainstream) and keeps in the radial direction (span-wise direction), showing by larger film cooling effectiveness in span-wise direction. Increasing density ratio to DR=1.5 (heavier coolant), coolant jets have lower momentum and adhere more to leading edge surface. Therefore, the film cooling effectiveness is with an overall increase. Contour plots for compound angle shaped holes are shown in Fig. 5.3 (d). From film cooling effectiveness traces for compound angle holes, traces are along the compound angle holes' direction for blowing ratio M=1.0 and 1.5 for both density ratios (DR=1.0 and 1.5). As for lower blowing ratio (M=0.5) case, film cooling effectiveness traces are slightly deflected to mainstream direction.

Coolant downstream accumulation shows from contour plots from s/d=9 to s/d=16.5 on Fig. 5.3. The general trend in the downstream region of leading edge surface is that the mainstream momentum increases. Therefore, the interaction or mixing between the coolant jet and mainstream enhances. In other words, the higher the jet momentum, the stronger the interaction or mixing with mainstream happens. From configuration (a) contour plot downstream portion, film coolant effectiveness traces still adhere to leading edge surface for lower blowing ratio M=0.5 (either DR=1.0 or 1.5) cases. However, the film cooling traces already mix together for higher blowing ratio

M=1.5 cases no matter density ratio 1.0 or 1.5 and result in reduced effectiveness. In a word, blowing ratio M=0.5 and 1.0 shows better film cooling effectiveness than M=1.5 at the downstream portion for both density ratios for first hole configuration. As for second configuration, the downstream effectiveness trend for lower blowing ratio (M=0.5) is similar to that of configuration 1: coolant trace shows that coolant still adheres to leading edge surface for both density ratios. As increasing blowing ratio, coolant jets mix together with mainstream and also reattach happen for medium and higher blowing ratios of lower density ratio (DR=1) cases. However, increasing density ratio with heavier coolant helps improve coolant lift-off indicating by longer film cooling effectiveness traces, especially at higher blowing ratio (M=1.5). For configuration (c) and (d), the trend of film cooling effectiveness traces are close to that of configuration (a) and (b). At DR=1.0, higher blowing ratio case has lower film cooling effectiveness than lower and medium blowing ratio cases due to film coolant mix more with mainstream at leading edge downstream portion. When density ratio increases to 1.5, heavier density coolant shows wider film coolant coverage and more coolant accumulation for all blowing ratios and results in higher downstream film cooling effectiveness.

5.3 Film Cooling Effectiveness Distribution for Three-Row Design

Three-row design with fewer film cooling holes is suitable to simulate film cooling of blade. There are twenty one film cooling holes in total to eject coolant out to protect leading edge for this design. The only difference between seven-row design and three-row design is the total holes' number. The hole configurations of three-row design is the same as the seven-row design such as radial angle cylindrical holes, compound angle cylindrical holes, radial angle shaped holes, and compound angle shaped holes. The blowing ratio selection also keeps the same as 0.5, 1.0, and 1.5. The density ratio except for 1.0 and 1.5, we extend to higher density ratio 2.0 to simulate realistic engine conditions. The x axis is s/d along mainstream direction and the y axis is z/d along the span-wise or radial direction. Stagnation line (row) locates at s/d = 0 and only follows by one row at s/d ≈ 6. Data presented are up to s/d =16.5. The film cooling effectiveness distributions for three-row design are shown Fig. 5.4. At the beginning, the discussion focus on film cooling along stagnation row (s/d=0) for all hole configurations. The mainstream momentum at stagnation region is smaller compared with first film row downstream the leading edge model. Coolant at stagnation row does not be easily deflected by mainstream and it still comes out in the radial direction. Another problem of stagnation row is highest static pressure at this row, and coolant becomes harder to eject out because coolant jet does not have high enough momentum. For the cylindrical hole such as first hole configuration: radial angle cylindrical holes and second hole configuration: compound angle cylindrical holes, coolant still can not come out from stagnation row of holes for all blowing ratios (M=0.5, 1.0, and 1.5) and density ratios

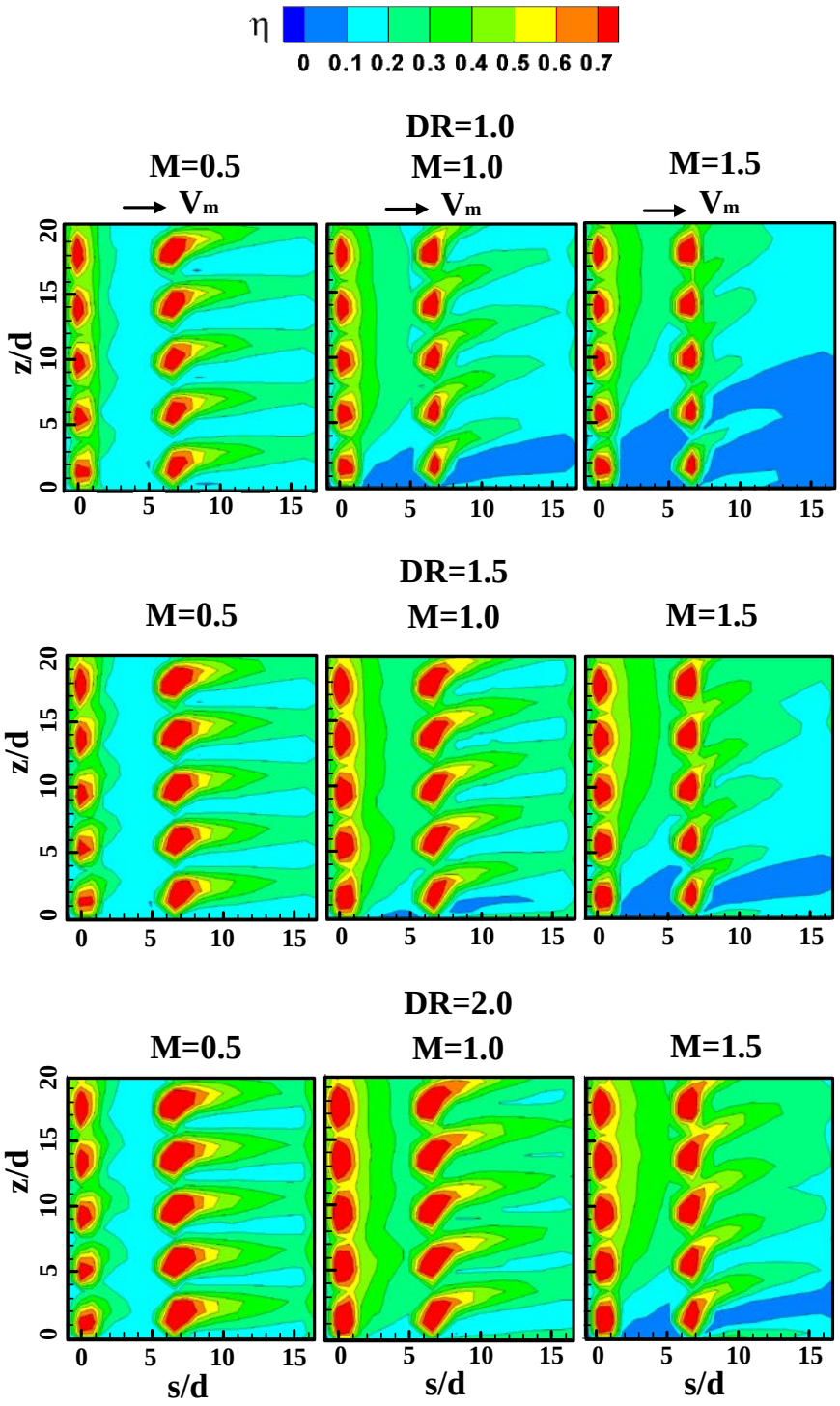

(a) Radial angle cylindrical holes

Fig. 5.4 Film cooling effectiveness distribution for three-row design

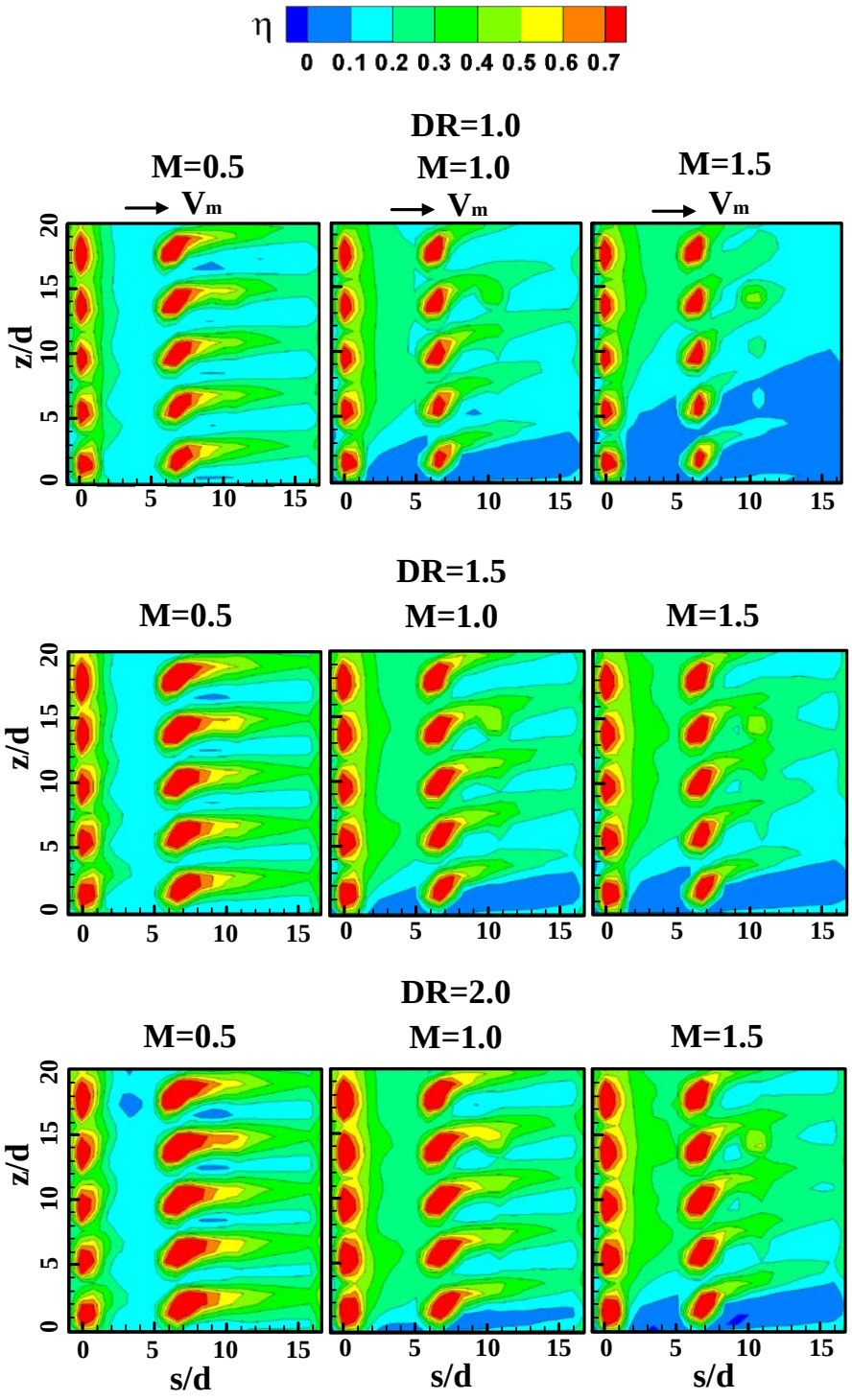

(b) Compound angle cylindrical holes

Fig. 5.4 Continued

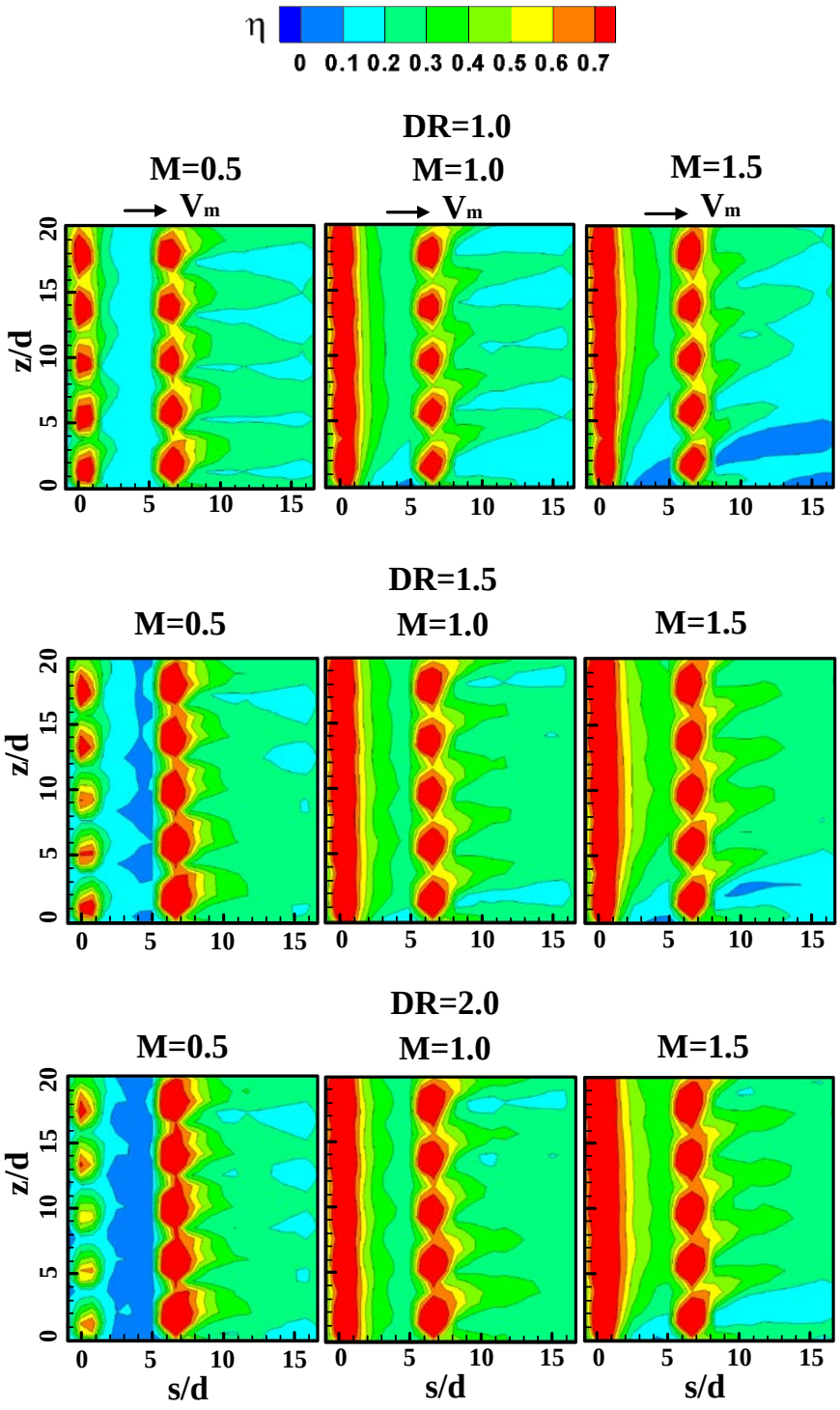

(c) Radial angle shaped holes

Fig. 5.4 Continued

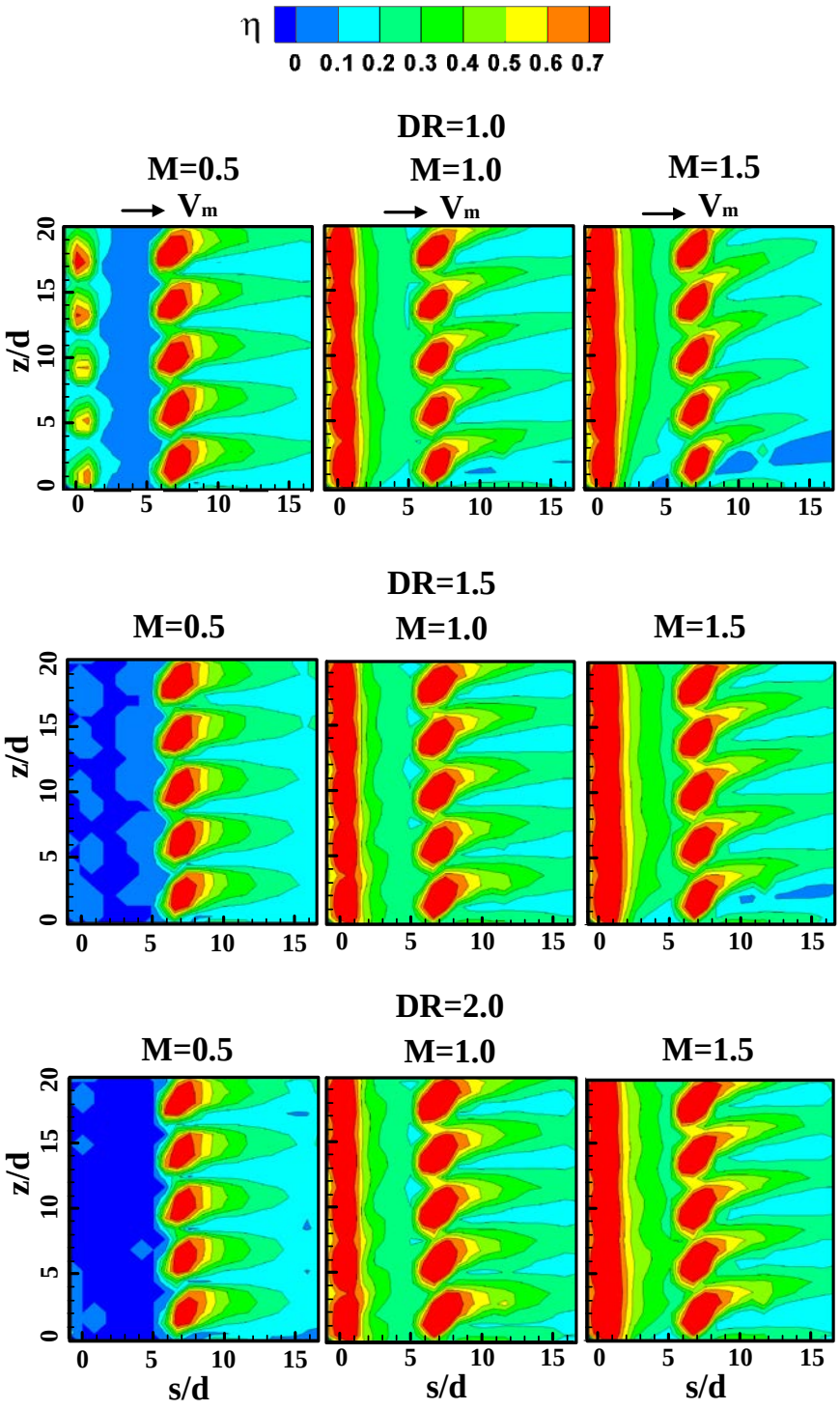

(d) Compound angle shaped holes

Fig. 5.4 Continued

(DR=1.0, 1.5, and 2.0) as shown in Fig 5.4 (a) and (b). Also, coolant jets at stagnation line have lower momentum and do not affect by mainstream flow. Therefore, all the film cooling traces are in the radial direction. For the shaped holes configuration, third hole configuration is the radial angle shaped holes (Fig 5.4 (c)) and forth hole configuration is the compound angle shaped holes (Fig. 5.4(d)). For both these two shaped holes configurations all density ratios (DR=1.0, 1.5, and 2.0), no matter medium blowing ratio (M=1.0) or higher blowing ratio (M=1.5) cases, coolant already has sufficient jet momentum to eject out from shaped film holes. Furthermore, coolant accumulate along the stagnation line (from z/d =0 to 20) in the radial direction. However, coolant has difficulty to come out from shaped film holes particularly at lower blowing ratio (M=0.5). The reason is that shaped hole itself with wider hole cross section area at hole exit, resulting in further lower film coolant jet momentum along stagnation row. For radial angle shaped hole lower blowing ratio (M=0.5), DR=1.0 case, film cooling traces along stagnation line are acceptable. Once increasing density ratio to DR=1.5 and 2.0 with a fixed blowing ratio M=0.5, coolant becomes heavier and has even lower coolant jet momentum. From contour plots (Fig. 5.4 (c)) present that coolant jets barely eject out from stagnation row of film holes and coolant even do not have enough momentum to go further downstream to the fist film cooling row shown in coolant traces. This situation is even worst for last film hole configuration: compound angle shaped holes (Fig. 5.4 (d)). For lower blowing ratio (M=0.5) with density ratio DR=1 case, coolant only slightly comes out from film hole and contains insufficient momentum to go further downstream. The worst two compound angle cases along stagnation line are lower blowing ratio

(M=0.5) with heavier density coolant (DR=1.5 and 2.0). The film cooling effectiveness value is in the range of 0 to 0.1. This indicates coolant cannot come out to protect leading edge surface due to heavier density coolant with lower jet momentum and compound angle itself.

There is only one row located at s/d ≈ 6 behind stagnation row for three-row design shown in contour plots for all hole configurations. The downstream portion is from s/d ≈ 6 to s/d=16.5. For the first configuration: radial angle cylindrical holes with density ratio DR=1.0, coolant traces are deflected from original holes' direction (radial direction) to mainstream direction for all blowing ratios (M=0.5 to 1.5). For lower blowing ratio, film coolant traces has better film cooling coverage, better protection. As increasing blowing ratio to M=1.0, lower z/d area (below z/d=4), coolant does not cover leading edge surface well no matter between two adjacent rows or downstream the first row. Further increasing blowing ratio to M=1.5, film coolant covers leading edge surface badly below the area z/d<10. When density ratio increase to DR=1.5 and 2.0, heavier density coolant adheres to leading edge surface and provides wider film coolant protection. This can been seen from contour plots (Fig. 5.4(a)) that the coolant uncover area reduces as increasing density ratio from 1.0 to 2.0 both between two adjacent rows and downstream first row. For second film hole configuration: compound angle cylindrical holes, compound angle hole's orientation is forty five degree away from radial direction. However, due to lower blowing ratio (M=0.5) with lower momentum, coolant jets are deflected to close to mainstream direction. For blowing ratio M=1.0 and 1.5 cases with higher momentum, coolant traces are in the compound angle direction.

Coolant traces for compound angle holes seem to interact more with mainstream compared with radial angle holes. This can be seen from contour plots: traces of compound angle holes do not flow downstream smoothly. As for increasing density ratio to 1.5 and 2.0 for all blowing ratios, the same conclusion as radial angle cylindrical holes can be made, coolant uncover area reducing indicating better film coolant protection. The results of shaped hole configurations can be seen from Fig. 5.4(c) and (d). No matter radial angle shaped holes or compound angle shaped holes, the coolant comes out smoothly from first row for all blowing ratios (M=0.5, 1.0, and 1.5) and density ratios (DR=1.0, 1.5, and 2.0). Coolant traces of all cases indicate film coolant deflected by mainstream into mainstream direction. About hole configuration 3 Fig. 5.4(c): radial angle shaped holes behind first row (downstream portion), only the case of higher blowing ratio (M=1.5) and lower density ratio (DR=1.0) shows that coolant does not cover leading edge surface well at lower location (z/d below 5). Fixed at density ratio DR=1.0, film coolant traces downstream first row become thinner and shorter indicating reducing film cooling effectiveness as blowing ratio increases from 0.5 to 1.0 and 1.5. As increasing density ratio from 1.0 to a higher one 1.5 and 2.0, film coolant traces become shorter. This implies heavier coolant which ejects out from radial angle shaped holes does not have enough momentum to flow toward downstream for all blowing ratios. The last film hole configuration is compound angle shaped holes for discussion. The overall trend for this configuration downstream first row is that coolant traces behind first row adhere to leading edge surface well no matter lower or higher blowing ratio, lower or higher density ratio. As mentioned before, lower blowing ratio (M=0.5) case with lower

coolant jet momentum for all density ratios, coolant is deflect by mainstream from compound angle direction (forty five degree) to mainstream direction. As increasing blowing ratio to higher ones (M=1.0 and 1.5), coolant jet have larger momentum and coolant is only partially deflected by mainstream away from compound angle direction. As the density ratio increases to a higher value, film cooling effectiveness downstream first row increases for higher blowing ratio M=1.0 and 1.5.

5.4 Blowing Ratio Effect

The general trends of blowing ratio effect on film cooling effectiveness are as follows. At lower blowing ratios, film coolant jets with lower momentum adhere to blade surface. Increasing blowing ratio means jet momentum increases. Film coolant jets mix and interact more with mainstream, resulting in reduction of film cooling effectiveness. In this section, three different blowing ratios: lower blowing ratio M=0.5, medium blowing ratio M=1.0, and higher blowing ratio M=1.5 are selected to see blowing ratio effect. Density ratios include DR=1.0 and 1.5 for these three blowing ratios. There are four holes configurations: radial angle cylindrical holes, compound angle cylindrical holes, radial angle shaped holes, and compound angle shaped holes. These four configurations are all tested based on three blowing ratios and two density ratios.

The span-wise averaged film cooling effectiveness for the seven-row design is shown in Fig. 5.5. The data are presented in terms of s/d and θ (angles to the stagnations line). In the bottom x-axis is s/d and in the top x-axis is θ. The stagnation row is at s/d=0, and first to three rows are at 15°, 30°, and 45°. As shown in the span-wise averaged film cooling effectiveness, the peak value of film cooling effectiveness is at the location of

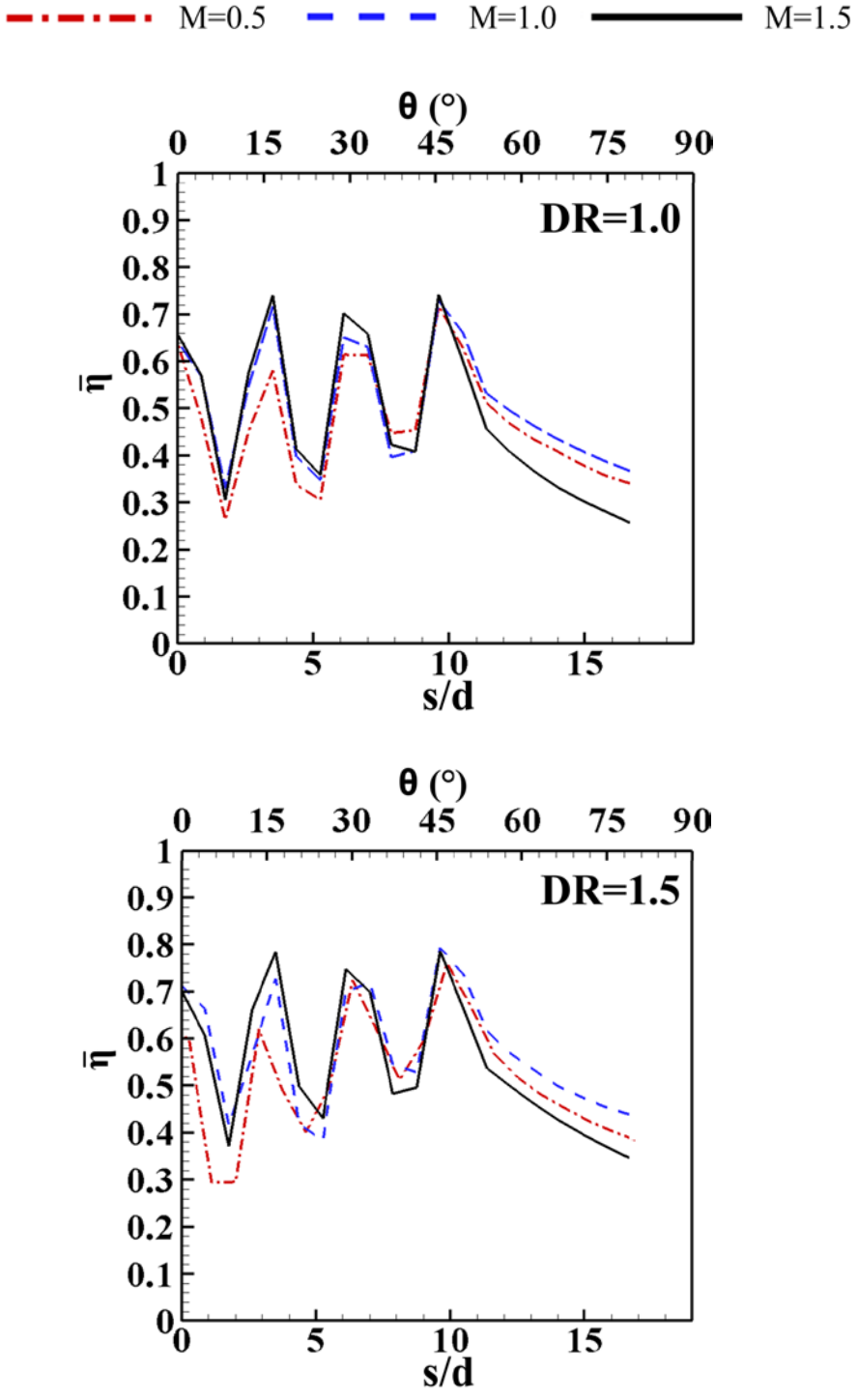

(a) Radial angle cylindrical holes

Fig. 5.5 Effect of blowing ratio on span-wise averaged film cooling effectiveness(7-row)

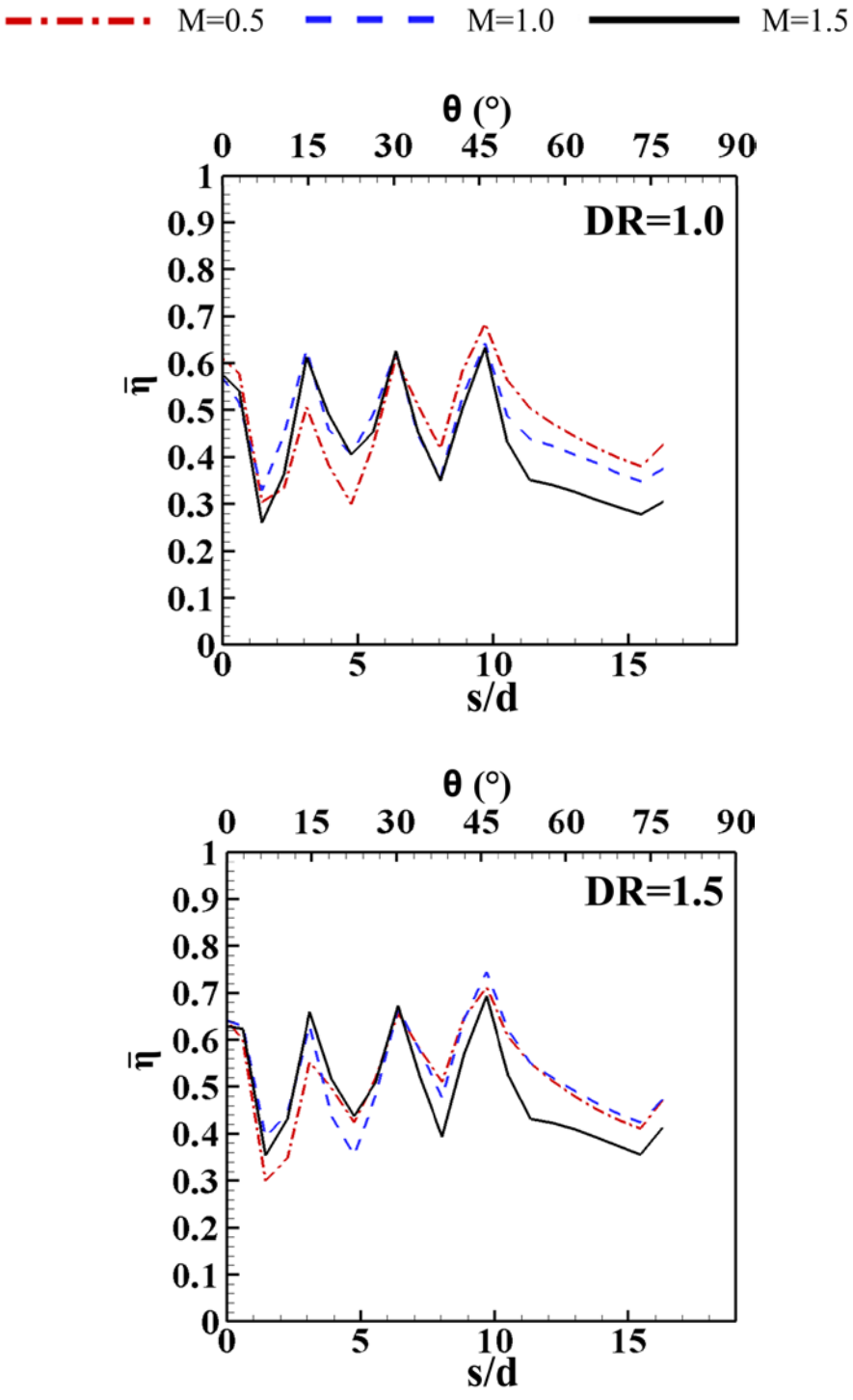

(b) Compound angle cylindrical holes

Fig. 5.5 Continued

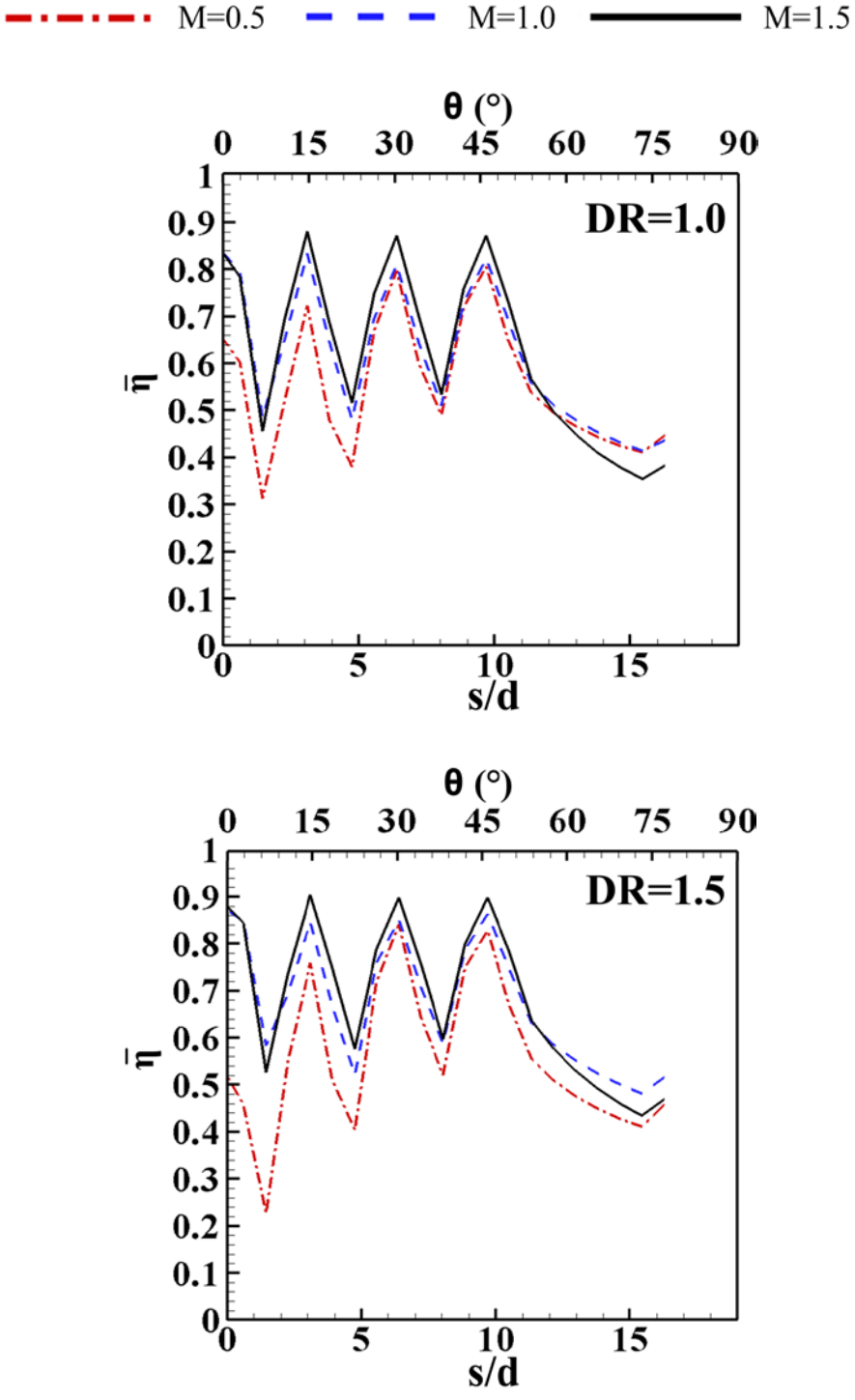

(c) Radial angle shaped holes

Fig. 5.5 Continued

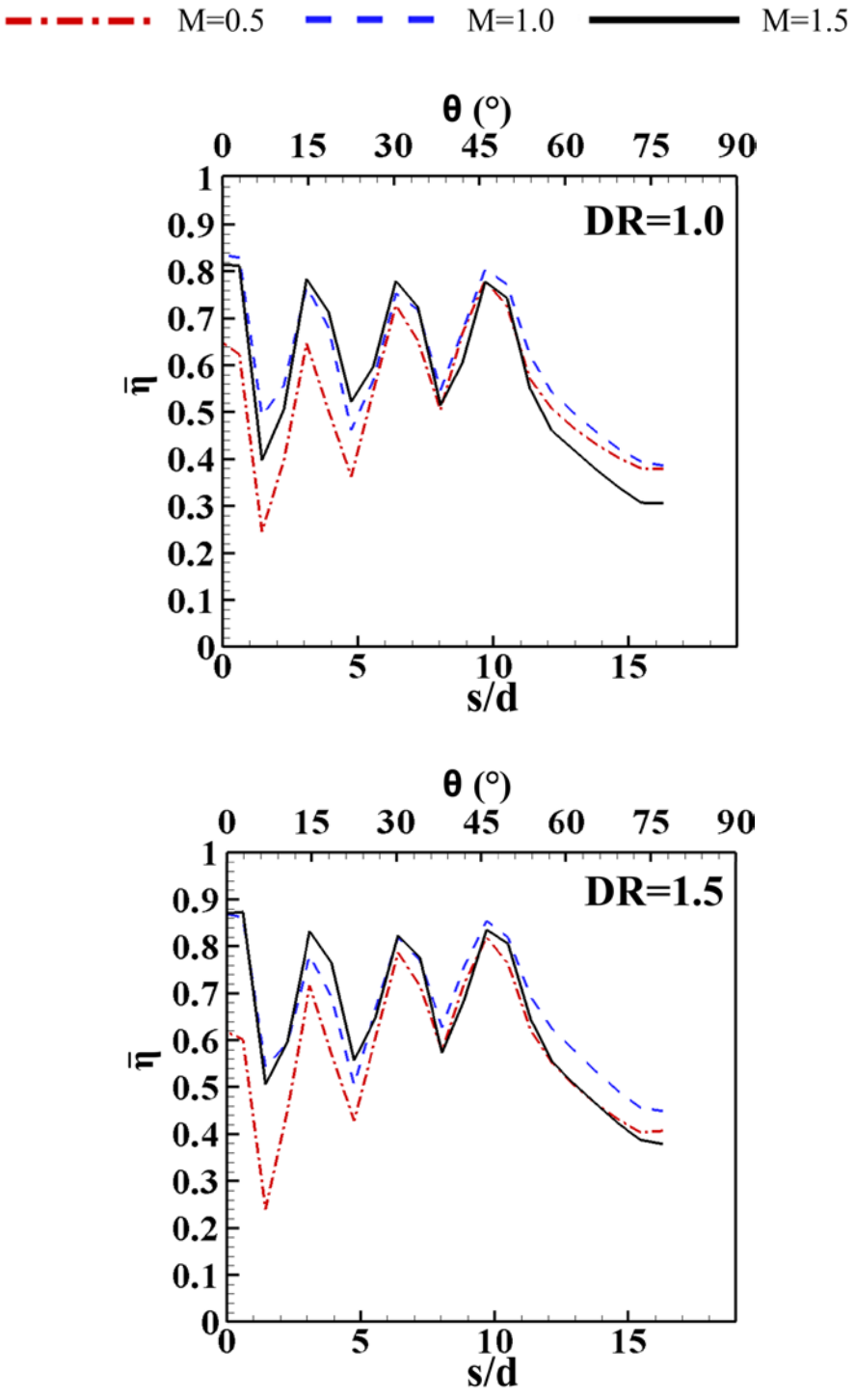

(d) Compound angle shaped holes

Fig. 5.5 Continued

film holes, indicating coolant just ejecting out from holes. As film coolant moves downstream away from holes, film cooling effectiveness starts to decrease and increases again as reaching next row of holes. Behind the $\theta = 45°$, this region is called downstream portion. Fig. 5.5 (a) contains two sub-figures of DR=1.0 and DR=1.5 for radial angle cylindrical holes. For DR=1 case, highest blowing ratio (M=1.5) has highest span-wise averaged film cooling effectiveness at hole locations (0°, 15°, 30°, and 45°). This can be explained as that higher blowing ratio with higher momentum so that coolant ejects and accumulates more in the span-wise (radial) direction. Between two adjacent rows, higher blowing ratio has higher effectiveness in general. In other words, the span-wise film cooling effectiveness increases with increasing of blowing ratio between any two rows.

At the downstream region, the span-wise averaged effectiveness of highest blowing ratio (M=1.5) becomes lowest among three blowing ratios. The reason is that highest blowing ratio contains strong coolant jet. Coolant most likely accumulates in the radial direction rather than moves further downstream along mainstream direction (with lowest coolant deflection by mainstream). Medium blowing ratio (M=1.0) case shows best downstream coolant accumulation. As increasing density ratio to DR=1.5, heavier density coolant with lower momentum has the tendency to adhere more to leading edge surface. Increasing density ratio has marginal effect on lower blowing ratio (M=0.5). This can be seen from the span-wise averaged film cooling effectiveness level for two cases: DR=1.0, M=0.5 and DR=1.5, M=0.5. They are close to each other. For higher blowing ratio cases (M=1.0 and 1.5), increasing density ratio makes span-wise effectiveness slightly increase. This also indicated heavier density coolant spreads better

in the span-wise or radial direction. Second film hole configuration is also cylindrical hole but the hole orientates in compound angle direction. In general, higher blowing ratio has higher effectiveness at the exit of hole for these two configurations. As density ratio equal to DR=1.0, lower blowing ratio (M=0.5) case has lower span-wise averaged effectiveness at hole location and between two adjacent rows of holes. Also, it has highest coolant accumulation at the downstream portion. As increasing density ratio to DR=1.5, there is almost no change for lower blowing ratio (M=0.5). However, as increasing density ratio for compound angel cylindrical holes, there is only small span-wise averaged effectiveness change for higher blowing ratios cases (M=1.0 and 1.5) at hole location and between two adjacent rows. As for downstream portion, coolant accumulates more for blowing ratio M=1.0 and 1.5 cases as increasing density ratio 1 to 1.5. No matter density ratio, the best blowing ratio is M=1.0 with overall higher effectiveness at hole location, between two rows, and downstream portion for these two configurations.

The results of third hole configuration: radial angle shaped holes and forth hole configuration: compound angle shaped holes can been seen from Fig. 5.5 (c) and (d) for the seven-row design. No matter density ratio 1.0 or 1.5, the higher blowing ratio has higher span-wise averaged film cooling effectiveness except downstream region for radial angle shaped holes configuration. For DR=1.0, lowest blowing ratio (M=0.5) had overall lowest effectiveness. As increasing blowing ratio to M=1.0, there is obvious effectiveness increment both at hole location and between any two rows of holes. Further increasing blowing ratio from 1.0 to 1.5, span-wise film cooling effectiveness increases

but only with smaller amount of increment. For DR=1.5, the film cooling trends is similar to that of DR=1.0 for three blowing ratios. The only different is that higher density ratio case (DR=1.5) has slightly higher effectiveness level than lower density case (DR=1.0). Next hole configuration is compound angle shaped holes as shown in Fig. 5.5 (d). The overall trend for this configuration is similar to that of radial angle shaped hole for all blowing and density ratios. The effectiveness difference between these two configurations is that radial angle holes have more accumulation in radial (span-wise) direction compared with compound angle holes, resulting in higher effectiveness at hole location. In summary, radial angle shaped with higher density ratio (DR=1.5) and medium blowing ratio (M=1.0) shows best span-wise averaged film cooling effectiveness among these four configurations.

The hole configuration for three-row design is the same as seven-row design except fewer film cooling holes. Blowing ratios are the same M=0.5, 1.0, and 1.5. Density ratios not only include 1.0 and 1.5 but also extend to realistic higher one 2.0. The span-wise averaged film cooling effectiveness for three-row design is shown in Fig. 5.6. The general trend for cylindrical holes (either radial angle (a) or compound angle (b)) is that lower blowing ratio (M=0.5) with lowest span-wise film cooling effectiveness between stagnation row (θ=0) and first row of holes (θ=30°) for all density ratios .The trend is reverse at downstream portion. Blowing ratio M=0.5 case has highest span-wise film cooling effectiveness indicating more coolant accumulation downstream.

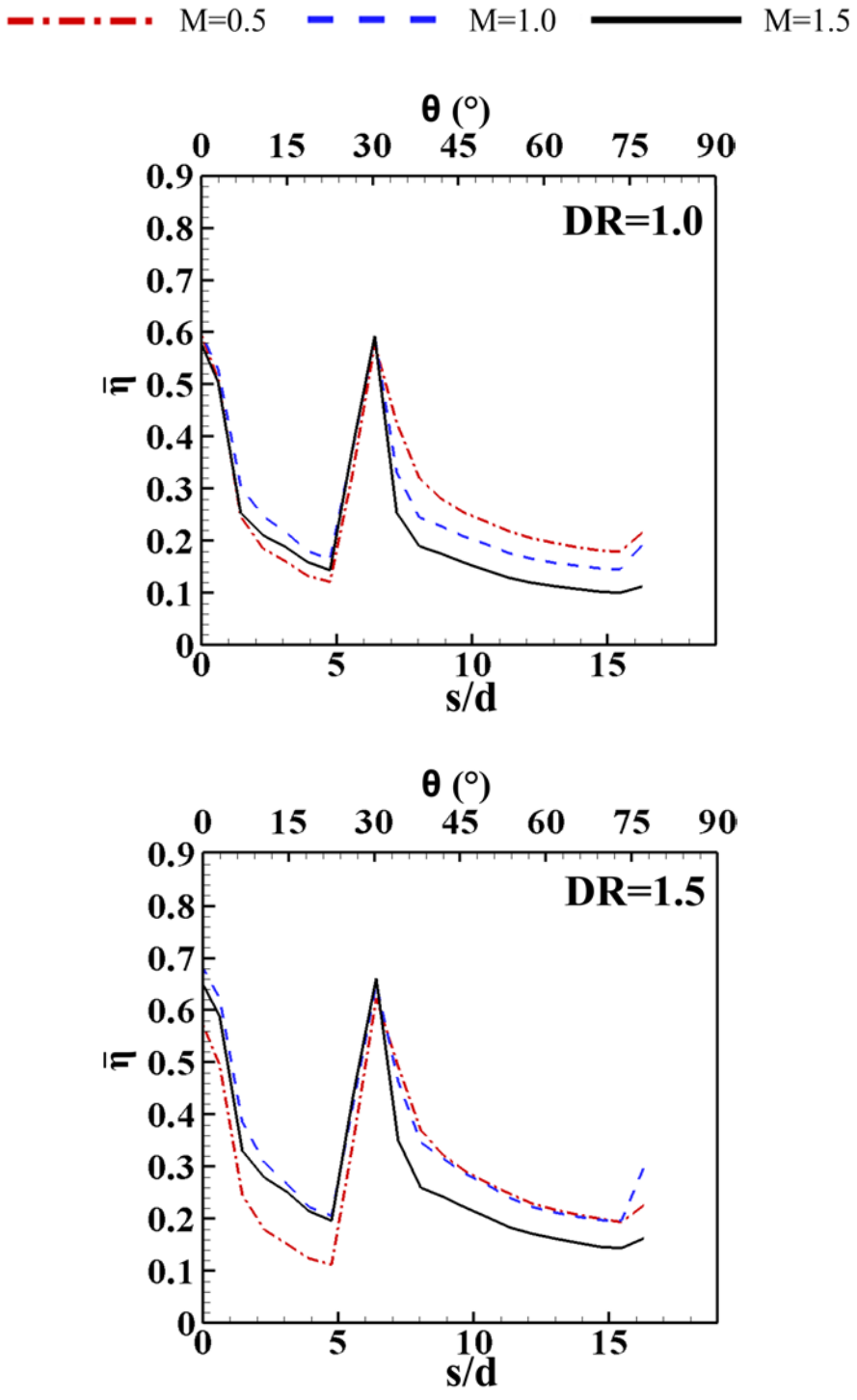

(a) Radial angle cylindrical holes

Fig. 5.6 Effect of blowing ratio on span-wise averaged film cooling effectiveness(3-row)

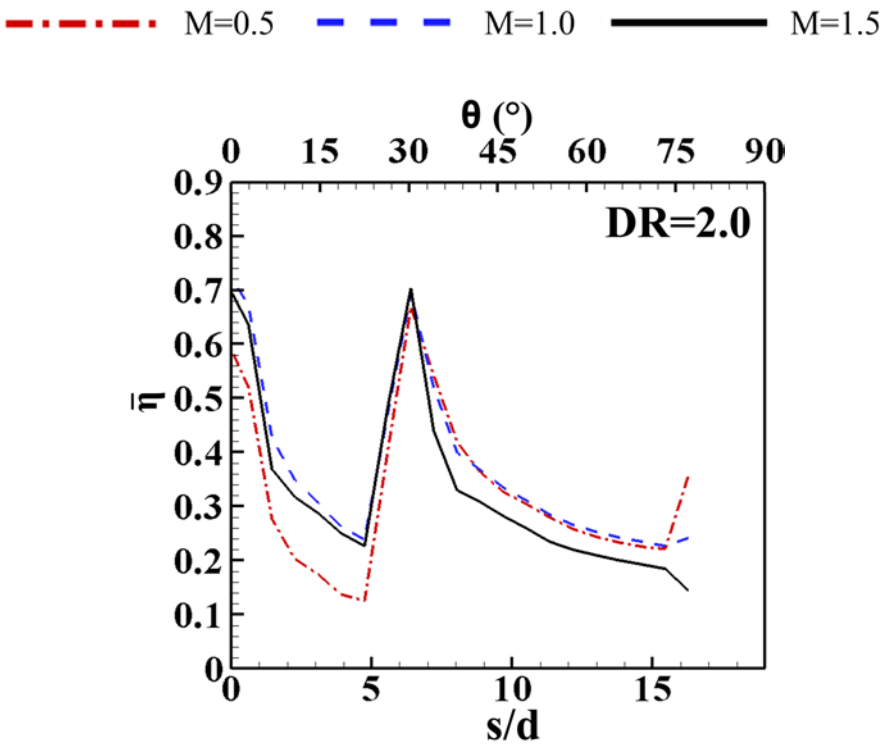

(a) Radial angle cylindrical holes

Fig. 5.6 Continued

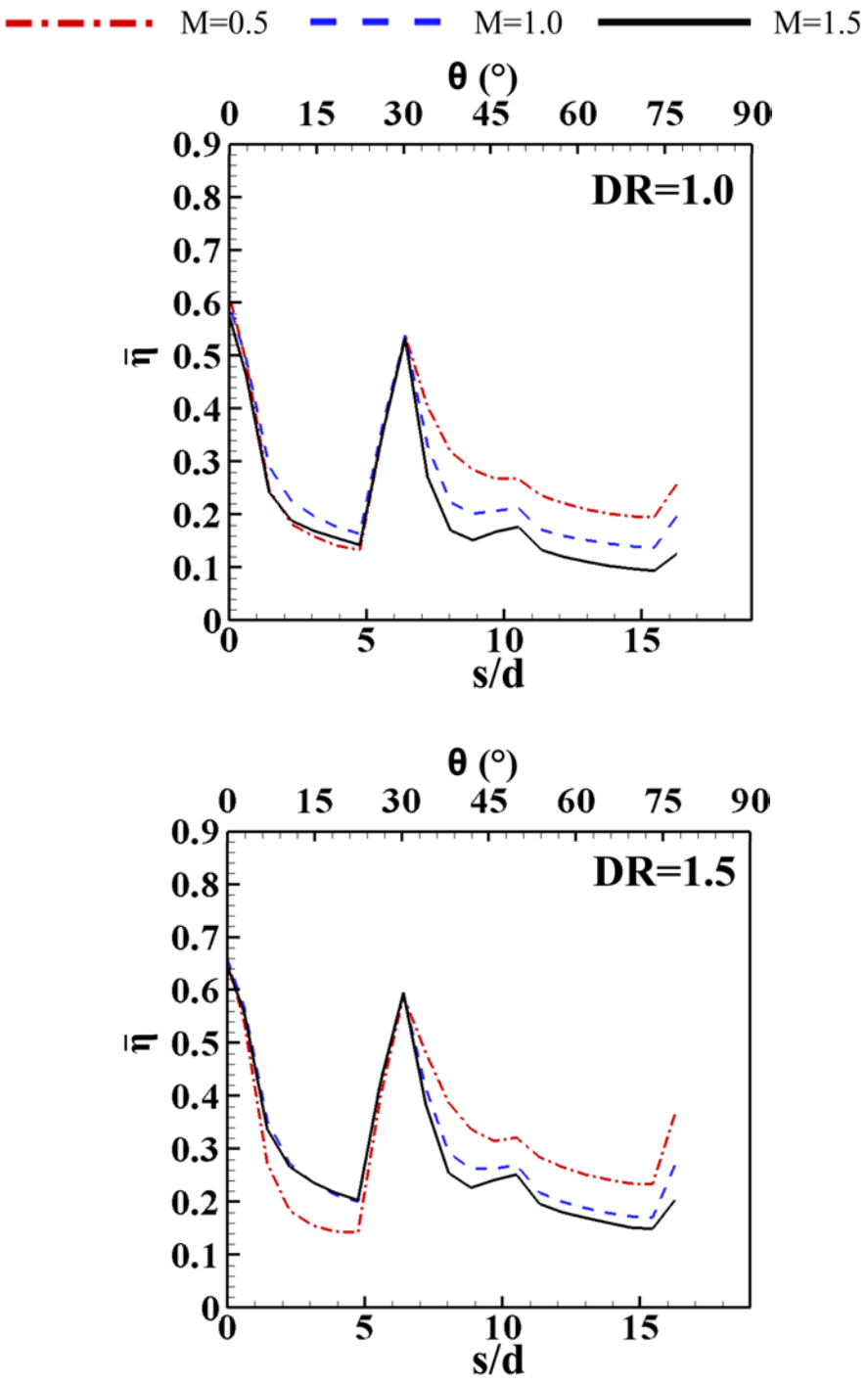

(b) Compound angle cylindrical holes

Fig. 5.6 Continued

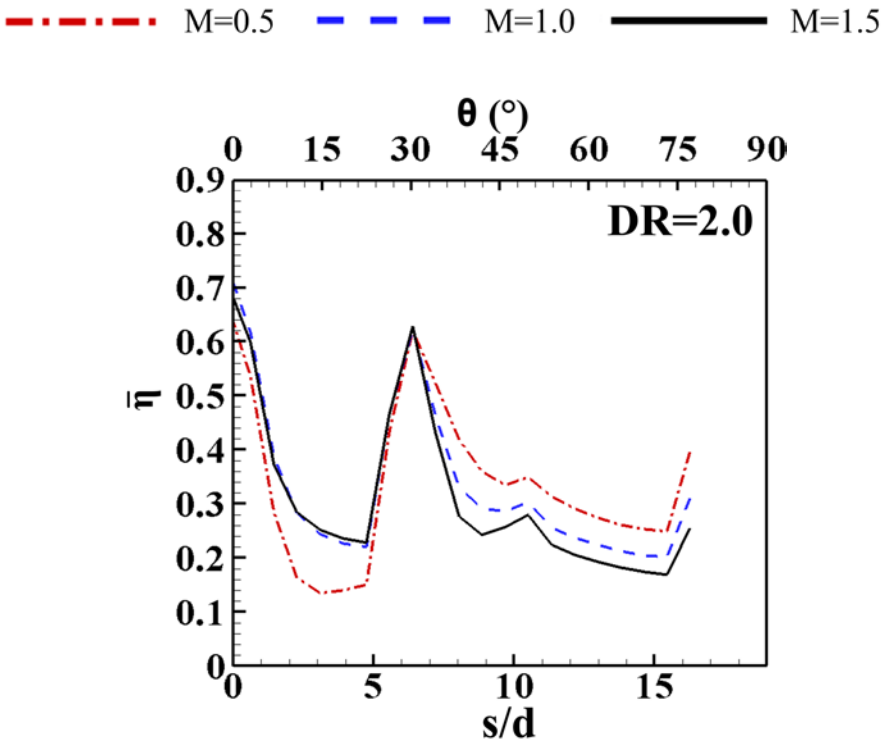

(b) Compound angle cylindrical holes

Fig. 5.6 Continued

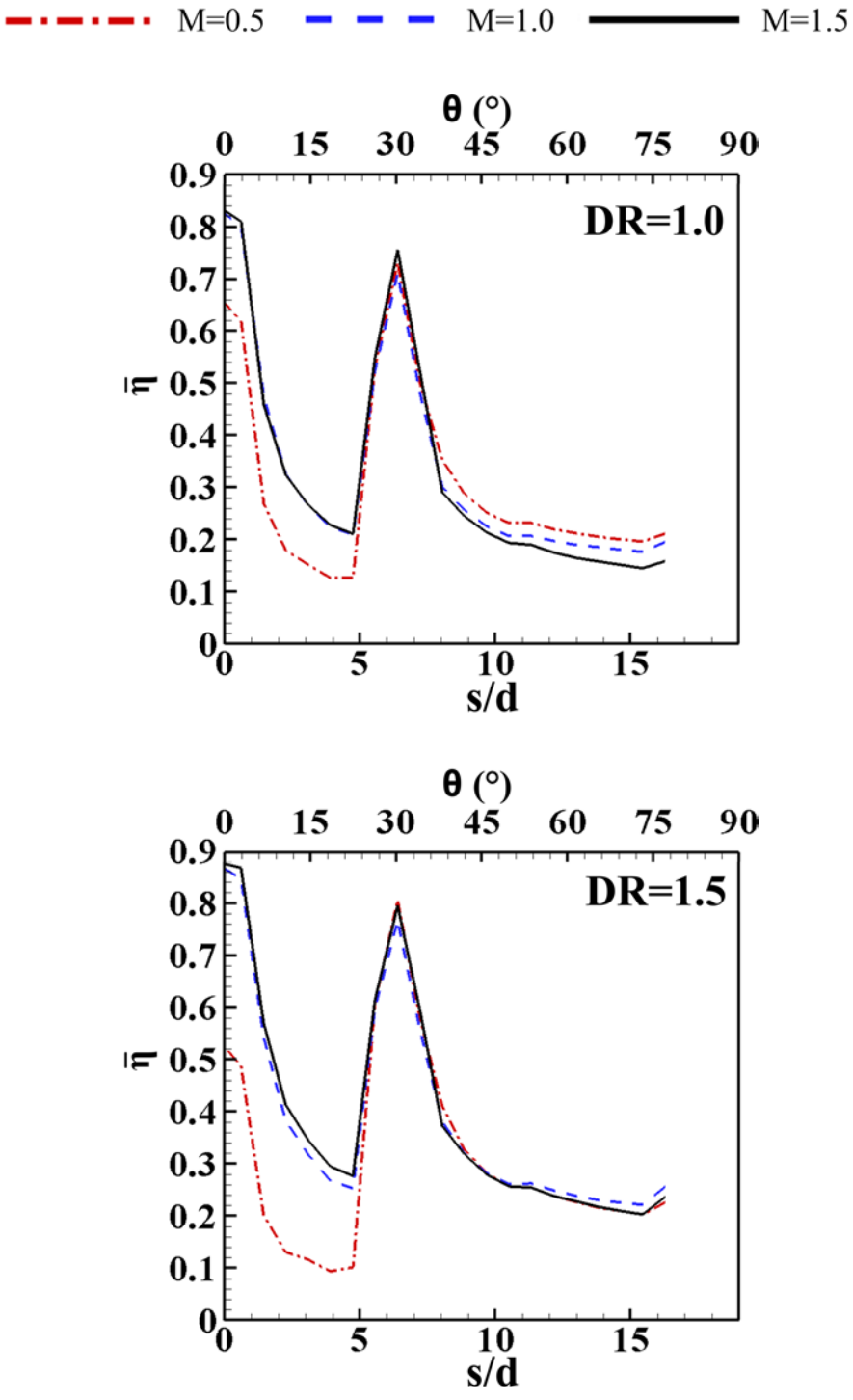

(c) Radial angle shaped holes

Fig. 5.6 Continued

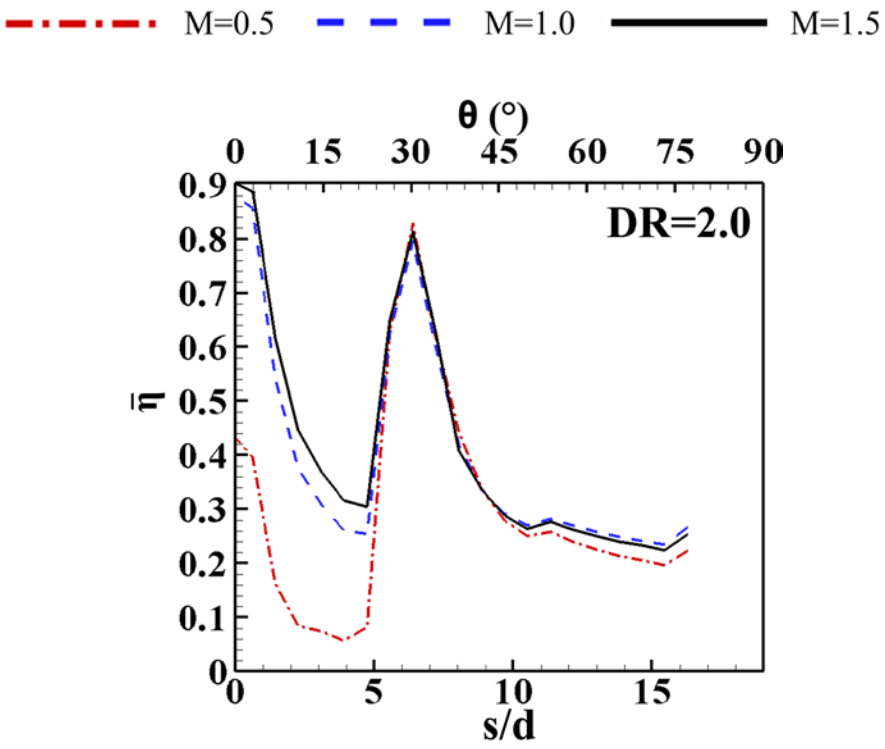

(c) Radial angle shaped holes

Fig. 5.6 Continued

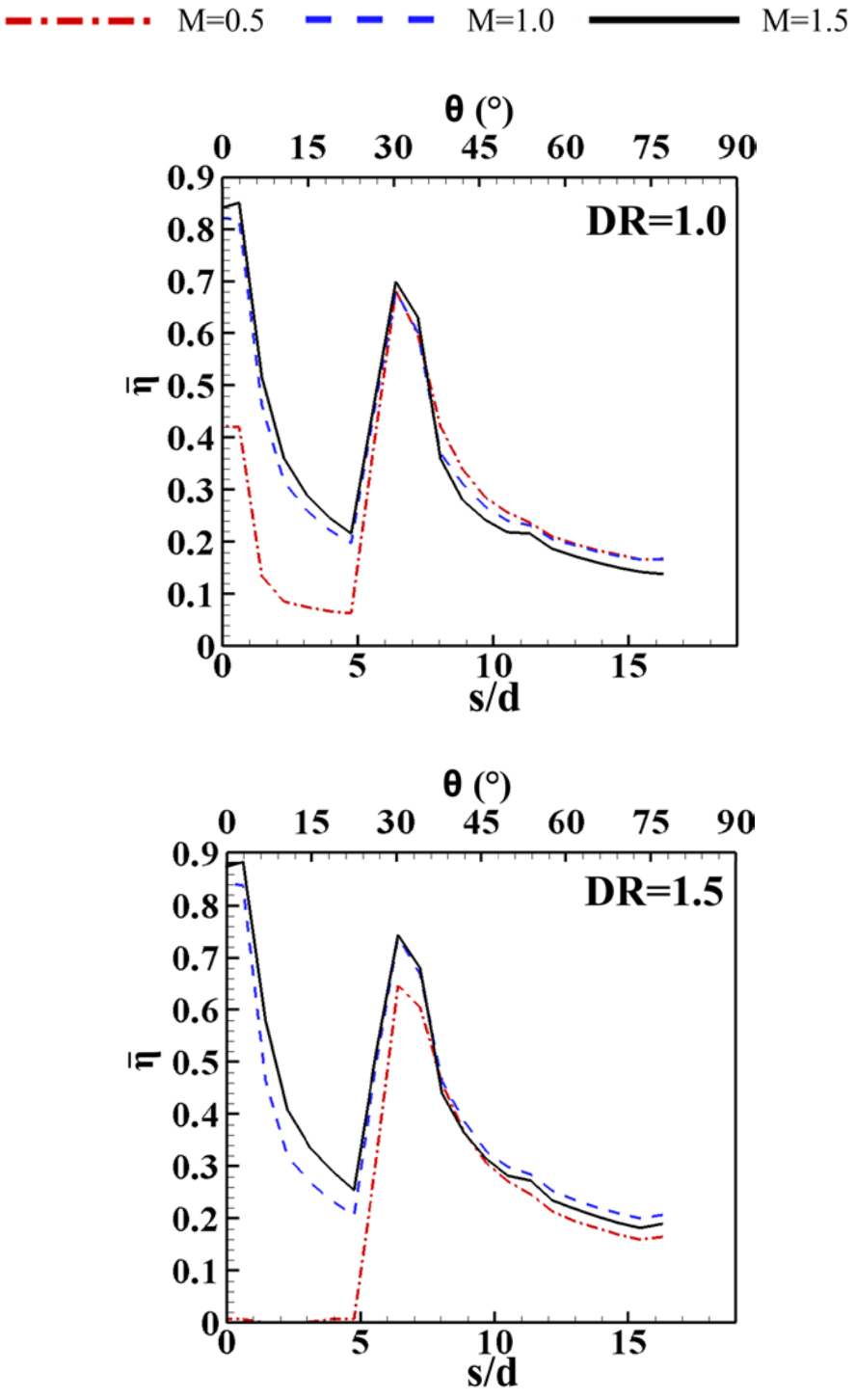

(d) Compound angle shaped holes

Fig. 5.6 Continued

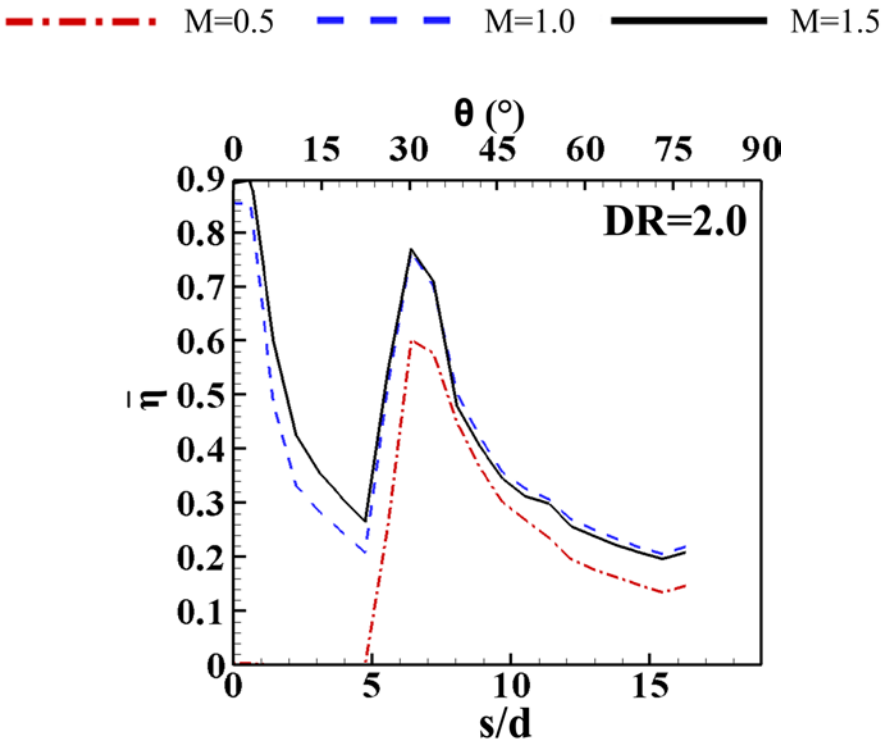

(d) Compound angle shaped holes

Fig. 5.6 Continued

At the first row of holes location, three blowing ratios all have the same value of span-wise averaged effectiveness in spite of density ratios. For the first hole configuration: radial angle cylindrical hole, as density ratio increases from 1.0 to 2.0, there is only minimal effectiveness change for lower blowing ratio (M=0.5). As for higher blowing ratio 1.0 and 1.5, the span-wise film cooling effectiveness increases as increasing density ratio from stagnation row to downstream portion. The same trend is for the compound angle cylindrical holes. Effectiveness of shaped holes can be seen

from Fig. 5.6 (c) radial angle shaped holes and (d) compound angle shaped holes. The overall trend for shaped hole (Fig. 5.6 (c) and (d)) is higher span-wise averaged film cooling effectiveness than cylindrical holes (Fig. 5.6 (a) and (b)) for all density ratio (DR=1.0 to 2.0) with higher blowing ratios (M=1.0 and 1.5) cases, particularly at location of stagnation row and first row. However, the lower blowing ratio (M=0.5) of radial angle shaped holes show pretty low effectiveness values from stagnation row to first low for three density ratios. This situation for compound angle shaped hole is even worst. Lowest blowing ratio (weak jet momentum) with heavier density coolant (density ratio 1.5 and 2.0) cases, coolant jet has insufficient momentum) and cannot eject out from shaped holes at stagnation row to protect leading edge surface. In summary, radial angle shaped with both higher density ratio and blowing ratio performs best film coverage among these four configurations.

5.5 Hole Configuration Effect

There are four kinds of film cooling holes for comparisons to see which one is better for both seven-row and three-row designs. The blowing ratio ranges from 0.5 to 1.5. The density ratio for seven-row design is 1.0 and 1.5 and for three-row design is 1.0 to 2.0. The film cooling hole shape can be categorized as cylindrical hole and shaped holes. The orientation of hole also includes two categories as radial angle and compound angle. These can be combined into four film hole configurations as radial angle cylindrical holes, compound angle cylindrical holes, radial angle shaped holes, and compound angle shaped holes. For cylindrical hole, the inlet and exit holes' cross section area are the same. For shaped hole, the laidback fan-shaped has been selected to

investigate. At the beginning of shaped hole (inlet), the hole is in cylindrical shape, the same hole inlet area as cylindrical hole. In the middle of length of film hole, the hole starts to expand until the exit of hole and the exit area is equal to two time of inlet area. This laidback fan-shaped contains film cooling hole lateral expansion angle and forward expansion angle. The advantage of the shaped holes is that the jet momentum reduces due to increase exit cross section area, coolant has larger tendency to adhere to blade surface for protection. By comparison of radial angle and compound angle, radial angle can direct coolant ejecting and accumulating in the radial or span-wise direction. However, as the coolant jet momentum is not sufficient enough to resist mainstream flow at lower blowing ratio, the coolant jet will be deflected by mainstream into stream-wise direction. As for compound angle hole, the purpose of this hole orientation is to increase the lateral spread of film coolant to increase span-wise coolant coverage.

The span-wise averaged film cooling effectiveness includes comparison of four hole configurations in the same plot for each single blowing and density ratio as shown in Fig. 5.7. There are six sub-figures for seven-row design and nine sub-figures for three-row design. From six-subfigures in the span-wise averaged film cooling effectiveness line plots, configuration of radial angle shaped hole shows best film cooling effectiveness among these four hole configurations at the hole location, between any two adjacent rows of holes, and downstream portion for all blowing ratios and density ratios, generally. For DR=1.0, increasing blowing ratio from M=0.5 to M=1.5, the peak film cooling effectiveness at hole location increases for all hole configurations. As for the downstream coolant accumulation, lower blowing ratio (M=0.5) and medium blowing

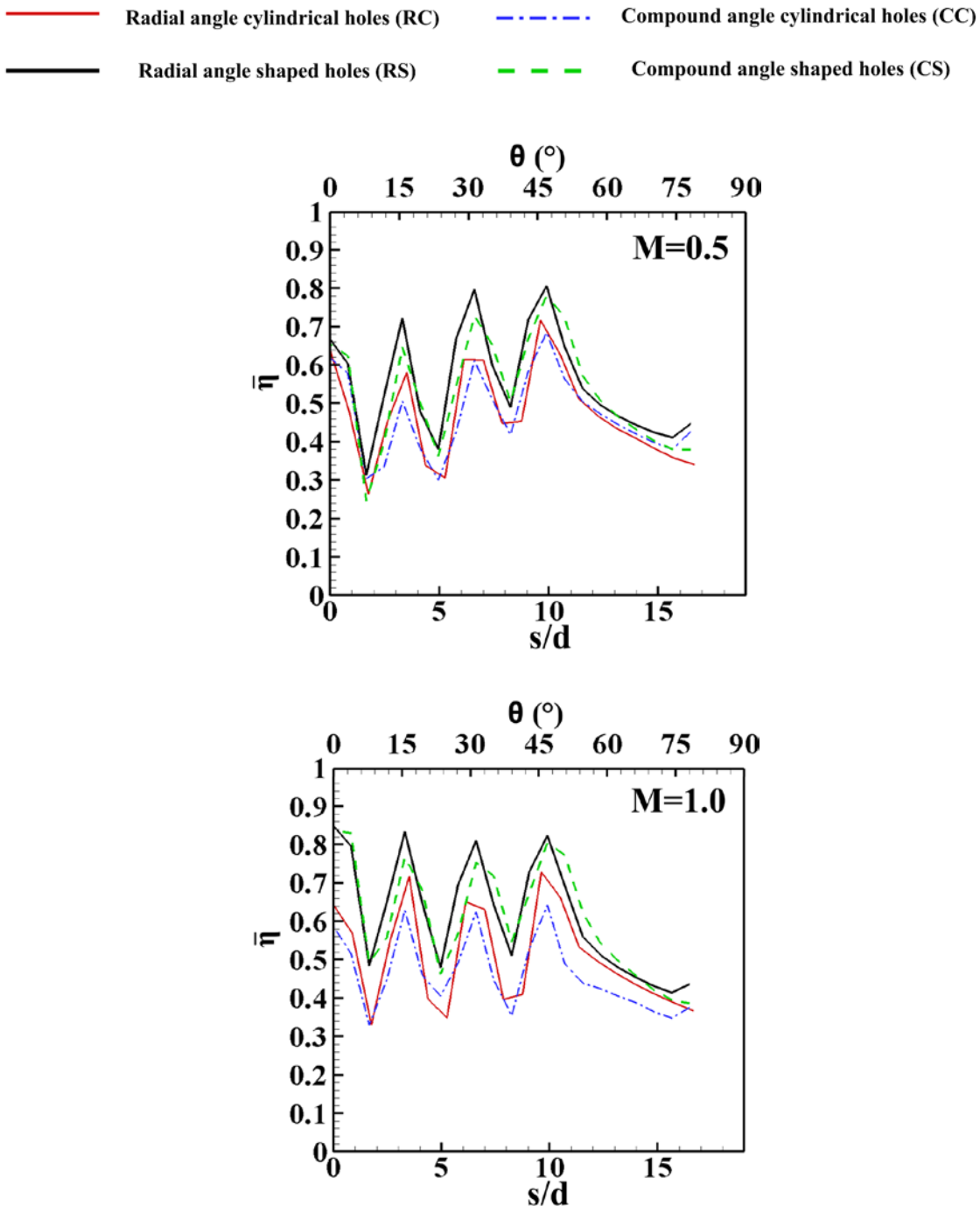

(a) DR=1.0

Fig. 5.7 Effect of hole configuration on span-wise averaged film cooling effectiveness (7-row)

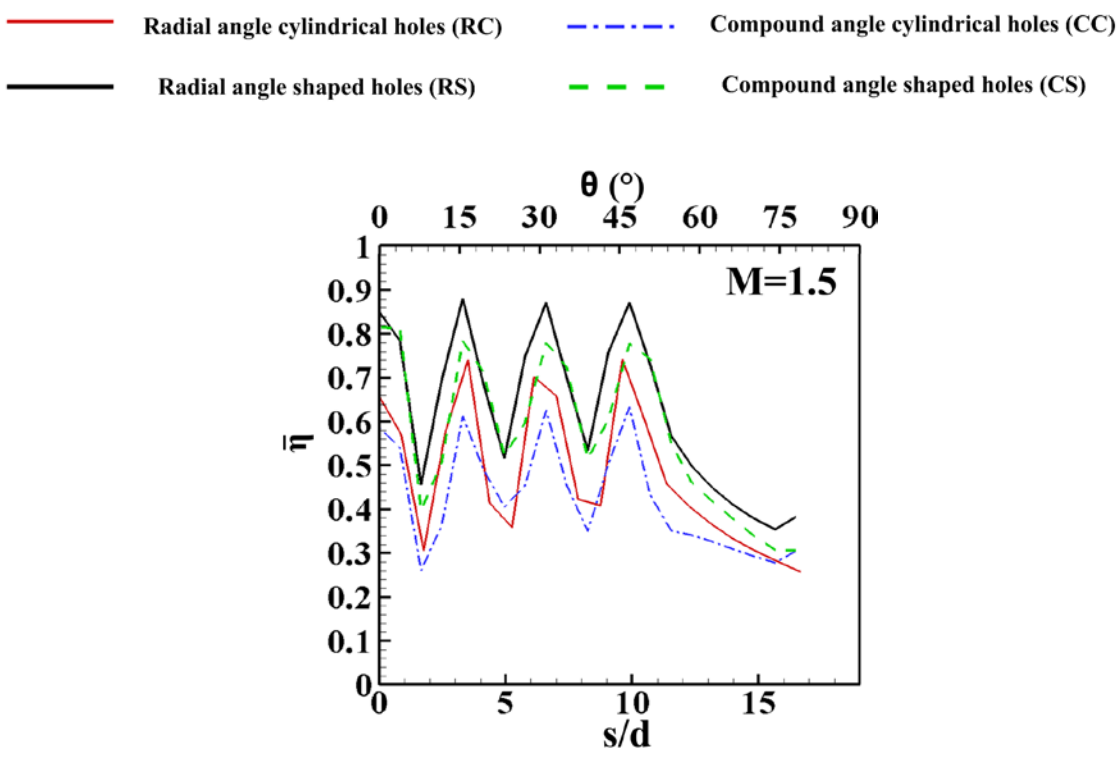

(a) DR=1.0

Fig. 5.7 Continued

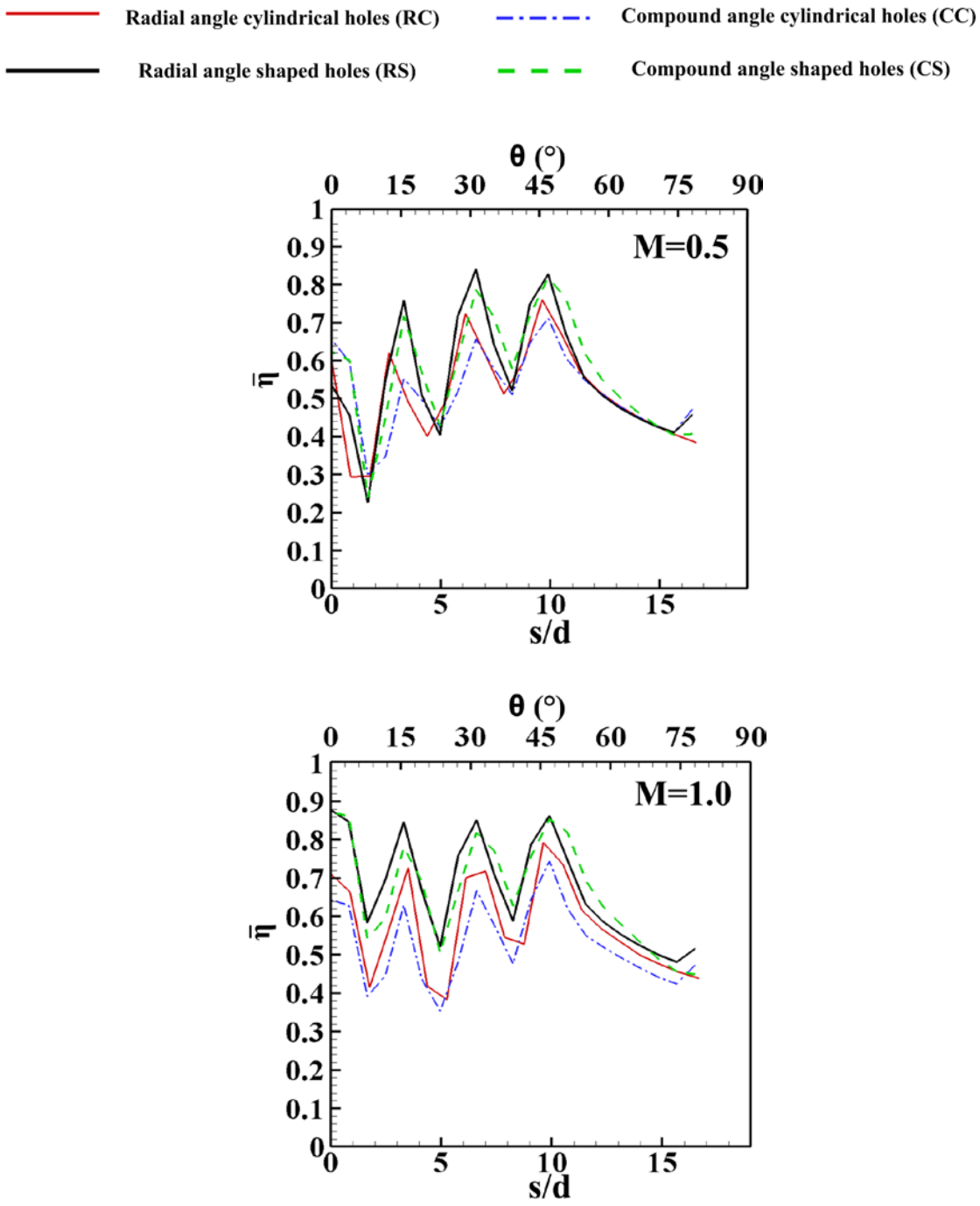

(b) DR=1.5

Fig. 5.7 Continued

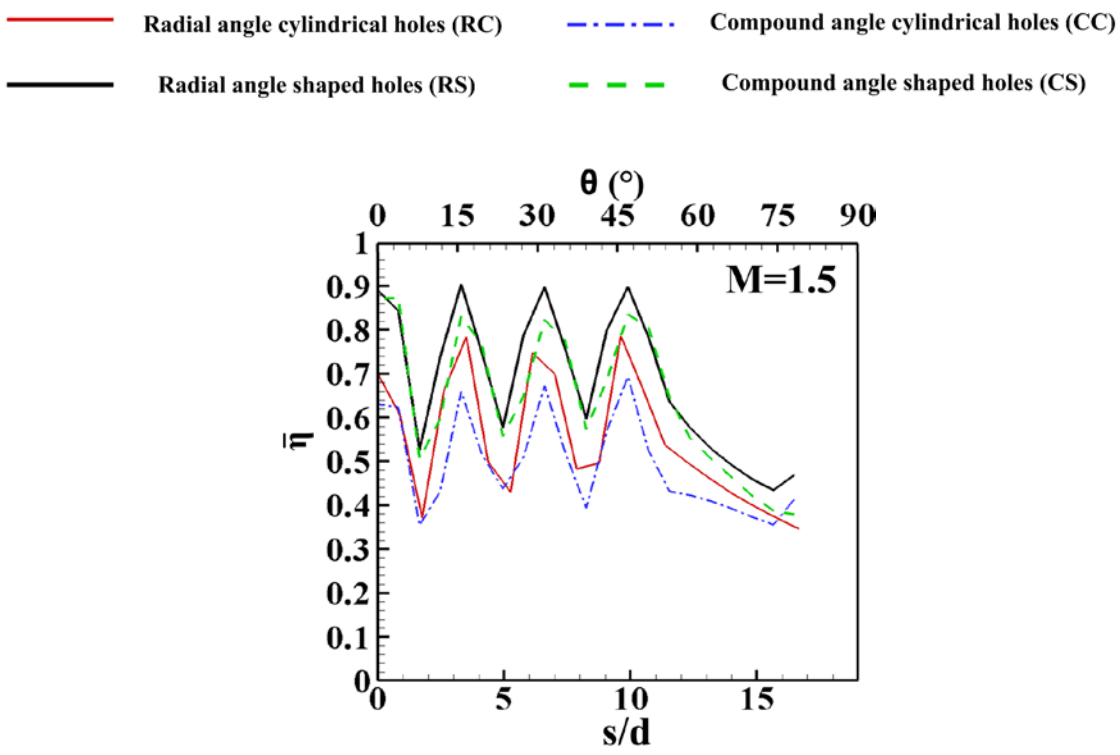

(b) DR=1.5

Fig. 5.7 Continued

ratio (M=1.0) provide the better film coolant accumulation than higher blowing ratio (M=1.5) case. As increasing density ratio from 1.0 to1.5, heavier density coolant is with lower jet momentum as ejecting out from film holes and is easier to adhere to leading edge surface. Therefore, span-wise film cooling effectiveness of three blowing ratios increase especially at hole location and near holes for four film holes configurations.

The span-wise averaged film cooling effectiveness for three-hole design can be seen from Fig. 5.8, the results of four configurations in the same plot for each blowing

ratio and density ratio. Overall, for density ratio 1.0, 1.5, and 2.0, radial angle shaped holes performs best film coverage from leading edge stagnation row to downstream portion among all configurations for medium and higher blowing ratios (M=1.0 and 1.5). This also indicates that the advantage of the shaped hole becomes more evident at higher blowing ratio cases. At lower blowing ratio lower coolant jet momentum cases, coolant jet at the exit of shaped hole has even lower momentum (due to hole expansion) than at the exit of cylindrical hole. This can be seen from Fig. 5.8, blowing ratio M=0.5 cases. Along the stagnation row, cylindrical hole (either radial or compound angles) perform better than shaped hole, especially for higher density ratio cases. The worse situation occurs for hole configuration of compound angle shaped holes along stagnation row, case of M=0.5, DR=1.5 and M=0.5, DR=2.0, coolant barely comes out from film holes to protect leading edge surface.

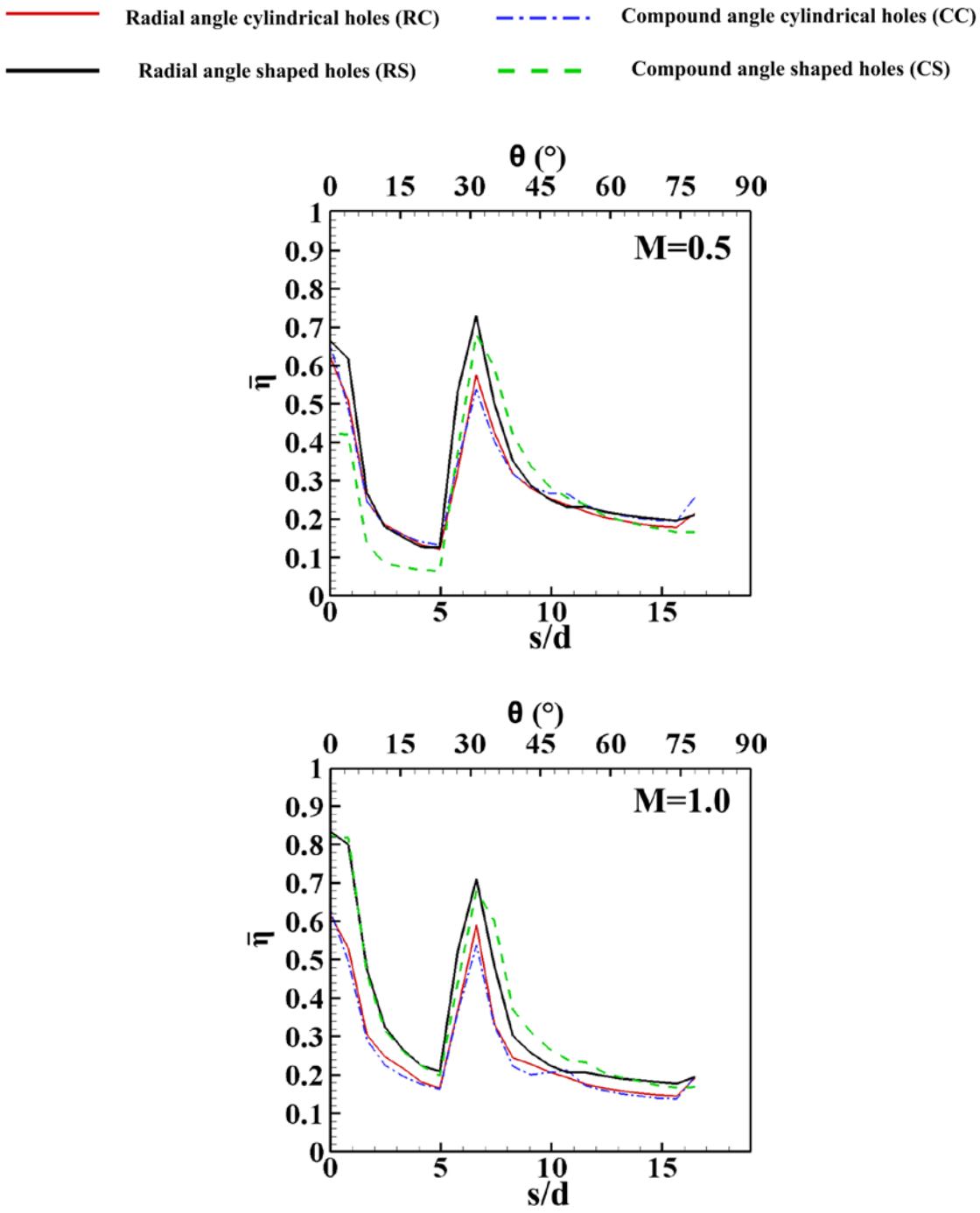

(a) DR=1.0

Fig. 5.8 Effect of hole configuration on span-wise averaged film cooling effectiveness (3-row)

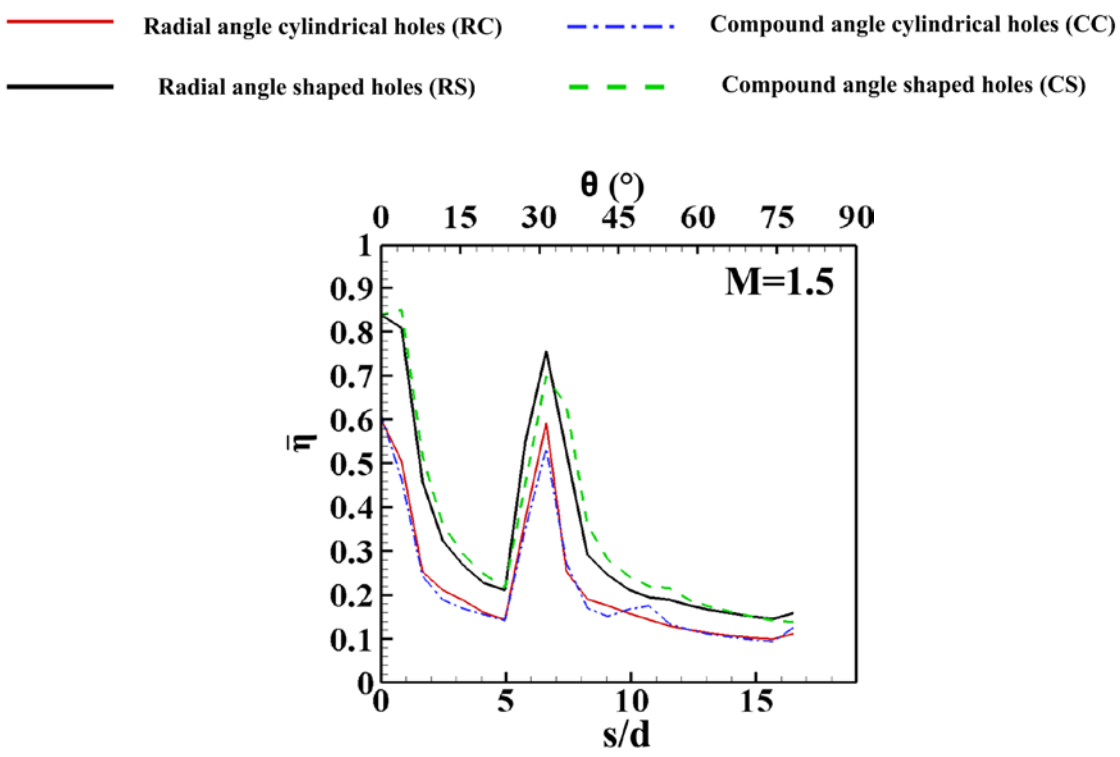

(a) DR=1.0

Fig. 5.8 Continued

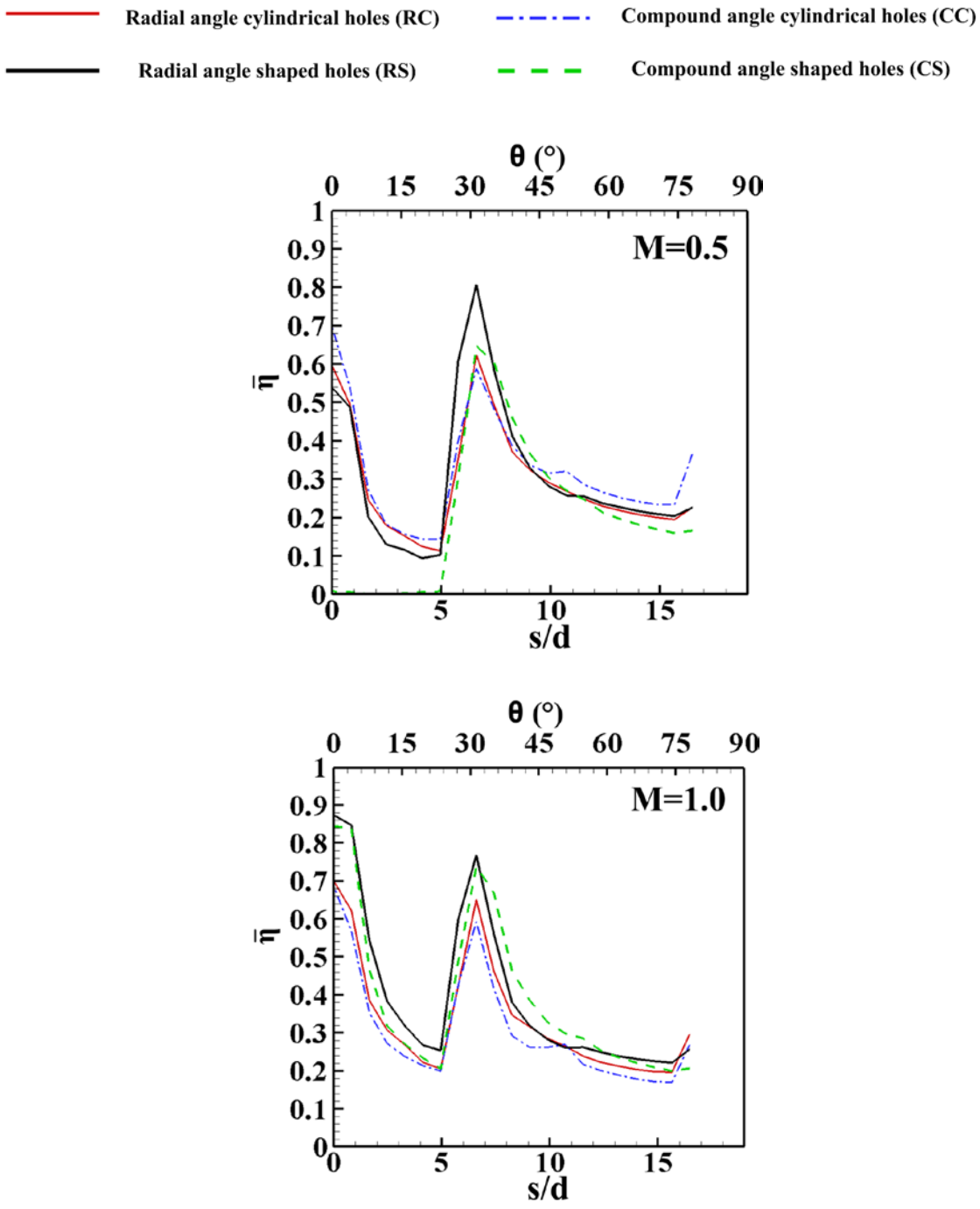

(b) DR=1.5

Fig. 5.8 Continued

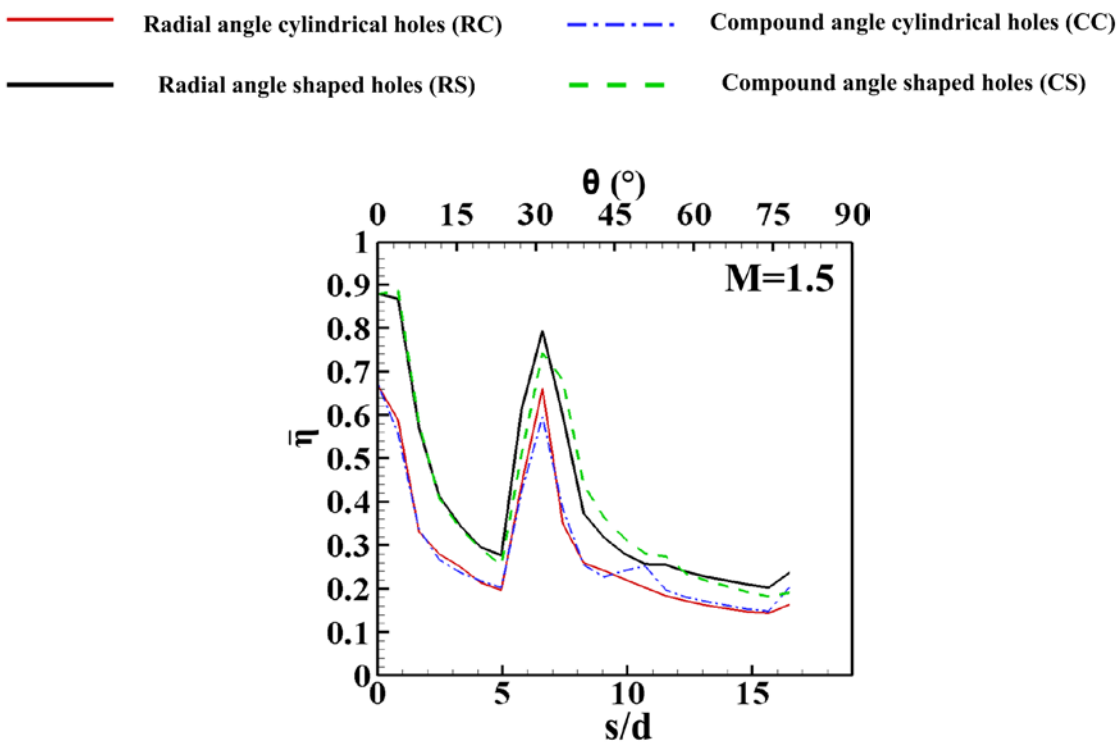

(b) DR=1.5

Fig. 5.8 Continued

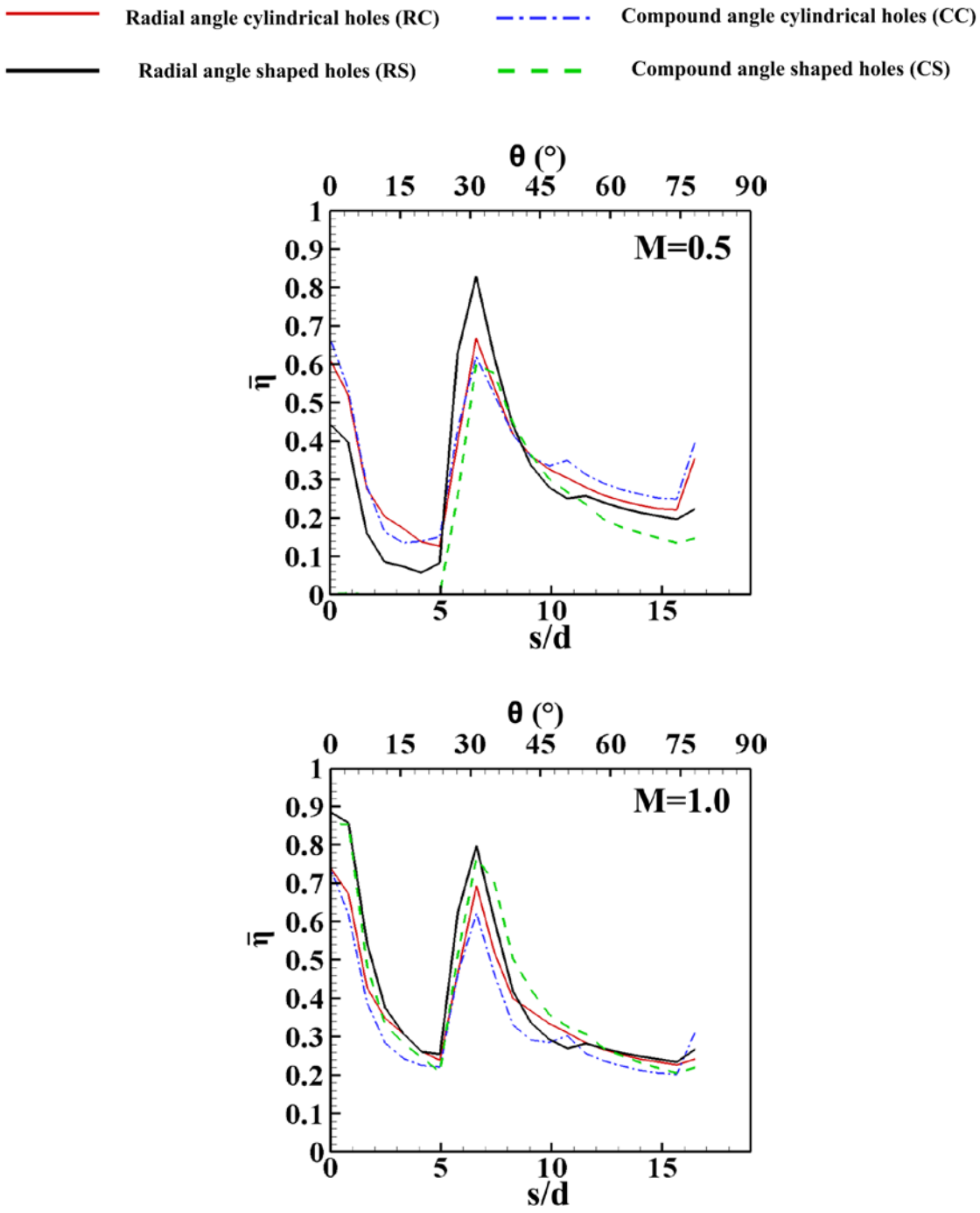

(c) DR=2.0

Fig. 5.8 Continued

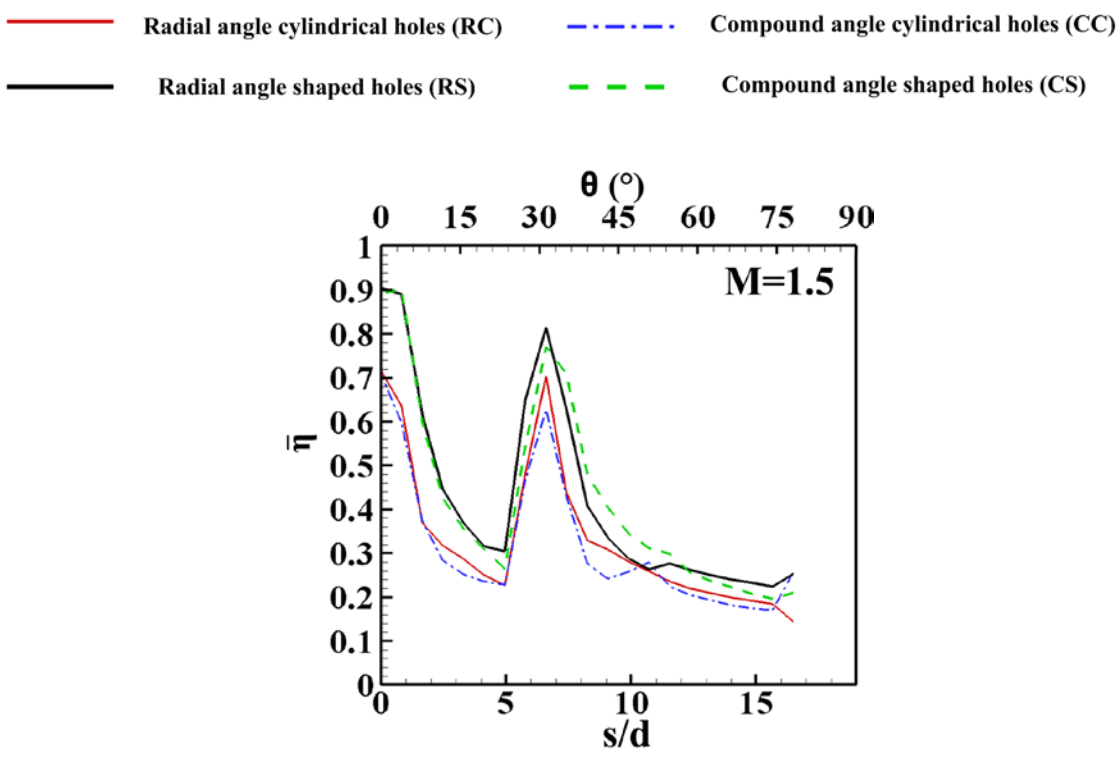

(c) DR=2.0

Fig. 5.8 Continued

5.6 Density Ratio Effect

For a fixed blowing ratio, momentum of the coolant jets decreases with increasing density ratios. Lower coolant momentum is less susceptible to coolant lift-off comparing with higher coolant momentum. Both seven-row design and three-row design are investigated the effect of density ratio. Density ratios for seven-row design are 1.0 and 1.5 and for three-row design are 1.0, 1.5, and 2.0 for four film cooling hole configurations. The blowing ratio varies from 0.5 to 1.5.

The span-wise averaged film cooling effectiveness for seven-row design can be seen from Fig. 5.9. The film cooling effectiveness of density ratio 1.5 provides overall better film cooling coverage than density ratio 1.0 for four film hole configurations no matter which blowing ratios. This means heavier density coolant can adhere more to leading edge surface for protection. For first two film cooling hole configurations: radial angle cylindrical holes (Fig. 5.9(a)) and compound angle cylindrical holes (Fig. 5.9(b)), DR=1.5 cases show higher span-wise averaged film cooling effectiveness at hole location, between any rows of holes, and also downstream portion for all three blowing ratios. As for shaped holes configurations: radial angle shaped hole (Fig. 5.9(c)) and compound angle shaped hole (Fig. 5.9(d)), heavier density ratio of 1.5 offers overall higher span-wise averaged film cooling effectiveness for medium (M=1.0) and higher (M=1.5) blowing ratio cases. As for lower blowing ratio (M=0.5) case, heavier density cooling (DR=1.5) provides higher effectiveness except for one place: stagnation row of holes. The reason is that the coolant jets are already harder to eject out along stagnation row than other downstream row. Also, shaped hole with expanded cross section area

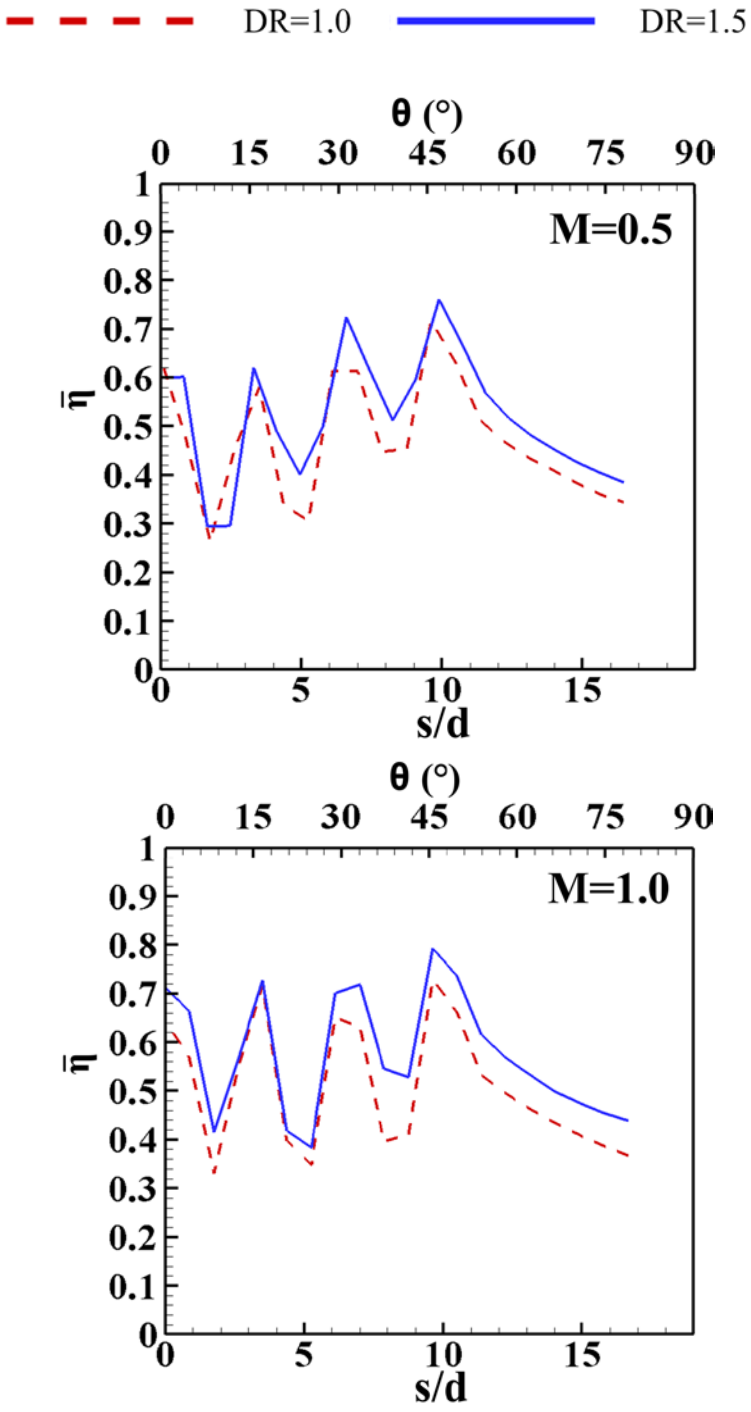

(a) Radial angle cylindrical holes

Fig. 5.9 Effect of density on span-wise averaged film cooling effectiveness (7-row)

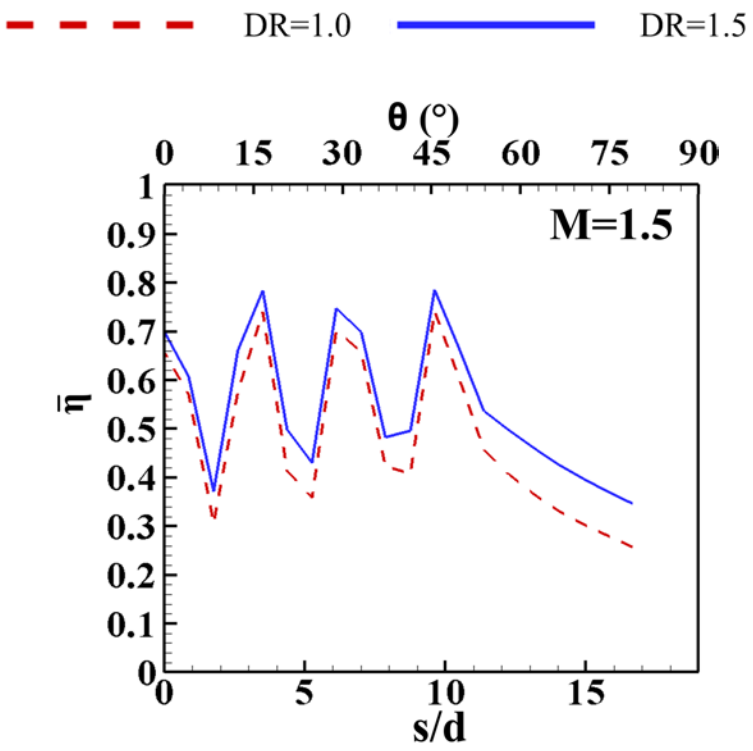

(a) Radial angle cylindrical holes

Fig. 5.9 Continued

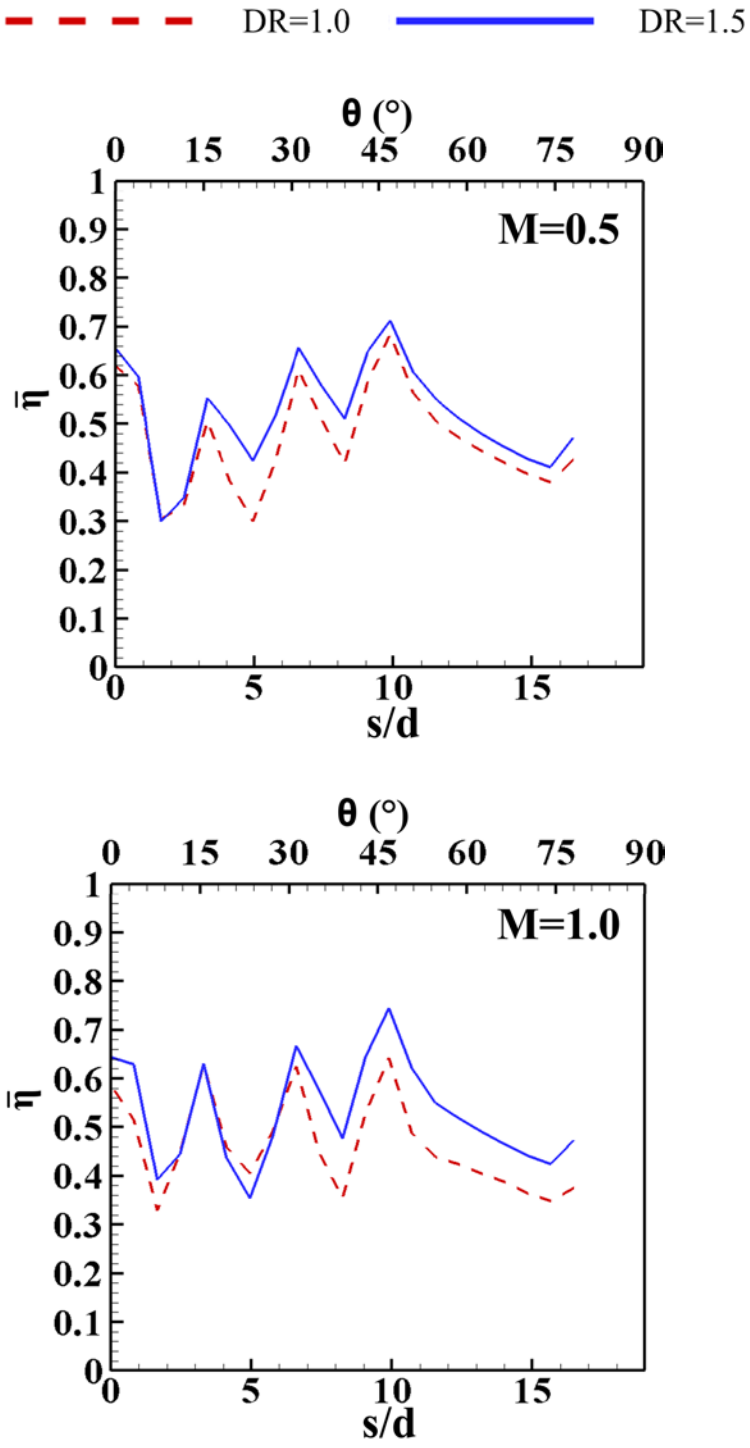

(b) Compound angle cylindrical holes

Fig. 5.9 Continued

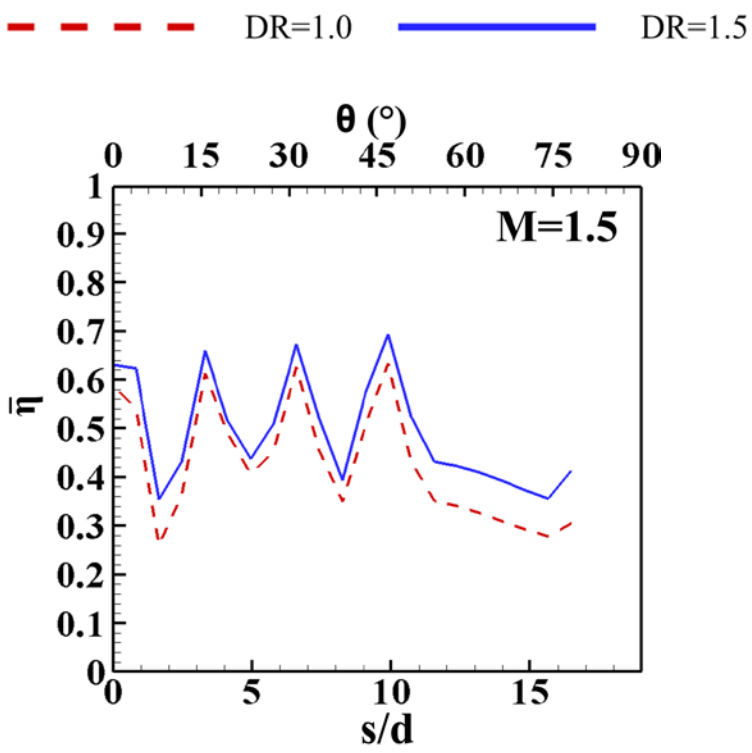

(b) Compound angle cylindrical holes

Fig. 5.9 Continued

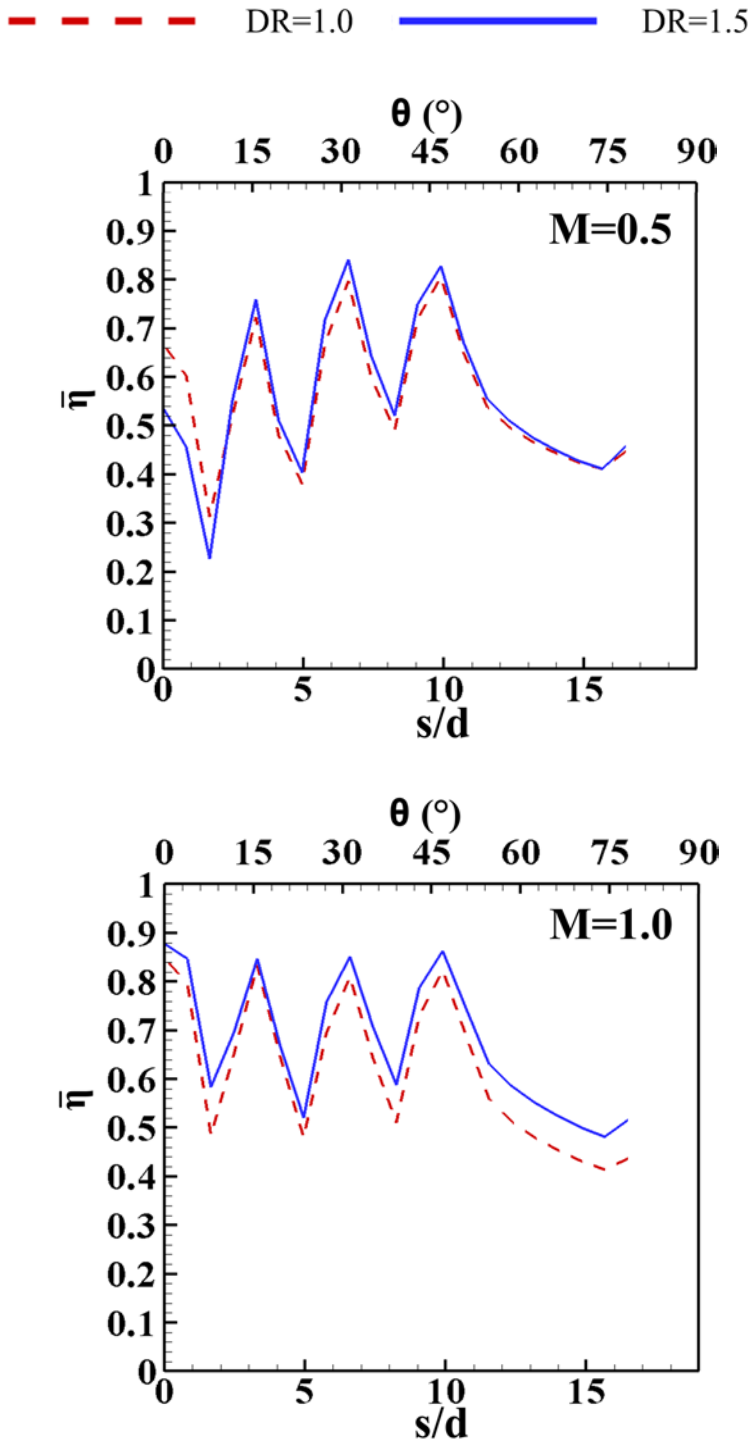

(c) Radial angle shaped holes

Fig. 5.9 Continued

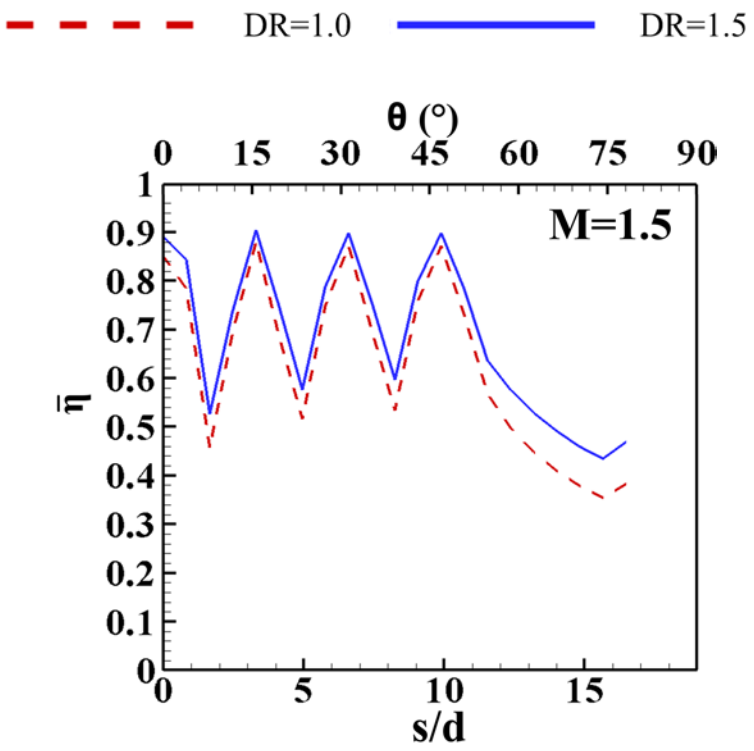

(c) Radial angle shaped holes

Fig. 5.9 Continued

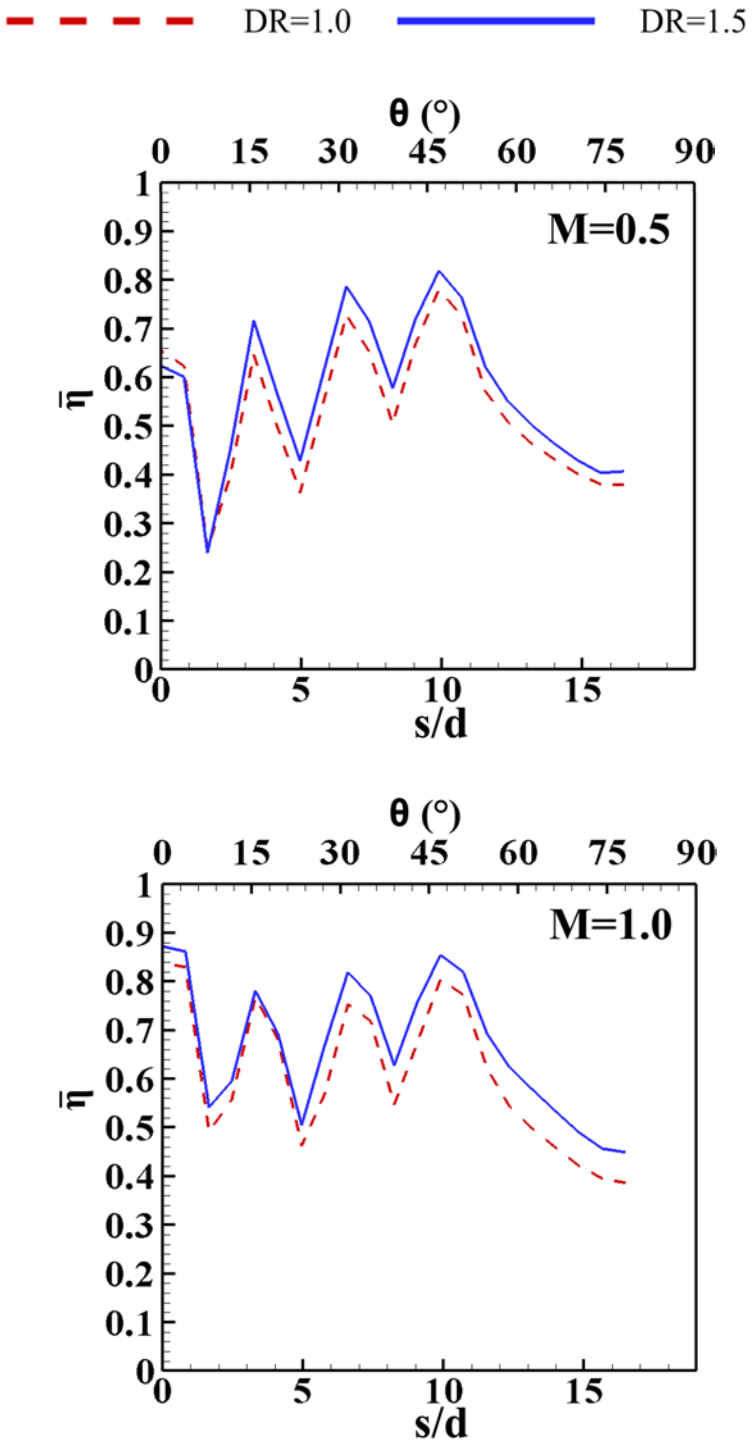

(d) Compound angle shaped holes

Fig. 5.9 Continued

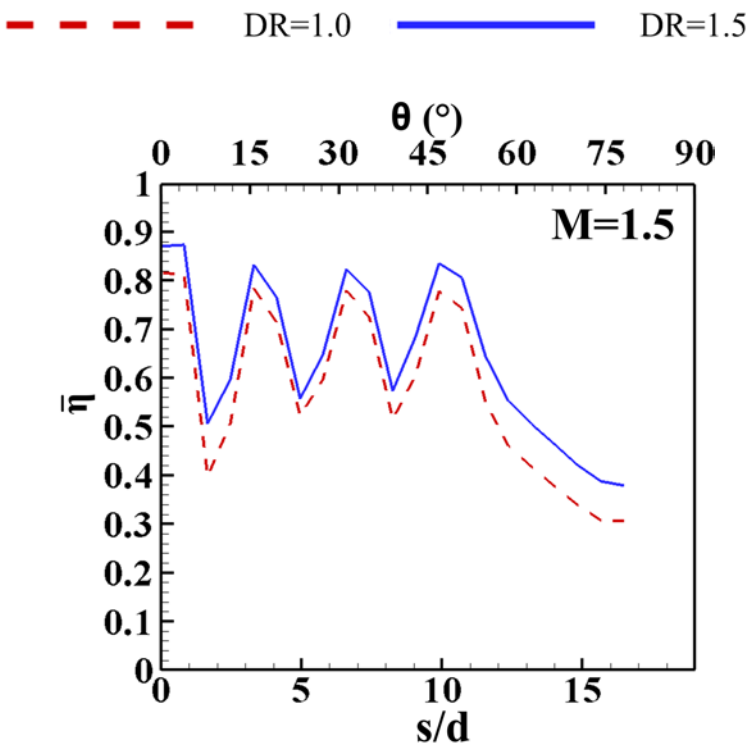

(d) Compound angle shaped holes

Fig. 5.9 Continued

further reduces coolant jet momentum at the exit of holes. Therefore, coolant jet of lower blowing ratio and higher density ratio (M=0.5, DR=1.5) becomes harder to eject coolant out from holes, indicating by lower film cooling effectiveness. Among these four configurations, radial angle shaped holes already show higher film cooling effectiveness at lower density ratio (1.0). Further increasing density ratio to 1.5 is only with marginal increment of film cooling effectiveness. There is obvious film cooling effectiveness increment for the three remaining configurations, particular for cases of cylindrical hole.

The span-wise averaged film cooling effectiveness for three-row design can be seen from Fig. 5.10. It can be seen that film cooling effectiveness level dramatically decreases with less number of film cooling holes compared with seven-row design. Also, some characteristics observed in seven-row design also take place in the three row design. Three blowing ratio (M=0.5, 1.0, and 1.5) and three density ratio (DR=1.0, 1.5, and 2.0) for each hole configuration. For cylindrical holes (either radial or compound angle), the higher the density ratio provides the higher span-wise averaged film cooling effectiveness for all blowing ratios. Density ratio effect is small for lower blowing ratio (M=0.5) cases with cylindrical hole (both angle), especially from stagnation row to leading edge first row. As increasing blowing ratio to M= 1.0 and 1.5, span-wise film cooling effectiveness obviously increases as density ratio increases from 1.0 to 2.0. As for shaped hole (both radial and compound angle), density ratio has marginal effect on film cooling effectiveness for lower blowing ratio M=0.5. For medium and higher blowing ratios, density ratio effect becomes obvious shown in film cooling effectiveness for shaped holes. As increasing density ratio to DR=1.5, film cooling effectiveness obviously increase. As further increasing density ratio from 1.5 to 2.0, there is only minimal increment of film cooling effectiveness.

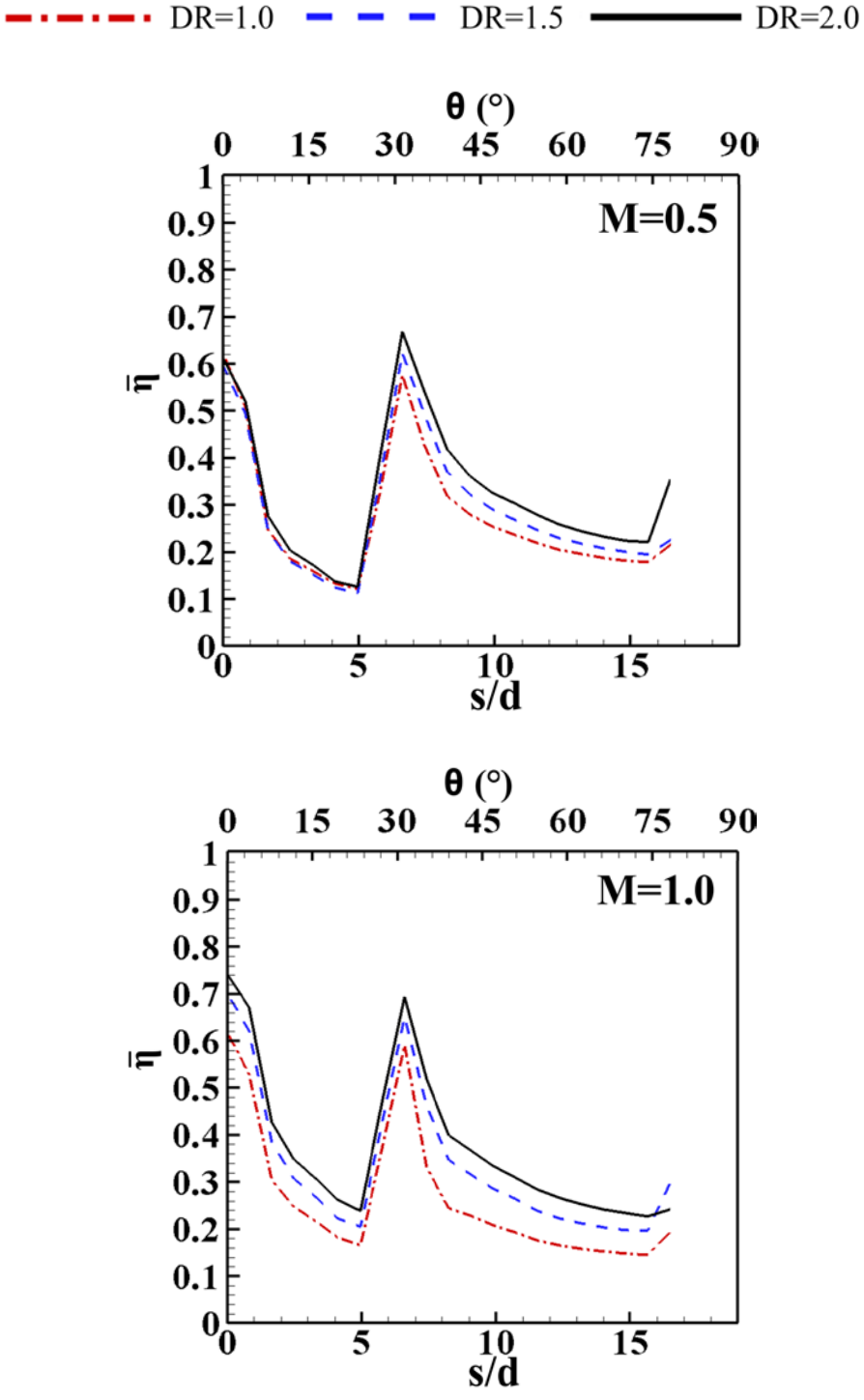

(a) Radial angle cylindrical holes

Fig. 5.10 Effect of density on span-wise averaged film cooling effectiveness (3-row)

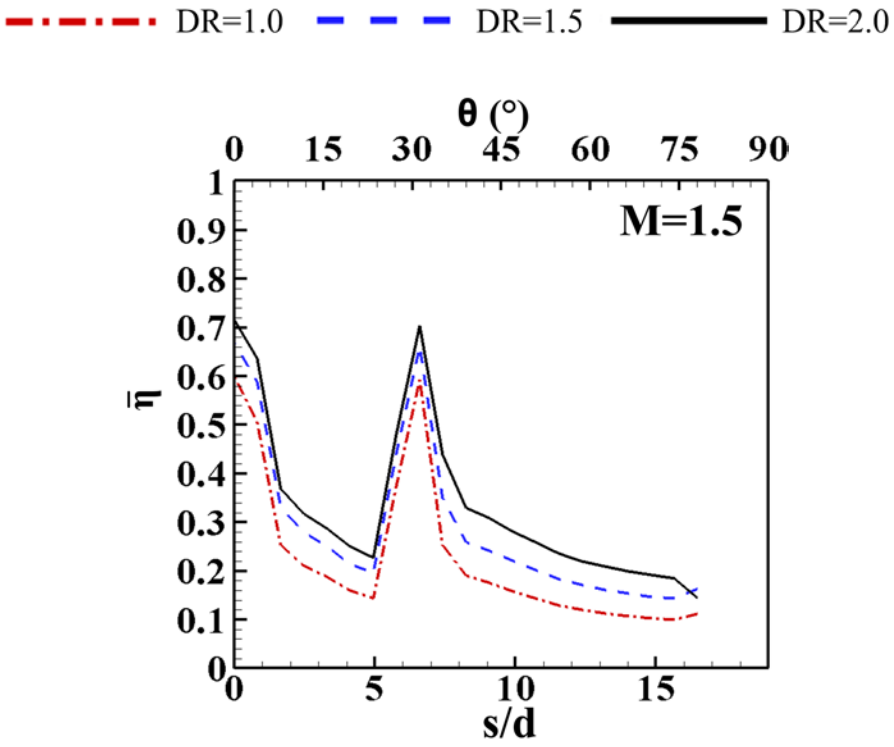

(a) Radial angle cylindrical holes

Fig. 5.10 Continued

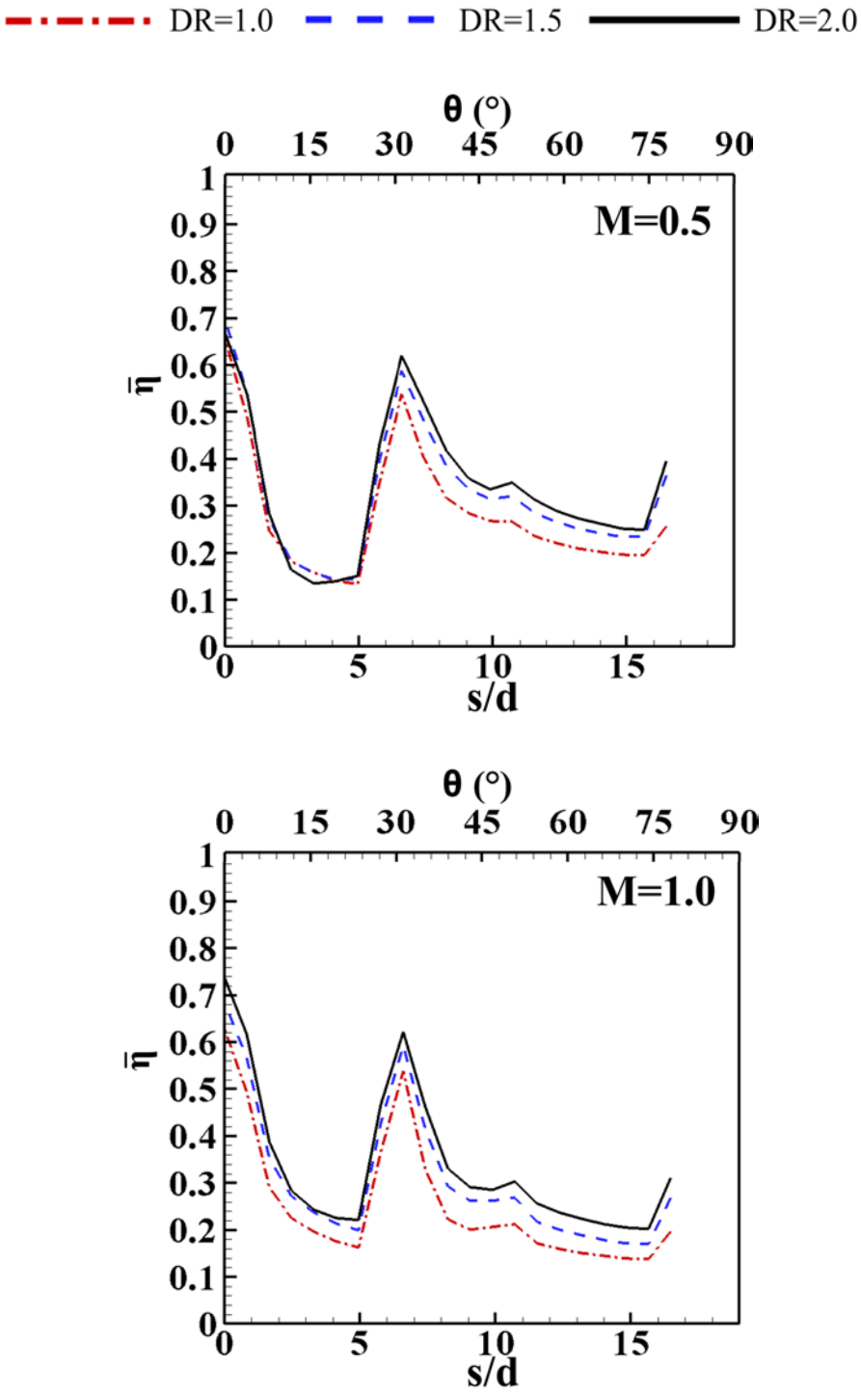

(b) Compound angle cylindrical holes

Fig. 5.10 Continued

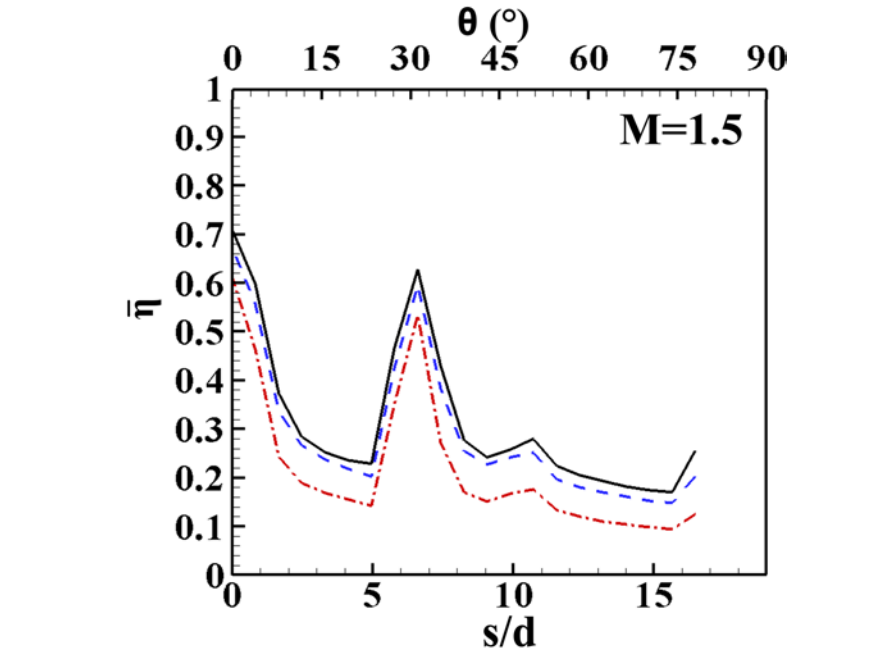

(b) Compound angle cylindrical holes

Fig. 5.10 Continued

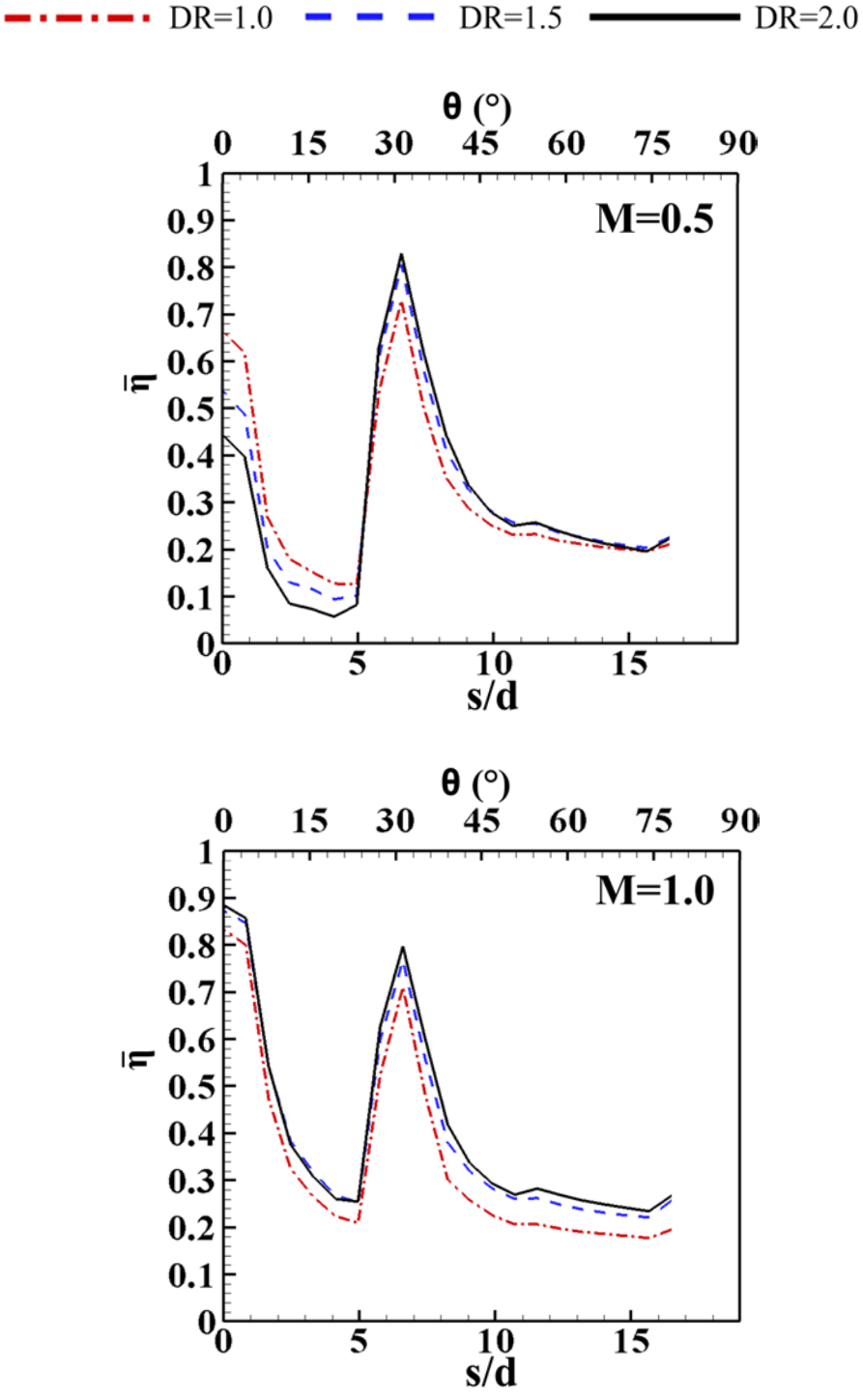

(c) Radial angle shaped holes

Fig. 5.10 Continued

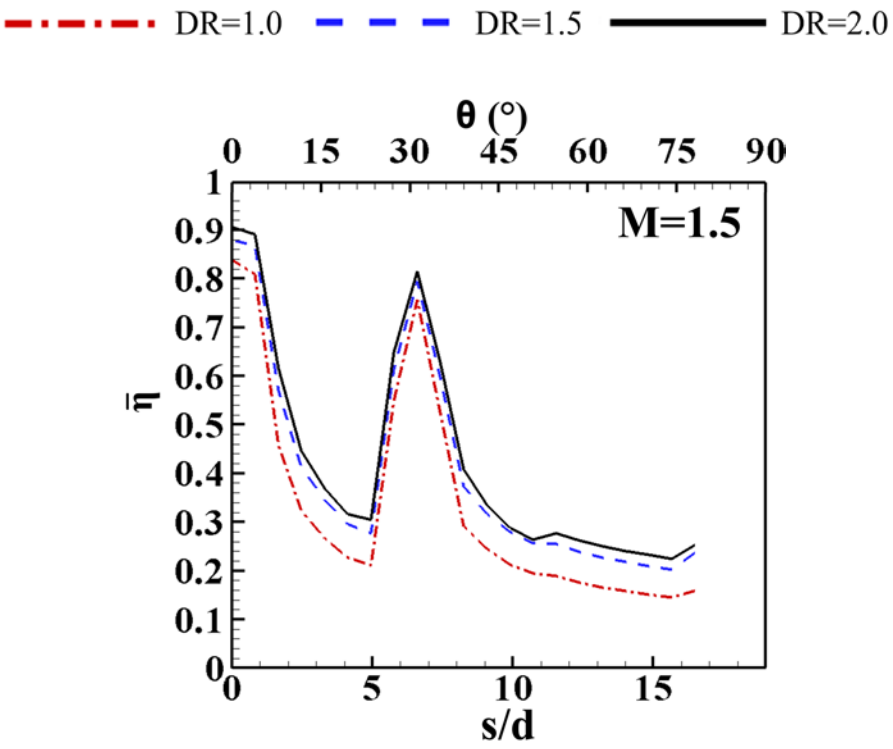

(c) Radial angle shaped holes

Fig. 5.10 Continued

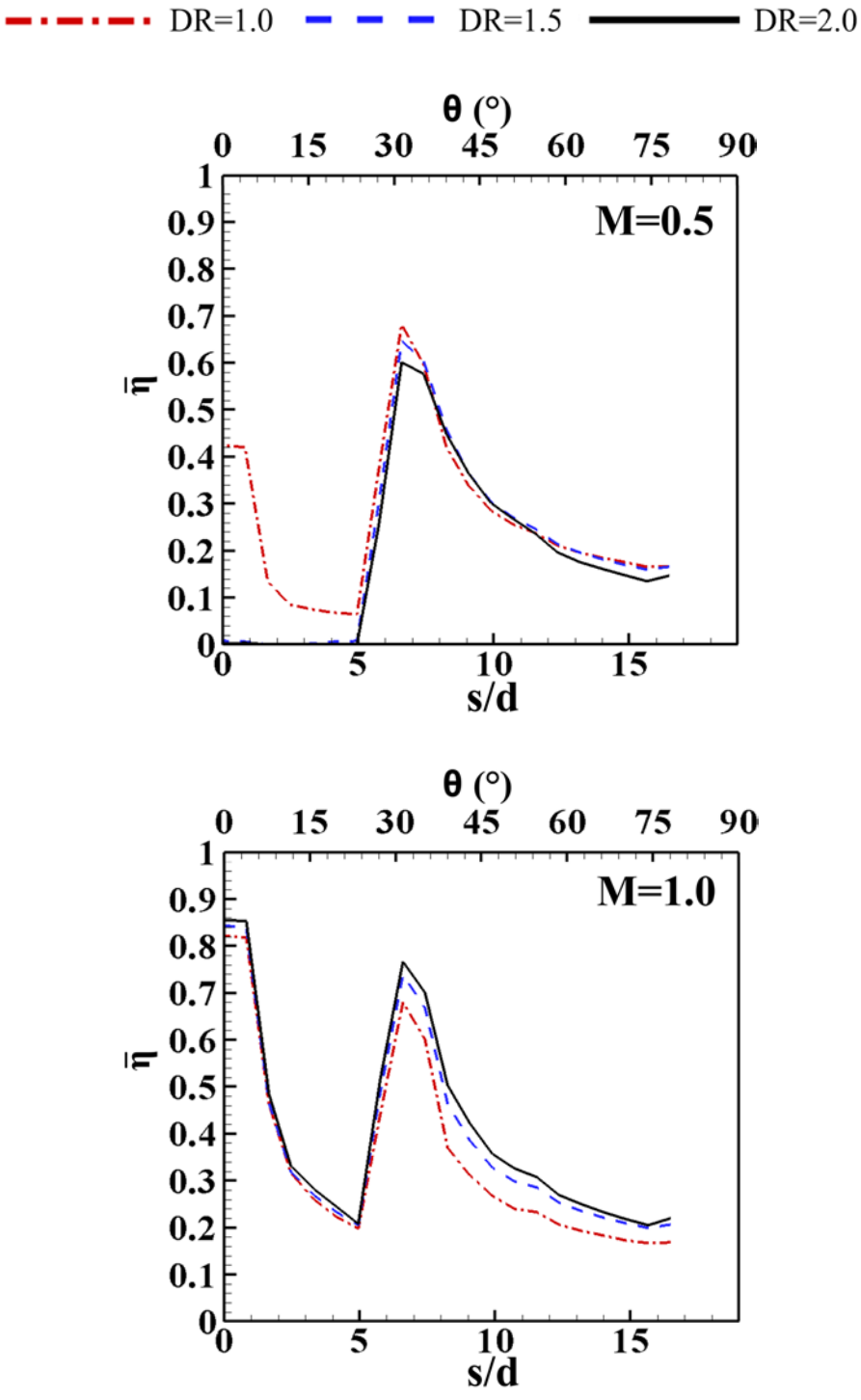

(d) Compound angle shaped holes

Fig. 5.10 Continued

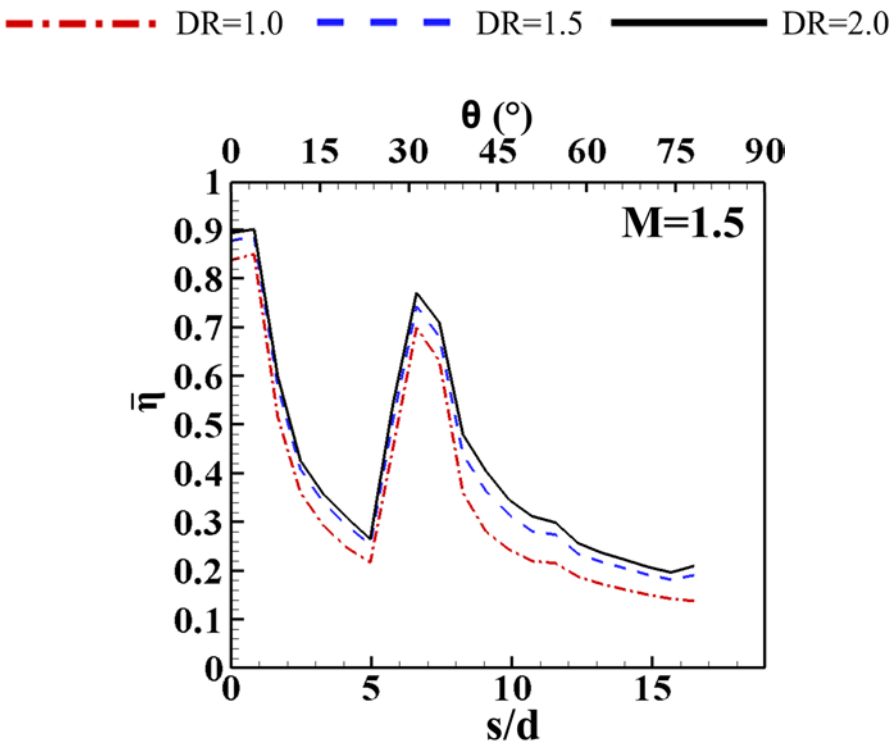

(d) Compound angle shaped holes

Fig. 5.10 Continued

5.7 Area Averaged Film Cooling Effectiveness

Area averaged film cooling effectiveness has been calculated for more directly and clearly comparing film cooling effectiveness for four film cooling holes configurations, different blowing ratios, and different density ratios. The region used to calculate area averaged film cooling effectiveness ranges from 0 to 16.5 of s/d, and 0 to 20 of z/d, and this region is exactly the same area as contour plot. Blowing ratios are M=0.5, 1.0, and 1.5 for both seven-row and three-row designs for all configurations. Density ratios are DR=1.0 and 1.5 for seven-row design and are DR=1.0, 1.5, and 2.0 for three-row design. There are twenty-four cases in total for seven-row design, and thirty-six cases in total for three-row design. Each film hole configuration is with results of various blowing ratios and density ratios in the same plot as shown in Fig. 5.11 (seven-row design) and Fig. 5.12 (three-row design).

First configuration for discussion is radial angle cylindrical hole for seven-row design in Fig. 5.11. As increasing blowing ratio from 0.5 to 1.5, the overall film cooling effectiveness increases at the beginning, and then decreases for both density ratios. The best overall film cooling effectiveness for this hole configuration occurs at the medium blowing ratio (M=1.0) for either DR=1.0 or DR=1.5 case. As density ratio increases from DR=1.0 to 1.5, the increment percentage of the overall film cooling effectiveness ranges from 13% to 18% for three blowing ratios. For the second hole configuration: compound angle cylindrical hole, the overall film cooling effectiveness decreases as increasing blowing ratio from 0.5 to 1.5 for lower density ratio DR=1.0 cases. The overall film cooling effectiveness increases slightly and then decreases again as

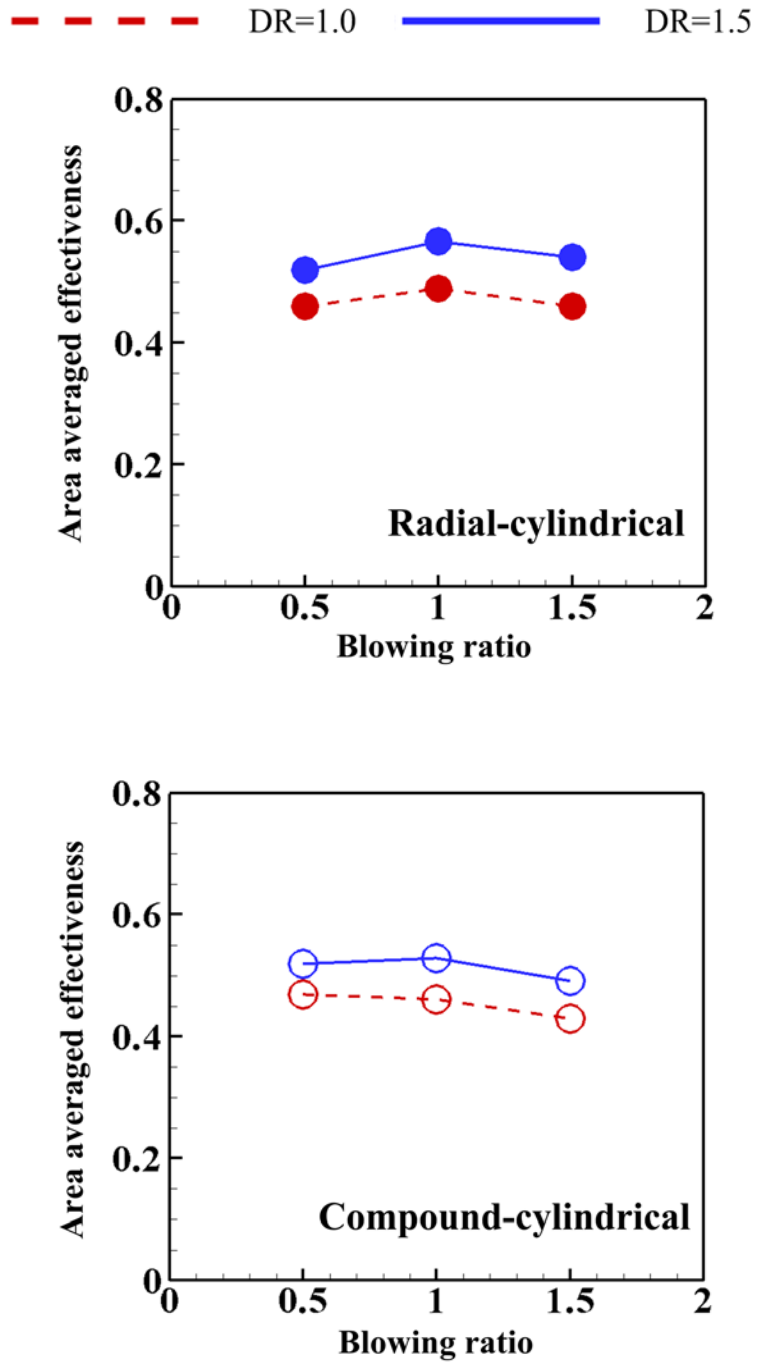

Fig. 5.11 Area averaged film cooling effectiveness for seven-row design

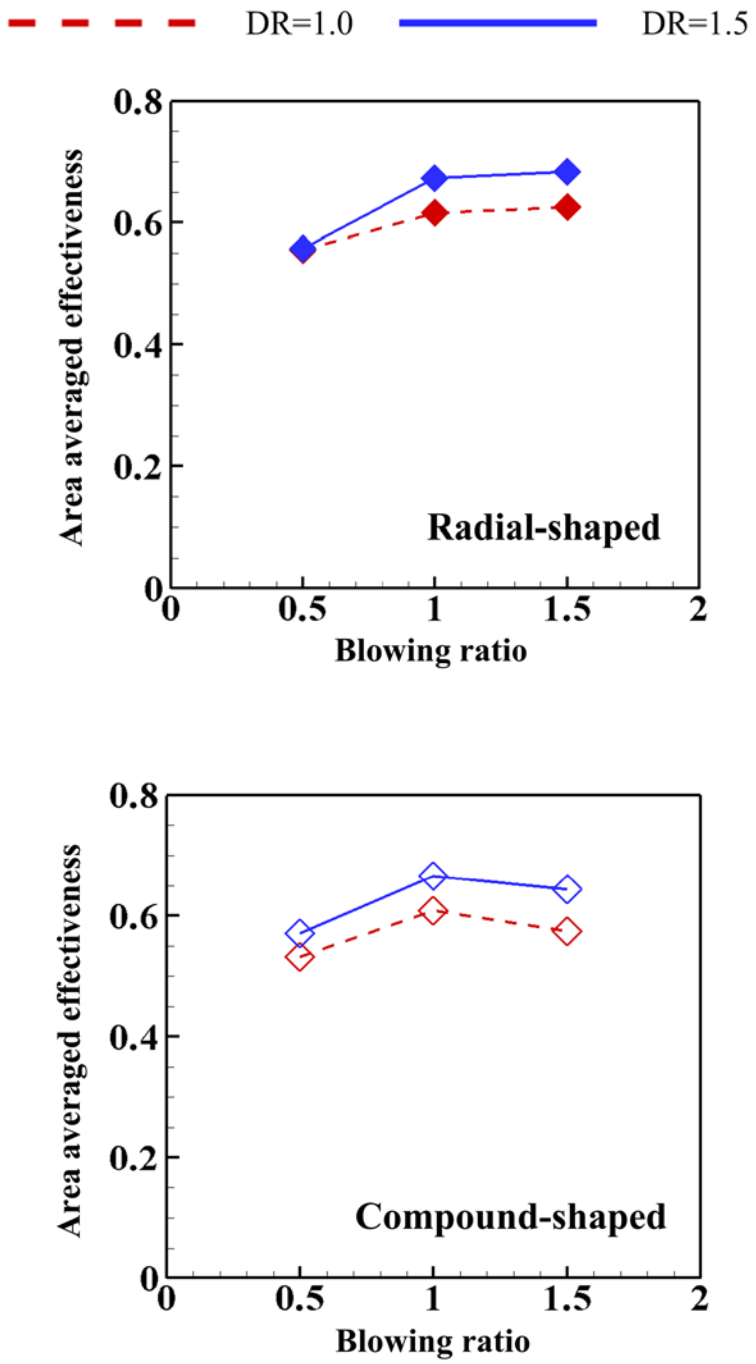

Fig. 5.11 Continued

increasing blowing ratio to 1.5 for higher density ratio DR=1.5 case. The increment percentage of overall film cooling for this configuration is from 11% to 15%. The next film hole configuration is radial angle shaped holes. This configuration performs very well than cylindrical holes, particularly at medium and higher blowing ratios. At lowest blowing ratio (M=0.5), there is no density effect indicating by two overall film cooling effectiveness overlap as increasing density ratio. Increasing blowing ratio from M=0.5 to 1.0, the overall effectiveness obviously increases for both density ratios. However, further increasing blowing ratio from M=1.0 to 1.5, there is only marginal increment of overall effectiveness either DR=1.0 or DR=1.5. Increasing density ratio from 1.0 to 1.5, the increment percentage of overall film cooling for this configuration is from 0% to 9% for three blowing ratios. The last film hole configuration for discussion is the compound angle shaped holes. The trend of increasing blowing ratio for this configuration is similar to that of radial angle cylindrical holes. The best overall film cooling effectiveness occurs at medium blowing ratio (M=1.0) for both density ratios. Enlarging the density ratio from 1.0 to 1.5, the increment percentage ranges from 7% to 12% for three blowing ratios. In summary, configuration of radial angle shaped hole performs best among all configurations by comparing four sub-figures of Fig. 5.11 for all blowing ratios and density ratios.

The overall film cooling effectiveness for three-row design for four configurations shows in Fig. 5.12. The same blowing ratio M=0.5, 1.0, and 1.5 for consideration. However, the blowing ratios are not only limited to DR=1.0, and 1.5 but also extended to realistic higher one 2.0. First configuration of radial angle cylindrical

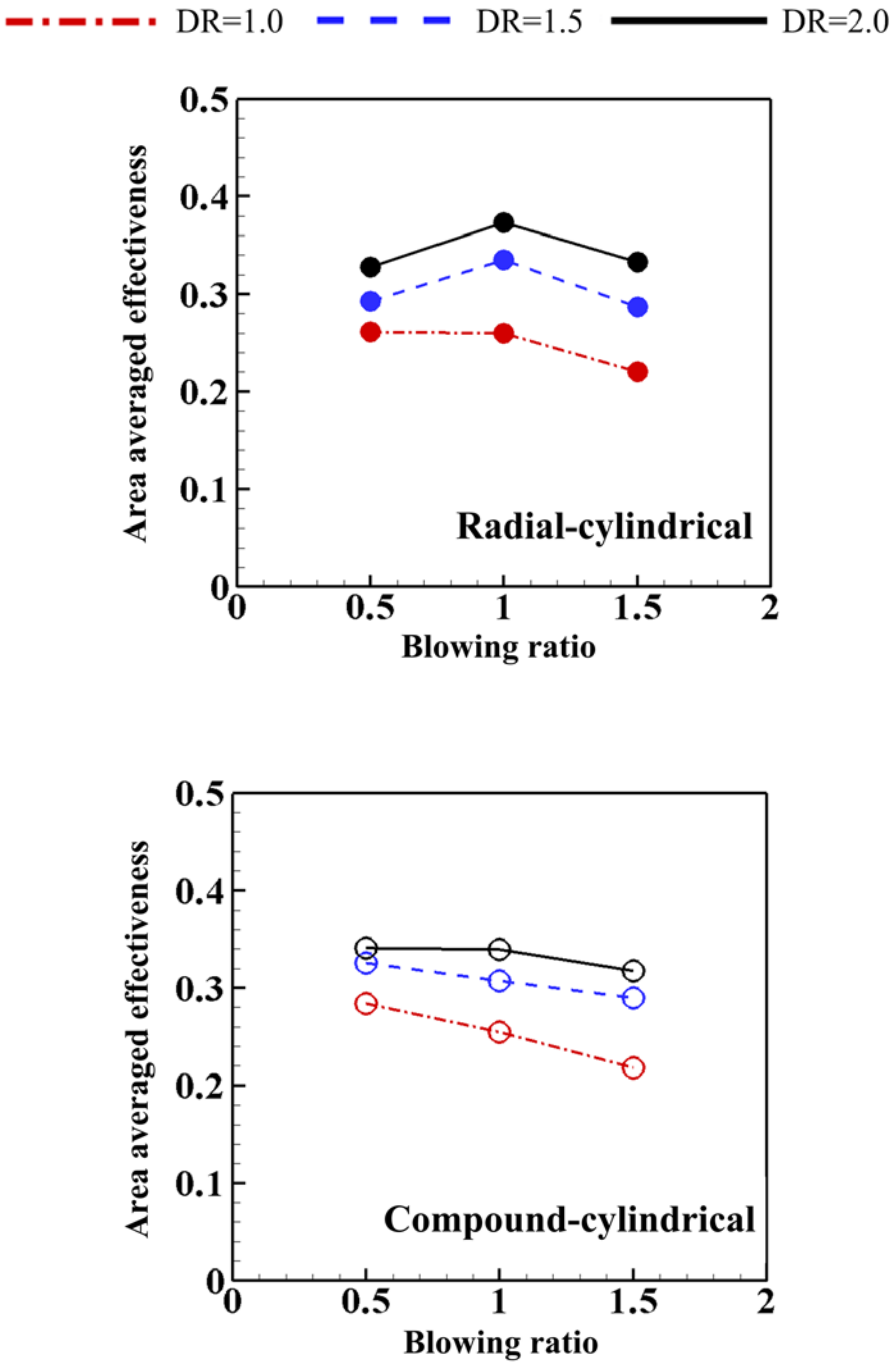

Fig 5.12 Area averaged film cooling effectiveness for three-row design

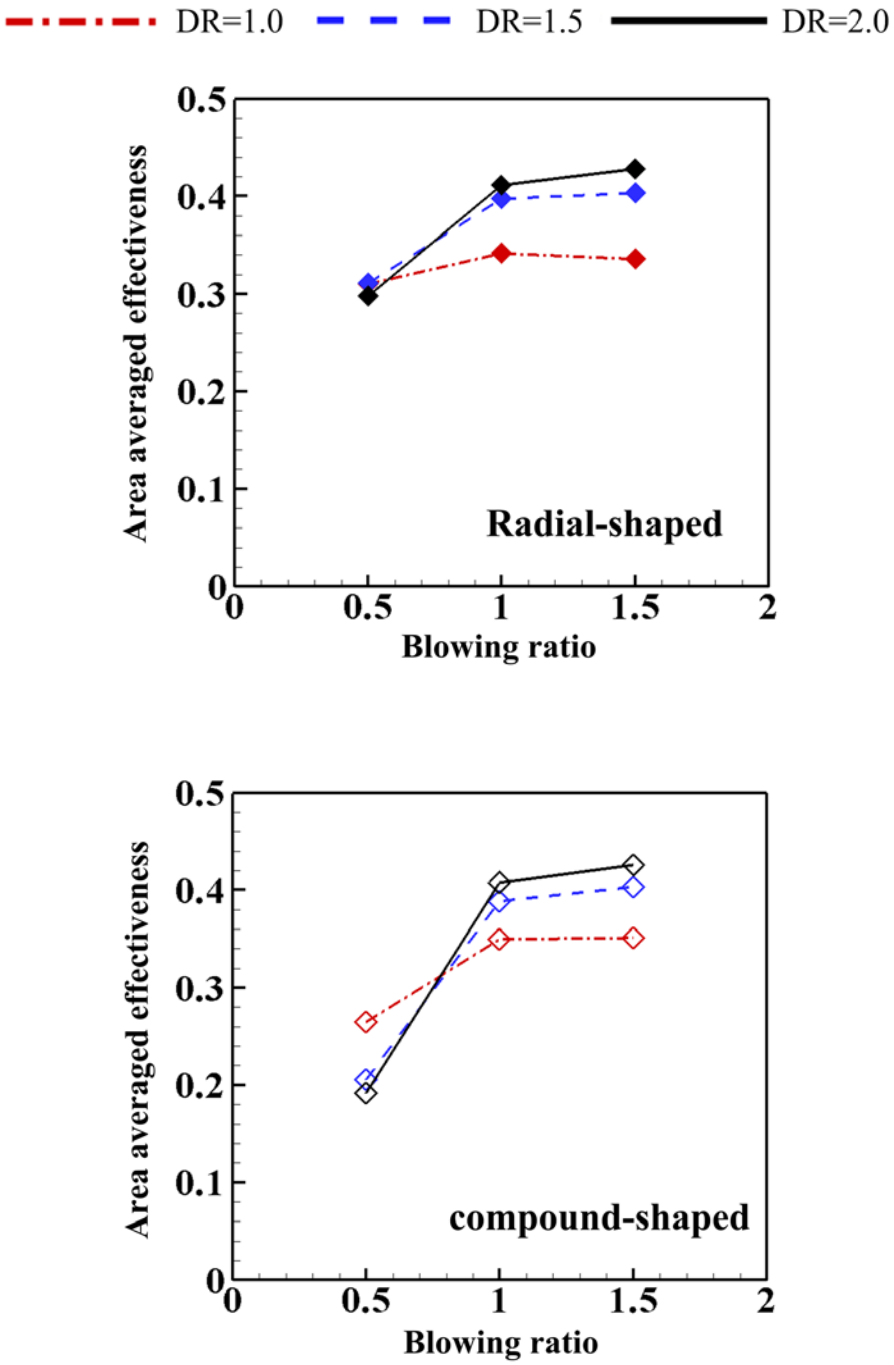

Fig. 5.12 Continued

holes, increasing blowing ratio decreases overall film cooling effectiveness for lowest density ratio (DR=1.0) case. As increasing density ratio to 1.5 and 2.0, heavier density helps coolant jet adheres to leading edge surface for protection, indicating by increment of effectiveness. At higher blowing ratio (M=1.5) with strong jet momentum, even increasing density ratio (DR=1.5 and 2.0) with heavier coolant still can not prevent coolant jet interact with mainstream, indicating by reduction of overall film cooling effectiveness. By increasing density ratio from DR=1.0 to 1.5, the increment percentage of overall film cooling effectiveness is in the range of 11% to 23% for three blowing ratios. Also, the range becomes from 10% to 14% as enlarging density ratio from DR=1.5 to 2.0. As for second configuration of compound angle cylindrical holes, increasing blowing ratio from M=0.5 to 1.5 decreases overall film cooling effectiveness for all density ratios (DR=1.0 to 2.0). As increasing density ratio from 1.0 to 1.5, the increment percentage of overall effectiveness is in the range of 13% to 25% for three blowing ratios. Further increasing density ratio from DR=1.5 to 2.0, the increment percentage becomes 4% to 10% for all blowing ratios. As for radial angle shaped holes, there is no density ratio effect for lowest blowing ratio (M=0.5), shown by three effectiveness of three different density ratios close to each other. Density ratio effect becomes apparent for medium (M=1.0) and higher (M=1.5) blowing ratios. The increment percentage is from 0% to 17% as increasing density ratio from to DR=1.0 to 1.5. Further increasing density ratio from DR=1.5 to 2.0, the increment percentage reduces to 4% to 6%. The last configuration for discussion is compound angle shaped

hole. For lowest blowing ratio (M=0.5) with lowest coolant jet momentum, increasing density ratio has an negative effect on overall film cooling effectiveness, indicating by reduction of overall effectiveness as increasing density ratio from DR=1.0 to 2.0. As for medium and higher blowing ratios, coolant jets already have higher enough momentum. Increasing density ratio (with heavier coolant) helps coolant stay close to leading edge surface and result in higher overall effectiveness. For lowest blowing ratio M=0.5, the reduction percentage of overall film cooling effectiveness as increasing density ratio from DR=1.0 to 1.5 is 29% and from DR=1.5 to 2.0 is 7%. For both medium (M=1.0) and higher (M=1.5) blowing ratios, increasing density ratio increases overall effectiveness. For blowing ratio M=1.0 and 1.5, the increment percentage is from 10% to 13% as density ratio increase to DR=1.5 but the increment becomes 4% to 5% as further increasing density ratio from DR=1.5 to 2.0. To summarize, among all four configurations, the third (radial angle shaped holes) and fourth (compound angle shaped holes) perform best overall film cooling effectiveness at higher blowing ratios and higher density ratios.

6. CONCLUSIONS

6.1 Unsteady Flow on Film Cooling

High resolution film cooling effectiveness contours and line plots have been presented for upstream trailing edge ejection combined with unsteady wake on downstream blade film cooling effectiveness using pressure sensitive paint measurement method. A comprehensive discussion is presented for no wake condition, wake condition, and combined wake and ejection condition. The key remarks are listed below:

1. Effect of blowing ratio**.** From leading edge to the second film row on both side of blade, lower blowing ratio provides higher effectiveness. However, the reverse is true at further downstream due to coolant accumulation.

2. Effect of unsteady wake. Using no wake condition as reference, passing unsteady wake increases the turbulence in mainstream, inducing more mixing between mainstream and film coolant. The overall effectiveness reduces.

3. Effect of trailing edge coolant ejection**.** Adding coolant ejection compensates the velocity defect resulted from passing wake. Also, coolant ejection is carried by wake to approach and protect blade surface. Therefore, the overall effectiveness slightly increases as compared with no coolant ejection.

4. High density film cooling and ejection. Using coolant with density ratio 2.0 simulates typical engine condition. Overall effectiveness increases due to high density coolant from ejection carried by unsteady wake to approach and protect blade surface as well as itself heavier density coolant adheres to blade.

6.2 Leading Edge Film Cooling

There are two leading edge film cooling designs investigated. Seven-row design with a heavily film cooled holes model to simulate vane. Another model is three-row design with a moderately film cooled holes to simulated blade. Four different film cooling hole configurations are investigated for both seven and three-row designs. The film cooling effectiveness on leading edge models are measured by Pressure Sensitive Paint (PSP). PSP is the superior method for determining detailed high resolution film cooling effectiveness contour, particularly for the surfaces with heavily distributed film holes. Because PSP bases on the mass transfer method rather than heat transfer one, inherent problems associated with heat transfer methods such as conduction error near film holes are avoided. A comprehensive discussions and key remarks are listed below:

1. At a fixed blowing ratio, the overall film cooling effectiveness of seven-row design is much higher than that of the three-row design due to more film holes on seven-row model with larger amount of coolant consumption. Due to larger row-to-row spacing for three-row design, the coolant accumulation is relatively insignificant. Film coolant accumulation in both span-wise and stream-wise direction is obvious for seven-row design. The superposition of the coolant jets leads to elevated effectiveness level for the seven-row designs.

2. The general trends is that lower blowing ratio case with lower coolant jet momentum, coolant jet is easily deflected by mainstream from original holes' radial or compound angle direction into stream-wise direction from stagnation row to downstream portion, and also has obvious downstream coolant accumulation along stream-wise direction. As

blowing ratio increases, coolant jets contain sufficient momentum and accumulate more along their holes' direction (either radial or compound angle direction). Furthermore, cylindrical film cooling holes are more sensitive to variations in blowing ratio than shaped holes. Shaped holes keep increase film cooling effectiveness as increasing blowing ratio. Cylindrical holes do not perform well at high blowing ratio because coolant interacts and mixes more with mainstream.

3. For both the seven-row and three-row designs, the advantage of shaped holes becomes evident as increasing blowing ratio. The shaped holes (either radial or compound angle) in general offer higher effectiveness than cylindrical holes at medium and higher blowing ratios (M=1.0~1.5). For shaped holes, due to increasing the exit area of the film holes, the jet momentum from the shaped holes is reduced. Therefore, the coolant jets can stay closer to the leading edge surface, and result in a higher effectiveness at higher blowing ratio.

4. For both designs, increasing density ratio increases film cooling effectiveness for all film hole configurations. For lower blowing ratio (M=0.5) case, there is minimal density effect on film cooling effectiveness. Coolant jet has higher tendency to lift-off at higher blowing ratio due to strong jet momentum. Increasing coolant density ratio will reduce momentum of the coolant jets. Heavier coolant can still adhere to blade surface and result in higher film cooling effectiveness. Density effect is more evident for cylindrical holes either radial or compound angle than for shape holes no matter seven or three-row design.

5. From the overall film cooling effectiveness points of view, radial angle shaped holes gives the best effectiveness for seven-row design, particularly at higher blowing ratio and higher density ratio. For three-row design, both radial angle shaped holes and compound angle shaped holes have best effectiveness at higher blowing ratio and higher density ratio. However, the worst case occurs from lowest blowing ratio (M=0.5), higher density ratio (DR=1.5 and 2.0) cases of three-row design: compound angle shaped holes along stagnation low. Coolant barely ejects from stagnation row due to insufficient jet momentum, resulting in lowest effectiveness.

REFERENCES

[1] Han, J.C., Dutta, S., and Ekkad, S.V., 2001, *Gas Turbine Heat Transfer and Cooling Technology*, Taylor & Francis, New York.

[2] Han, J.C., and Rallabandi, A.P., 2010, "Turbine Blade Film Cooling Using PSP Technique", Frontiers in Heat and Mass Transfer, Vol. 1, n1, pp. 1–21.

[3] Goldstein, R.J., Eckert, E.R.G., and Burggraf, F., 1974, "Effects of Hole Geometry and Density on Three-Dimensional Film Cooling", International Journal of Heat and Mass Transfer, Vol. 17(5), pp. 595 – 607.

[4] Goldstein, R.J., and Jin, P., 2001, "Film Cooling Downstream of a Row of Discrete Holes with Compound Angle", Journal of Turbomachinery, Vol. 123(2), pp. 222–230.

[5] Rallabandi, A.P., Grizzle, J., and Han, J.C., 2011, "Effect of Upstream Step on Flat Plate Film Cooling Effectiveness using PSP", Journal of Turbomachinery, Vol. 133(4), p. 041024.

[6] Gritsch, M., Schulz, A., and Wittig, S., 1998, "Adiabatic Wall Effectiveness Measurements of Film-Cooling Holes With Expanded Exits", Journal of Turbomachinery, Vol. 120(3), pp. 549 – 556.

[7] Gao, Z., Han, J.C., 2009, "Influence of Film-Hole Shape and Angle on Showerhead Film Cooling Using PSP Technique", Journal of Heat Transfer, Vol. 131, p. 061701.

[8] Waye, S.K., and Bogard, D.G., 2007, "High-Resolution Film Cooling Effectiveness Measurements of Axial Holes Embedded in a Transverse Trench with Various Trench Configurations", Journal of Turbomachinery, Vol. 129(2), pp. 294 – 302.

[9] Sinha, A.K., Bogard, D., and Crawford, M., 1991, “Film Cooling Effectiveness Downstream of a Single Row of Holes with Variable Density Ratio”, Journal of Turbomachinery, Vol. 113(3), pp. 442–449.

[10] Ekkad, S., Zapata, D., and Han, J.C., 1997, “Film Effectiveness Over a Flat Surface With Air and CO2 Injection Through Compound Angle Holes Using a Transient Liquid Crystal Image Method”, Journal of Turbomachinery, Vol. 119(3), pp. 587 – 593.

[11] Wright, L.M., Gao, Z., Varvel, T.A., and Han, J.C., 2005, “Assessment of Steady State PSP, TSP, and IR Measurement Techniques for Flat Plate Film Cooling”, In Proceedings of the ASME Summer Heat Transfer Conference, Paper no. HT2005–72363 pp. 37-46.

[12] Goldstein, R.J., Eckert, E.G., Eriksen, V.L., and Ramsey, J.W., 1970, “Film Cooling Following Injection through Inclined Circular Tubes”, Israel J. of Technology, Vol. 8, pp. 145–154.

[13] Jubran, B., and Brown, A., 1985, “Film Cooling from Two Rows of Holes Inclined in the Streamwise and Spanwise Directions”, ASME J. Eng. Gas Turbines Power, Vol. 107, pp. 84 – 91.

[14] Ethridge, M.I., Cutbirth, J.M., and Bogard, D.G., 2001, “Scaling of Performance for Varying Density Ratio Coolants on an Airfoil with Strong Curvature and Pressure Gradient Effects”, Journal of Turbomachinery, Vol. 123(2), pp. 231–237.

[15] Jones, T., 1999, “Theory for the use of foreign gas in simulating film cooling”, International Journal of Heat and Fluid Flow, Vol. 20(3), pp. 349–354.

[16] Wright, L.M., McClain, S.T., and Clemenson, M.D., 2011, “Effect of Density Ratio

on Flat Plate Film Cooling With Shaped Holes Using PSP", Journal of Turbomachinery, Vol. 133(4), p. 041011

[17] Choi, J, Teng S, Han, J.C., and Ladeinde, F, 2004, "Effect of Free-Stream Turbulence on Turbine Blade Heat Transfer and Pressure Coefficients in Low Reynolds Number Flows", International Journal of Heat and Mass Transfer, Vol. 47 pp. 3441–3452.

[18] Ekkad, S.V., Han, J.C., and Du, H., 1998, "Detailed Film Cooling Measurements on a Cylindrical Leading Edge Model: Effect of Free-Stream Turbulence and Coolant Density", Journal of Turbomachinery, Vol. 120(4), pp. 799–807.

[19] Bons, J.P., MacArthur, C.D., and Rivir, R.B., 1996, "The Effect of High Free-Stream Turbulence on Film Cooling Effectiveness", Journal of Turbomachinery, Vol. 118(4), pp. 814–824.

[20] Saumweber C., Schulz A., and Wittig S., 2003, "Free-Stream Turbulence Effects on Film Cooling With Shaped Holes", Journal of Turbomachinery, Vol. 125(1), pp. 65–73.

[21] Ethridge, M.I., Michael C.J., and Bogard, D.G., 2001, "Scaling of Performance for Varying Density Ratio Coolants on an Airfoil With Strong Curvature and Pressure Gradient Effects", Journal of Turbomachinery, Vol. 123(2), pp. 231–237.

[22] El-Gabry, Lamyaa A., and Rivir, R.B., 2012, "Effect of Pulsed Film Cooling on Leading Edge Film Effectiveness", Journal of Turbomachinery, Vol. 134(4), p. 041005.

[23] Maikell J., Bogard D., Piggush J., and Kohli A., 2011, "Experimental Simulation of a Film Cooled Turbine Blade Leading Edge Including Thermal Barrier Coating Effects", Journal of Turbomachinery, Vol. 133(1), p. 011014.

[24] Rozati A., Tafti, D.K., and Sreedharan S.S., 2011, “Effects of Syngas Ash Particle Size on Deposition and Erosion of a Film Cooled Leading Edge”, Journal of Turbomachinery, Vol. 133(1), p. 011010.

[25] Gao, Z., Yang, H., Wright, L.M., and Han, J.C., 2006, “Conjugate Prediction of Leading Edge Film Cooling and Heat Transfer”, Proceedings of ISROMAC, Paper no. ISROMAC11-2006-45.

[26] Mayle, R., 1991, “The Role of Laminar-Turbulent Transition in Gas Turbine Engines”, Journal of Turbomachinery, Vol. 113(4), pp. 509 – 536.

[27] Mayle, R., and Dullenkopf, K., 1990, “A Theory for Wake Induced Transition”, Journal of Turbomachinery, Vol. 112(2), pp. 188 – 195.

[28] Han, J.C., Zhang, L., and Ou, S., 1993, “Influence of Unsteady Wake on Heat Transfer Coefficient from a Gas Turbine Blade”, Journal of Heat Transfer, Vol. 115(4), pp. 904–911.

[29] Zhang, L., and Han, J.C., 1995, “Combined Effect of Free Stream Turbulence and Unsteady Wake on Heat Transfer Coefficients from a Gas Turbine Blade”, Journal of Heat Transfer, Vol. 117, p. 296.

[30] Ou, S., Han, J.C., Mehendale, A., and Lee, C., 1994. “Unsteady Wake Over a Linear Turbine Blade Cascade With Air and CO2 Film Injection: Part I Effect on Heat Transfer Coefficients”. Journal of Turbomachinery, Vol. 116, pp. 721 – 729.

[31] Guenette, G., Epstein, A., Giles, M., Haimes, R., and Norton, R., 1989, “Fully Scaled Transonic Turbine Rotor Heat Transfer Measurements”, Journal of Turbomachinery, Vol. 111(1), pp. 1 – 7.

[32] Doorly, D., and Oldfield, M., 1985, “Simulation of the Effects of Shock Wave Passing on a Turbine Rotor Blade”, Journal of Engineering for Gas Turbines and Power, Vol. 107(4), pp. 998 – 1006.

[33] Funazaki, K., Yokota, M., and Yamawaki, S., 1997, “Effect of Periodic Wake Passing on Film Effectiveness of Discrete Cooling Holes around the Leading Edge of a Blunt Body”, Journal of Turbomachinery, Vol. 119(2), pp. 292 – 301.

[34] Stieger, R., and Hodson, H., 2005, “The Unsteady Development of a Turbulent Wake through a Downstream Low Pressure Turbine Blade Passage”, Journal of Turbomachinery, Vol. 127(2), pp. 388 – 394.

[35] Bijak-Bartosik, E., and Elsner, W., 2009, “Investigation of Wake Transport in a Turbine Blade Channel and its Effect on the Boundary Layer Development”, In ASME, International Gas Turbine Conference and Exhibit, Orlando, Paper no. GT2009-59123, pp. 1509 – 1517.

[36] Mehendale, A., Han, J.C., Ou, S., and Lee, C., 1994, “Unsteady Wake over a Linear Turbine Blade Cascade with Air and CO2 Film Injection: Part II Effect on Film Effectiveness and Heat Transfer Distributions”, Journal of Turbomachinery, Vol. 116(4), pp. 730 – 737.

[37] Du, H., Han, J.C., and Ekkad, S., 1998, “Effect of Unsteady Wake on Detailed Heat Transfer Coefficient and Film Effectiveness Distributions for a Gas Turbine Blade”, Journal of Turbomachinery, Vol(4). 120, pp. 808 – 817.

[38] Rallabandi, A.P., Li, S.J., and Han, J.C., 2012, “Unsteady Wake and Coolant

Density Effects on Turbine Blade Film Cooling Using PSP Technique", Journal of Heat Transfer, Vol. 134, p. 081701.

[39] Teng, S., Sohn, D., and Han, J.C., 2000, "Unsteady Wake Effect on Film Temperature and Effectiveness Distributions for a Gas Turbine Blade", Journal of Turbomachinery, Vol. 122(2), pp. 340 – 347.

[40] Heidmann, J., Lucci, B., and Reshotko, E., 2001, "An Experimental Study of the Effect of Wake Passing on Turbine Blade Film Cooling", Journal of Turbomachinery, Vol. 123(2), pp. 214 – 221.

[41] Du, H., Ekkad, S., and Han, J.C., 1997, "Effect of Unsteady Wake with Trailing Edge Coolant Ejection on Detailed Heat Transfer Coefficient Distributions for a Gas Turbine Blade", Journal of Heat Transfer, Vol. 119, p. 242.

[42] Du, H., Ekkad, S., and Han, J.C., 1999, "Effect of Unsteady Wake with Trailing Edge Coolant Ejection on Film Cooling Performance for a Gas Turbine Blade", Journal of Heat Transfer, Vol. 121, p. 448.

[43] Li, S.J., Rallabandi, A.P., and Han, J.C., 2012, " Influence of Unsteady Wake with Trailing Edge Coolant Ejection on Turbine Blade Film Cooling", Journal of Turbomachinery, Vol. 134(6), p. 061026.

[44] Schulz A., 2000, "Infrared Thermography as Applied to Film Cooling of Gas Turbine Components", Measurement Science and Technology, Vol. 11, Num. 7, pp. 948- 956.

[45] Lu, Y., Dhungel, A., Ekkad, S.V., and Bunker, R.S., 2012, "Effect of Trench Width

and Depth on Film Cooling From Cylindrical Holes Embedded in Trenches", Journal of Turbomachinery, Vol. 131(1), p. 011003.

[46] Ou, S., and Rivir, R.B., 2001, "Leading Edge Film Cooling Heat Transfer with High Free Stream Turbulence using a Transient Liquid Crystal Image Method", International Journal of Heat and Fluid Flow, Vol. 22(6), pp. 614 – 623

[47] Nicoll, W., and Whitelaw, J., 1967, "The Effectiveness of the Uniform Density, Two-Dimensional Wall Jet (Two-Dimensional Wall Jet Effectiveness Measurements and Calculation Procedures for Injection Conditions)", International Journal of Heat and Mass Transfer, Vol. 10, pp. 623 – 639.

[48] Goldstein, R.J., and Cho, H.H., 1995, "A Review of Mass Transfer Measurements using Naphthalene Sublimation", Experimental Thermal and Fluid Science, Vol. 10(4), pp. 416 – 434.

[49] Nicoll, W., and Whitelaw, J., 1967, "The effectiveness of the uniform density, two-dimensional wall jet (Two-dimensional wall jet effectiveness measurements and calculation procedures for injection conditions)", International Journal of Heat and Mass Transfer, Vol. 10, pp. 623 – 639.

[50] Wright, L.M., McClain, S.T., and Clemenson, M.D., 2011, "Effect of Freestream Turbulence Intensity on Film Cooling Jet Structure and Surface Effectiveness Using PIV and PSP", Journal of Turbomachinery, Vol. 133(4), p. 041023.

[51] Gao, Z., Narzary D., Mhetras, S., and Han, J.C., 2009, "Effect of Inlet Flow Angle on Gas Turbine Blade Tip Film Cooling", Journal of Turbomachinery, Vol. 131(3), p. 031005.

[52] Gao, Z., Narzary D., and Han, J.C., 2009, “Film-Cooling on a Gas Turbine Blade Pressure Side or Suction Side With Compound Angle Shaped Holes”, Journal of Turbomachinery, Vol. 131(1), p. 011019.

[53] Kline, S., and McClintock, F., 1953, “Describing Uncertainties in Single-Sample Experiments”, Mechanical Engineering, Vol. 75(1), pp. 3 – 8.